



Calhoun: The NPS Institutional Archive DSpace Repository

Theses and Dissertations

1. Thesis and Dissertation Collection, all items

1987

A numerical modeling study of the transmission line antenna for use as an HF combat survivable shipboard antenna

Choi, Seung Kyu

Monterey, California: U.S. Naval Postgraduate School

<http://hdl.handle.net/10945/22389>

Copyright is reserved by the copyright owner.

Downloaded from NPS Archive: Calhoun



<http://www.nps.edu/library>

Calhoun is the Naval Postgraduate School's public access digital repository for research materials and institutional publications created by the NPS community.

Calhoun is named for Professor of Mathematics Guy K. Calhoun, NPS's first appointed -- and published -- scholarly author.

Dudley Knox Library / Naval Postgraduate School
411 Dyer Road / 1 University Circle
Monterey, California USA 93943



MONTEREY COUNTY HIGH SCHOOL
MONTEREY, CALIFORNIA 93945 5002

NAVAL POSTGRADUATE SCHOOL

Monterey, California



THEESIS

C448861

A NUMERICAL MODELING STUDY OF THE
TRANSMISSION LINE ANTENNA
FOR USE AS AN HF
COMBAT SURVIVABLE SHIPBOARD ANTENNA

by

Seung Kyu, Choi

December 1987

Thesis Advisor:

Richard W. Adler

Approved for public release; distribution is unlimited

Prepared for:
Naval Ocean Systems Center
San Diego, CA 92152

T238765

NAVAL POSTGRADUATE SCHOOL

Monterey, CA 93943-5000

Rear Admiral R.C. Austin
Superintendent

Kneale T. Marshal
Acting Provost

This thesis is prepared in conjunction with research
sponsored in part by Naval Ocean Systems Center under
N6227186WR60125.

Reproduction of all or part of this report is authorized.

Released by:

UNCLASSIFIED

SECURITY CLASSIFICATION OF THIS PAGE

REPORT DOCUMENTATION PAGE

1a. REPORT SECURITY CLASSIFICATION UNCLASSIFIED		1b. RESTRICTIVE MARKINGS			
2a. SECURITY CLASSIFICATION AUTHORITY		3. DISTRIBUTION/AVAILABILITY OF REPORT Approved for public release; distribution is unlimited			
2b. DECLASSIFICATION/DOWNGRADING SCHEDULE					
4. PERFORMING ORGANIZATION REPORT NUMBER(S) NPS-62-88-005		5. MONITORING ORGANIZATION REPORT NUMBER(S)			
6a. NAME OF PERFORMING ORGANIZATION Naval Postgraduate School	6b. OFFICE SYMBOL (If applicable) 62	7a. NAME OF MONITORING ORGANIZATION Naval Postgraduate School			
6c. ADDRESS (City, State, and ZIP Code) Monterey, California 93943-5000		7b. ADDRESS (City, State, and ZIP Code) Monterey, California 93943-5000			
8a. NAME OF FUNDING / SPONSORING ORGANIZATION Naval Ocean Systems Center	8b. OFFICE SYMBOL (If applicable) Code 744	9. PROCUREMENT INSTRUMENT IDENTIFICATION NUMBER N6227186WR60125			
8c. ADDRESS (City, State, and ZIP Code) San Diego, California 92152		10. SOURCE OF FUNDING NUMBERS			
		PROGRAM ELEMENT NO.	PROJECT NO.	TASK NO.	WORK UNIT ACCESSION NO.
11. TITLE (Include Security Classification) A NUMERICAL MODELING STUDY OF THE TRANSMISSION LINE ANTENNA FOR USE AS AN HF COMBAT SURVIVABLE SHIPBOARD ANTENNA					
12. PERSONAL AUTHOR(S) Seung Kyu, Choi					
13a. TYPE OF REPORT Master's Thesis	13b. TIME COVERED FROM _____ TO _____	14. DATE OF REPORT (Year, Month, Day) 1987 December		15. PAGE COUNT 162	
16. SUPPLEMENTARY NOTATION					
17. COSATI CODES		18. SUBJECT TERMS (Continue on reverse if necessary and identify by block number) Transmission Line Antenna, Ship Antenna; Numerical Electromagnetic Code (NEC)			
FIELD	GROUP	SUB-GROUP			
19. ABSTRACT (Continue on reverse if necessary and identify by block number) This thesis investigates computer numerical models to improve combat survivability for HF shipboard antenna systems. The trend for the next generation of ships will be the elimination of tall and large structures to make antennas more survivable during combat. The use of a transmission line antenna on the bow and the stern of a ship seems to be a good candidate for solving these problems. The ship and antennas are modeled using wire grids. The computer models are developed by the Numerical Electromagnetics Code (NEC). Average power gain, input impedance, and radiation patterns of driven antennas are presented.					
20. DISTRIBUTION/AVAILABILITY OF ABSTRACT <input checked="" type="checkbox"/> UNCLASSIFIED/UNLIMITED <input type="checkbox"/> SAME AS RPT. <input type="checkbox"/> DTIC USERS			21. ABSTRACT SECURITY CLASSIFICATION UNCLASSIFIED		
22a. NAME OF RESPONSIBLE INDIVIDUAL R. W. Adler			22b. TELEPHONE (Include Area Code) (408) 646-2352	22c. OFFICE SYMBOL 62Ab	

Approved for public release; distribution is unlimited.

A Numerical Modeling Study of the Transmission Line Antenna
for Use as an IIF
- Combat Survivable Shipboard Antenna

by

Seung Kyu, Choi
Major, Republic of Korean Air Force
B.S., Korean Air Force Academy, 1977

Submitted in partial fulfillment of the
requirements for the degree of

MASTER OF SCIENCE IN ELECTRICAL ENGINEERING

from the

NAVAL POSTGRADUATE SCHOOL
December 1987

ABSTRACT

This thesis investigates computer numerical models to improve combat survivability for HF shipboard antenna systems. The trend for the next generation of ships will be the elimination of tall and large structures to make antennas more survivable during combat. The use of a transmission line antenna on the bow and the stern of a ship seems to be a good candidate for solving these problems. The ship and antennas are modeled using wire grids. The computer models are developed by the Numerical Electromagnetics Code (NEC). Average power gain, input impedance, and radiation patterns of driven antennas are presented.

TABLE OF CONTENTS

I.	INTRODUCTION	13
	A. NEED FOR THE STUDY	13
	B. TRANSMISSION LINE ANTENNA BACKGROUND	13
	C. SCOPE AND LIMITATION	14
II.	TRANSMISSION LINE ANTENNA COMPUTER MODEL AND RESULTS	16
	A. TRANSMISSION LINE ANTENNA COMPUTER MODEL	16
	B. COMPUTER MODEL RESULTS	17
	1. Average Power Gain	17
	2. Input Impedance	20
	3. Radiation Patterns	21
III.	SHIP - ANTENNA COMPUTER MODELS AND RESULTS	48
	A. SHIP COMPUTER MODELS	48
	B. COMPUTER RESULTS	52
	1. Average Power Gain	52
	2. Input Impedance	54
	3. Radiation Patterns	63
IV.	CONCLUSIONS AND RECOMMENDATIONS	84
	A. CONCLUSIONS	84
	B. RECOMMENDATIONS	85
APPENDIX A:	GEOMETRY DATA SETS	86
	a. Ship NGF Geometry	86
	b. End Feed Transmission Line Antenna on the Bow	91
	c. End Feed Transmission Line Antenna on the Stern	92
	d. End Feed Transmission Line Antenna on the Bow and the Stern	92

e. Top Feed Transmission Line Antenna on the Bow	92
f. Top Feed Transmission Line Antenna on the Stern	93
g. Top Feed Transmission Line Antenna on the Bow and the Stern	93
 APPENDIX B: AVERAGE POWER GAIN FOR REACTIVELY LOADED TRANSMISSION LINE ANTENNAS VS FREQUENCY	95
 APPENDIX C: INPUT IMPEDANCE FOR AN END FEED TRANSMISSION LINE ANTENNA WITH DIFFERENT RADII, SEGMENTATION, FEED LOCATION AND LOADING	98
 APPENDIX D: RADIATION PATTERNS FOR A CENTER-END FEED TRANSMISSION LINE ANTENNA	110
 APPENDIX E: RADIATION PATTERNS FOR TRANSMISSION LINE ANTENNAS ON THE BOW AND ON THE STERN	119
 LIST OF REFERENCES	152
 BIBLIOGRAPHY	153
 INITIAL DISTRIBUTION LIST	154

LIST OF TABLES

1. AVERAGE POWER GAIN FOR TLA WITH THREE DIFFERENT WIRE RADII	18
2. AVERAGE POWER GAIN FOR TLA WITH FOUR DIFFERENT SEGMENTATIONS	19
3. AVERAGE POWER GAIN FOR TLA WITH THREE DIFFERENT FEED POINTS	20
4. AVERAGE POWER GAIN FOR END FEED-TLA	53
5. AVERAGE POWER GAIN FOR TOP FEED-TLA	53
6. RESISTANCE FOR END FEED-TLA	55
7. REACTANCE FOR END FEED-TLA	55
8. RESISTANCE FOR TOP FEED-TLA	59
9. REACTANCE FOR TOP FEED-TLA	59
10. AVERAGE POWER GAINS OF TLA WITH CAPACITIVE LOADS	95
11. AVERAGE POWER GAINS OF TLA WITH INDUCTIVE LOADS	96
12. AVERAGE POWER GAINS FOR EF-TLA FROM 4.0 - 6.9 MHZ WITH 9 SEGMENTS AND A 0.05 METER RADIUS	97
13. RESISTANCE OF TLA WITH THREE DIFFERENT RADII	98
14. REACTANCE OF TLA WITH THREE DIFFERENT RADII	99
15. RESISTANCE OF TLA WITH FOUR DIFFERENT SEGMENTATIONS	100
16. REACTANCE OF TLA WITH THREE DIFFERENT SEGMENTATIONS	101
17. RESISTANCE OF TLA WITH THREE DIFFERENT FEED POINTS	102
18. REACTANCE OF TLA WITH THREE DIFFERENT FEED POINTS	103
19. RESISTANCE OF TLA WITH THREE DIFFERENT CAPACITORS	104
20. REACTANCE OF TLA WITH THREE DIFFERENT CAPACITORS	105
21. RESISTANCE OF TLA WITH THREE DIFFERENT INDUCTORS	106
22. REACTANCE OF TLA WITH THREE DIFFERENT INDUCTORS	107

23. INPUT IMPEDANCE FOR EF-TLA FROM 4.0 - 6.9 MHZ WITH 9 SEGMENTS AND A 0.05 METER RADIUS	108
23. INPUT IMPEDANCE FOR EF-TLA FROM 4.0 - 6.9 MHZ WITH 9 SEGMENTS AND A 0.05 METER RADIUS	109

LIST OF FIGURES

1.1	Transmission Line Antenna	14
2.1	Transmission Line Antenna Dimensions	16
2.2	Resistance vs Frequency for a 9 Segment EF-TLA with Three Different Wire Radii	23
2.3	Reactance vs Frequency for a 9 Segment EF-TLA with Three Different Wire Radii	24
2.4	Resistance vs Frequency for EF-TLA with Four Different Segmentations	25
2.5	Reactance vs Frequency for EF-TLA with Four Different Segmentations	26
2.6	Resistance vs Frequency for TLA with Three Different Feed Points	27
2.7	Reactance vs Frequency for TLA with Three Different Feed Points	28
2.8	Resistance vs Frequency for EF-TLA with Three Different Capacitive Loads	29
2.9	Reactance vs Frequency for EF-TLA with Three Different Capacitive Loads	30
2.10	Resistance vs Frequency for EF-TLA with Three Different Inductive Loads	31
2.11	Reactance vs Frequency for EF-TLA with Three Different Inductive Loads	32
2.12	Impedance Plot of EF-TLA from 4.0 - 6.9 MHz with 9 Segments and a 0.05 Meter Radius	33
2.13	E-Field Azimuth Pattern at 2 MHz for EF-TLA	34
2.14	E-Field Elevation Pattern at 2 MHz for EF-TLA	35
2.15	E-Field Azimuth Pattern at 5 MHz for EF-TLA	36
2.16	E-Field Elevation Pattern at 5 MHz for EF-TLA	37
2.17	E-Field Azimuth Pattern at 7 MHz for EF-TLA	38
2.18	E-Field Elevation Pattern at 7 MHz for EF-TLA	39
2.19	E-Field Azimuth Pattern at 10 MHz for EF-TLA	40
2.20	E-Field Elevation Pattern at 10 MHz for EF-TLA	41

2.21	E-Field Azimuth Pattern at 2 MHz for TF-TLA	42
2.22	E-Field Elevation Pattern at 2 MHz for TF-TLA	43
2.23	E-Field Azimuth Pattern at 6 MHz for TF-TLA	44
2.24	E-Field Elevation Pattern at 6 MHz for TF-TLA	45
2.25	E-Field Azimuth Pattern at 10 MHz for TF-TLA	46
2.26	E-Field Elevation Pattern at 10 MHz for TF-TLA	47
3.1	FFG-45 Frigate	48
3.2	Wire Grid Model of an FFG-45 Frigate without Antenna	49
3.3	Wire Grid Model of an FFG-45 Frigate with Antenna on the Bow	50
3.4	Wire Grid Model of an FFG-45 Frigate with Antenna on the Stern	51
3.5	Wire Grid Model of an FFG-45 Frigate with Antenna on the Bow and the Stern	52
3.6	Input Impedance vs Frequency for EF-TLA on the Bow	56
3.7	Input Impedance vs Frequency for EF-TLA on the Stern	57
3.8	Input Impedance vs Frequency for EF-TLA on the Bow and the Stern	58
3.9	Input Impedance vs Frequency for TF-TLA on the Bow	60
3.10	Input Impedance vs Frequency for TF-TLA on the Stern	61
3.11	Input Impedance vs Frequency for TF-TLA on the Bow and the Stern	62
3.12	Smith Chart Showing 3:1 VSWR Impedance Plot of EF-TLA : $Z_0 = 50$ Ohm	63
3.13	Smith Chart Showing 3:1 VSWR Impedance Plot of TF-TLA : $Z_0 = 50$ Ohm	64
3.14	Smith Chart Showing 3:1 VSWR Impedance Plot of EF-TLA : $Z_0 = 500$ Ohm	65
3.15	Smith Chart Showing 3:1 VSWR Impedance Plot of TF-TLA : $Z_0 = 500$ Ohm	66
3.16	E-Field Azimuth Pattern at 2.0 MHz for EF-TLA on the Bow and the Stern	68
3.17	E-Field Elevation Pattern at 2.0 MHz for EF-TLA on the Bow and the Stern	69
3.18	E-Field Azimuth Pattern at 4.5 MHz for EF-TLA on the Bow and the Stern	70
3.19	E-Field Elevation Pattern at 4.5 MHz for EF-TLA on the Bow and the Stern	71

3.20	E-Field Azimuth Pattern at 7.5 MHz for EF-TLA on the Bow and the Stern	72
3.21	E-Field Elevation Pattern at 7.5 MHz for EF-TLA on the Bow and the Stern	73
3.22	E-Field Azimuth Pattern at 10.0 MHz for EF-TLA on the Bow and the Stern	74
3.23	E-Field Elevation Pattern at 10.0 MHz for EF-TLA on the Bow and the Stern	75
3.24	E-Field Azimuth Pattern at 2.0 MHz for TF-TLA on the Bow and the Stern	76
3.25	E-Field Elevation Pattern at 2.0 MHz for TF-TLA on the Bow and the Stern	77
3.26	E-Field Azimuth Pattern at 4.5 MHz for TF-TLA on the Bow and the Stern	78
3.27	E-Field Elevation Pattern at 4.5 MHz for TF-TLA on the Bow and the Stern	79
3.28	E-Field Azimuth Pattern at 7.5 MHz for TF-TLA on the Bow and the Stern	80
3.29	E-Field Elevation Pattern at 7.5 MHz for TF-TLA on the Bow and the Stern	81
3.30	E-Field Azimuth Pattern at 10.0 MHz for TF-TLA on the Bow and the Stern	82
3.31	E-Field Elevation Pattern at 10.0 MHz for TF-TLA on the Bow and the Stern	83
D.1	E-Field Azimuth Pattern at 2 MHz for CEF-TLA	111
D.2	E-Field Elevation Pattern at 2 MHz for CEF-TLA	112
D.3	E-Field Azimuth Pattern at 5 MHz for CEF-TLA	113
D.4	E-Field Elevation Pattern at 5 MHz for CEF-TLA	114
D.5	E-Field Azimuth Pattern at 7 MHz for CEF-TLA	115
D.6	E-Field Elevation Pattern at 7 MHz for CEF-TLA	116
D.7	E-Field Azimuth Pattern at 10 MHz for CEF-TLA	117
D.8	E-Field Elevation Pattern at 10 MHz for CEF-TLA	118
E.1	E-Field Azimuth Pattern at 2.0 MHz for EF-TLA on the Bow	120
E.2	E-Field Elevation Pattern at 2.0 MHz for EF-TLA on the Bow	121
E.3	E-Field Azimuth Pattern at 2.0 MHz for EF-TLA on the Stern	122
E.4	E-Field Elevation Pattern at 2.0 MHz for EF-TLA on the Stern	123

E.5	E-Field Azimuth Pattern at 4.5 MHz for EF-TLA on the Bow	124
E.6	E-Field Elevation Pattern at 4.5 MHz for EF-TLA on the Bow	125
E.7	E-Field Azimuth Pattern at 4.5 MHz for EF-TLA on the Stern	126
E.8	E-Field Elevation Pattern at 4.5 MHz for EF-TLA on the Stern	127
E.9	E-Field Azimuth Pattern at 7.5 MHz for EF-TLA on the Bow	128
E.10	E-Field Elevation Pattern at 7.5 MHz for EF-TLA on the Bow	129
E.11	E-Field Azimuth Pattern at 7.5 MHz for EF-TLA on the Stern	130
E.12	E-Field Elevation Pattern at 7.5 MHz for EF-TLA on the Stern	131
E.13	E-Field Azimuth Pattern at 10.0 MHz for EF-TLA on the Bow	132
E.14	E-Field Elevation Pattern at 10.0 MHz for EF-TLA on the Bow	133
E.15	E-Field Azimuth Pattern at 10.0 MHz for EF-TLA on the Stern	134
E.16	E-Field Elevation Pattern at 10.0 MHz for EF-TLA on the Stern	135
E.17	E-Field Azimuth Pattern at 2.0 MHz for TF-TLA on the Bow	136
E.18	E-Field Elevation Pattern at 2.0 MHz for TF-TLA on the Bow	137
E.19	E-Field Azimuth Pattern at 2.0 MHz for TF-TLA on the Stern	138
E.20	E-Field Elevation Pattern at 2.0 MHz for TF-TLA on the Stern	139
E.21	E-Field Azimuth Pattern at 4.5 MHz for TF-TLA on the Bow	140
E.22	E-Field Elevation Pattern at 4.5 MHz for TF-TLA on the Bow	141
E.23	E-Field Azimuth Pattern at 4.5 MHz for TF-TLA on the Stern	142
E.24	E-Field Elevation Pattern at 4.5 MHz for TF-TLA on the Stern	143
E.25	E-Field Azimuth Pattern at 7.5 MHz for TF-TLA on the Bow	144
E.26	E-Field Elevation Pattern at 7.5 MHz for TF-TLA on the Bow	145
E.27	E-Field Azimuth Pattern at 7.5 MHz for TF-TLA on the Stern	146
E.28	E-Field Elevation Pattern at 7.5 MHz for TF-TLA on the Stern	147
E.29	E-Field Azimuth Pattern at 10.0 MHz for TF-TLA on the Bow	148
E.30	E-Field Elevation Pattern at 10.0 MHz for TF-TLA on the Bow	149
E.31	E-Field Azimuth Pattern at 10.0 MHz for TF-TLA on the Stern	150
E.32	E-Field Elevation Pattern at 10.0 MHz for TF-TLA on the Stern	151

ACKNOWLEDGEMENT

I thank GOD.

I would like to express my sincere appreciation to Dr. Richard W. Adler, my thesis advisor, for his assistance and guidance throughout this thesis and to Dr. H. A. Atwater, my second reader.

I thank my wife, Hyun Hee, my son, Young Kwang, and my daughter, Ju Ea, for their continuing support, understanding, and patient help throughout NPS.

Finally, I wish to thank the 40,000,000 Korean taxpayers for having paid for my course of studies.

I. INTRODUCTION

A. NEED FOR THE STUDY

Shipboard HF and VHF antennas tend to protrude from the ship's silhouette and are quite fragile. This implementation increases the ship's profile and causes the antennas to be vulnerable to gun fire and bomb blast. Should a HF/VHF antenna be destroyed or damaged by gun fire or bomb blast the ship would suffer a loss in its HF/VHF communication capability. A loss of HF/VHF communications would degrade its fighting ability. Therefore, a study of methods to make HF/VHF antennas more survivable is needed. The elimination of tall and large structures will make the antennas more survivable during combat.

There are many survivable antenna designs which may be investigated. One option might be to use a transmission line antenna on the bow and/or the stern of a ship. Another possible design might take the form of a telescoping antenna. These survivable antenna designs should be investigated.

B. TRANSMISSION LINE ANTENNA BACKGROUND

An early concept of a transmission line antenna was the Beverage antenna. This antenna utilized a terminating resistor as a load at the far end of a long wire to avoid both detuning and the high voltages which could result from resonances. If the line insulators can tolerate the high voltages, more current can be obtained by operating the line in a resonant mode and the terminating resistor can be eliminated as a source of power loss. The Beverage antenna, or wave antenna [Ref. 1], is a traveling-wave long wire operated in the presence of a lossy ground plane. A wave traveling outward from the feed point end toward the far end of the wire is reflected, setting up a standing-wave type current distribution. If the reflected wave is not present on the antenna it is referred to as a Traveling-wave antenna. A Traveling-wave antenna acts as a guiding structure for traveling waves, whereas a resonant antenna supports standing waves. Traveling waves can be created by using matched loads at the ends to prevent reflections. Also, very long antennas will radiate most of the power, leading to small reflected waves by virtue of the fact that very little power is incident on the ends.

In Figure 1.1, an example of the implementation of a transmission line antenna is shown being fed from a coaxial transmission line. A transmission line antenna can be

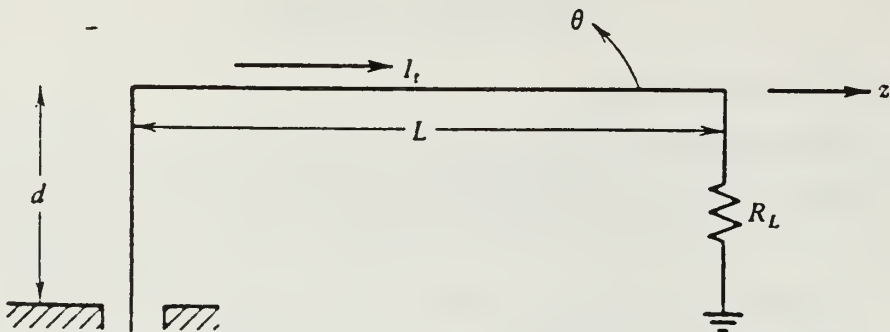


Figure 1.1 Transmission Line Antenna.

considered a rectangular loop antenna with current going out on the transmission line wires and returning to the ground at the far end.

C. SCOPE AND LIMITATION

This study is an investigation of the performance of a transmission line deployed over perfect ground, on the bow and the stern of an FFG-45 frigate, created by a wire grid model and using a special computer program called NEC - Numerical Electromagnetic Code [Ref. 2]. Understanding of linear antennas has been advanced since the late 1960's by the introduction of the METHOD OF MOMENTS into electromagnetic system analysis. Versatile computer codes based on this method, like NEC, allow very complex antenna systems to be analyzed, a task which is impossible via analytical methods.

The transmission line antenna is derived from its functional relationship to that of a shorted transmission line. This antenna is a transmission line with a ground at one end and a feed from the other end. The basic concept of this approach is that the transmission line is attached on the bow and the stern of a ship. The frequency range of the investigation is limited to 2-10 MHz. As frequency increases, the wavelength decreases, and the object size in wavelengths increases. This limitation is imposed by computer storage and time restraints.

This thesis begins with a discussion of a transmission line antenna numerical model and presents the computed results. Next, a description of the FFG-45 frigate

computer model used for this study is presented with results. This will form the basis for the conclusions and recommendations. Finally the appendices include the simulation data such as geometry cards for each model, average power gain, input impedance, and radiation patterns.

II. TRANSMISSION LINE ANTENNA COMPUTER MODEL AND RESULTS

This chapter presents the transmission line antenna computer models used in this thesis. The models are transmission lines with dimensions 13.5 x 0.6 meters and were run over a perfect ground.

A. TRANSMISSION LINE ANTENNA COMPUTER MODEL

In the simplest configuration, a transmission line antenna (hereafter referred to as "TLA") can be considered a rectangular loop antenna with current running on the transmission line wire and returning to the ground at the far end. A 13.5 x 0.6 meter transmission line above a perfect ground, Figure 2.1, was modeled as a 0.05 meter radius wire over the frequency range 2 - 10 MHz.

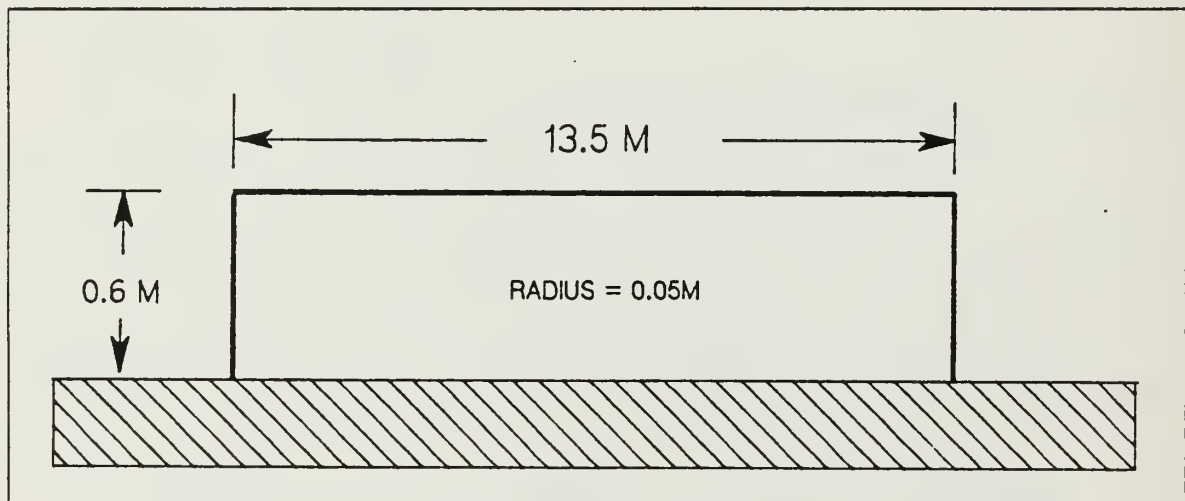


Figure 2.1 Transmission Line Antenna Dimensions.

The important design considerations required to develop this computer model were the segmentation size, the radii of the segments, and the proper geometrical model. Wire segments were modeled in NEC such that both geometric and electrical factors were involved. Segments, which were defined by coordinates of their end points, should follow the paths of conductors as closely as possible. Only axial currents were considered and there was no allowance for circumferential variation of the current. The accuracy of the mathematical solution depended on many constraints which

formed the following electrical considerations for single wire segments or wire-grid models of conducting surfaces: [Ref. 3: pp. 3-6]

- (a) The segment length Δ relative to a wavelength λ is a key parameter.
 - Δ should be less than 0.1λ for accurate results in most cases.
 - Δ should be less than 0.05λ in critical regions.
 - Δ could be less than 0.2λ on long, straight segments.
 - Δ should not be less than $10^{-4} \lambda$.
- (b) The radius a should be small relative to both λ and Δ .
 - a should be less than 0.5Δ .
 - a should be less than 0.1λ .
- (c) The user should avoid large changes in the radius, especially in short segments, and also avoid sharp bends in thick segments.
- (d) Wires that are connected must contact at segment ends. If the separation of two segment ends is less than 10^{-3} times the length of the shortest segment, then they are considered connected.
- (e) Segments before and after the segment on which a voltage source is applied should be equal in length and radius. When the source is at the base of a segment connected to a ground plane, this segment should be vertical.
- (f) The more segments used in a wire grid to model a solid structure, the more accurate the solution due to the avoidance of high inductances normally present in sparse grids.
- (g) The segments on either sides of the excitation source should be parallel and have the same lengths and radii.

B. COMPUTER MODEL RESULTS

1. Average Power Gain

Average power gain was obtained by integrating the radiated power and comparing that to the total input power at the feed points. These should be equal for a valid solution. An average power gain of 2.0 was used to represent a theoretical antenna radiating in a half space over a perfect ground. A common criterion applied to antenna computer models is to calculate the accuracy of the model with average power gain.

Table 1 lists the calculated average power gains for three different radii of the 9 segment transmission line antenna in the frequency range 2 - 10 MHz. The wire radius, a , was limited in that the relationship $2\pi a/\lambda << 1$ must hold. The 0.03 and 0.04 meter radii have the same gain as the 0.05 meter radius in the frequency range 2 - 9 MHz but differ by an insignificant amount at the 10 MHz.

TABLE 1
AVERAGE POWER GAIN FOR TLA
WITH THREE DIFFERENT WIRE RADII

Frequency in MHz	$r = 0.03$	$r = 0.04$	$r = 0.05$
2	1.99	1.99	1.99
3	1.99	1.99	1.99
4	1.99	1.99	1.99
5	1.99	1.99	1.99
6	1.99	1.99	1.99
7	1.99	1.99	1.99
8	1.99	1.99	1.99
9	1.99	1.99	1.99
10	2.00	2.00	1.99

Table 2 lists the calculated average power gains for four different numbers of segments of the transmission line antenna in the frequency range 2 - 10 MHz. For wire modeling, the main electrical consideration was segment length, Δ , relative to the wavelength, λ , and Δ should be less than approximately 0.1λ at the desired frequency. The smaller number of segments show slightly high average gain at low frequencies, and the larger number of segments show slightly higher gain at high frequencies. The average gain of the 9 segment was slightly better than that of 5, 15, and 21 segments.

Table 3 lists the calculated average power gains for three different feed points of the transmission line antenna in the frequency range 2 - 10 MHz. The end feed is located at the end of one side of the transmission line with a segment length of 0.6 meters (hereafter referred to as "EF-TLA"), the center end feed is located at the center

TABLE 2
AVERAGE POWER GAIN FOR TLA
WITH FOUR DIFFERENT SEGMENTATIONS

Frequency in MHz	5 segment	9 segment	15 segment	21 segment
2	2.04	1.99	1.97	1.96
3	2.03	1.99	1.97	1.96
4	2.02	1.99	1.97	1.97
5	2.01	1.99	1.97	1.97
6	2.00	1.99	1.98	1.97
7	1.99	1.99	1.98	1.98
8	1.99	1.99	1.99	1.98
9	1.99	1.99	1.99	1.99
10	1.99	1.99	2.00	2.00

of one side of the transmission line with a segment length of 0.2 meters ("CEF-TLA"), and the top feed is located at the center of the upper transmission line with a segment length of 0.71 meters ("TF-TLA"). As frequency increased, the average power gain of the CEF-TLA decreased. The TF-TLA had slightly high average power gain over the entire frequency range.

There are three tables listing the three different average power gains in Appendix B. Table B.1 lists the calculated average power gain for three different terminating capacitors of the 9 segment transmission line antenna, with the capacitor at the far end of the transmission line in the frequency range 2 - 10 MHz. The low capacitance loads produced low gain at high frequencies.

Table B.2 lists the calculated average power gain for three different terminating inductors for the 9 segment transmission line antenna, with the inductor at

TABLE 3
AVERAGE POWER GAIN FOR TLA
WITH THREE DIFFERENT FEED POINTS

Frequency in MHz	EF-TLA	CEF-TLA	TF-TLA
2	1.99	1.98	2.05
3	1.99	1.97	2.05
4	1.99	1.96	2.05
5	1.99	1.94	2.05
6	1.99	1.92	2.05
7	1.99	1.90	2.06
8	1.99	1.88	2.06
9	1.99	1.87	2.06
10	1.99	1.86	2.06

the far end of the transmission line in the frequency range 2 - 10 MHz. The inductors of 10^{-2} and 10^{-4} Henry had low gain at high frequencies.

Table B.3 lists the calculated average power gain for the 9 segment transmission line antenna with a short at the far end in the frequency range 4.0 - 6.9 MHz. The average power gain had almost the theoretical value over the entire range of frequencies.

2. Input Impedance

The input impedance is illustrated on two different curves, one for resistance (R), and the other for reactance (JX). Figures 2.2 - 2.12 are plots of input resistance and reactance versus frequency.

Figures 2.2 - 2.3 show the resistance and reactance of a wire versus frequency. The graphs show that the thickness of the wire had negligible effect on the resistance,

however, it did reduce values of reactance. Therefore, the thick wire was more acceptable than the thin wire.

Figures 2.4 - 2.5 show the same resistance for different segment numbers over the entire frequency range, however, the reactance increased as the segment number increased. High reactance was noted in 5 - 6 MHz range.

In Figures 2.6 - 2.7, the CEF-TLA displayed slightly higher resistance and reactance over the entire frequency range. The TF-TLA had increased resistance and reactance as the frequency increased. The EF-TLA and the CEF-TLA had the highest resistance and reactance at 5 MHz, and the TF-TLA had the highest resistance and reactance at 10 MHz.

Figures 2.8 - 2.9 show that the resistance decreased as the termination capacitance decreased. A capacitance of 10^{-12} Farads produced high input resistance at 10 MHz.

Figures 2.10 - 2.11 show that the resistance increased for termination inductances of 10^{-2} and 10^{-4} Henry. The inductance of 10^{-6} Henry had no change in resistance and reactance when compared to the EF-TLA case.

Figure 2.12 shows the resistance increased at 5.3 MHz. Above 5.3 MHz the resistance decreased. Reactance increased to 5.2 MHz, with the highest value at 5.3 MHz.

Figures 2.2 - 2.12 show that resistance was low and reactance was high except for very low load capacitance and inductance. Reactance could be reduced by using capacitance or inductance but resistances were very low. Particularly in the 5.0 - 5.5 MHz range, resistances were high and reactances were very high. Input impedance data are shown in Appendix C.

3. Radiation Patterns

Radiation patterns for the transmission line antenna computer model with 3 different feed points were obtained in the frequency range 2 - 10 MHz. For the EF-TLA and the CEF-TLA, the radiation patterns had almost the same azimuth and elevation patterns over the entire frequency range. Figures 2.13 - 2.20 show that for the EF-TLA, the azimuth patterns became omnidirectional at 5 and 6 MHz. At 2 MHz, the azimuth pattern had nulls at the side (like a figure eight). These side nulls filled in as frequency increased. At frequencies over 6 MHz, the azimuth patterns had decreasing front and back lobes. At 10 MHz, the pattern was a figure eight with nulls front and back and lobes to the sides. With increasing frequency, the elevation

patterns became less lobing near the vertical. The CEF-TLA case is shown in Appendix D.

Figures 2.21 - 2.28 show the TF-TLA case. The azimuth and elevation radiation patterns looked the same with a slight change in the lobe pattern over the entire frequency range. The azimuth patterns had less lobing near the side like a figure eight and the elevation patterns had almost the same 5 dBI in the entire frequency range but with a slightly smaller vertical size at the high frequency. The TF-TLA displayed a stable pattern in 2-10 MHz range.

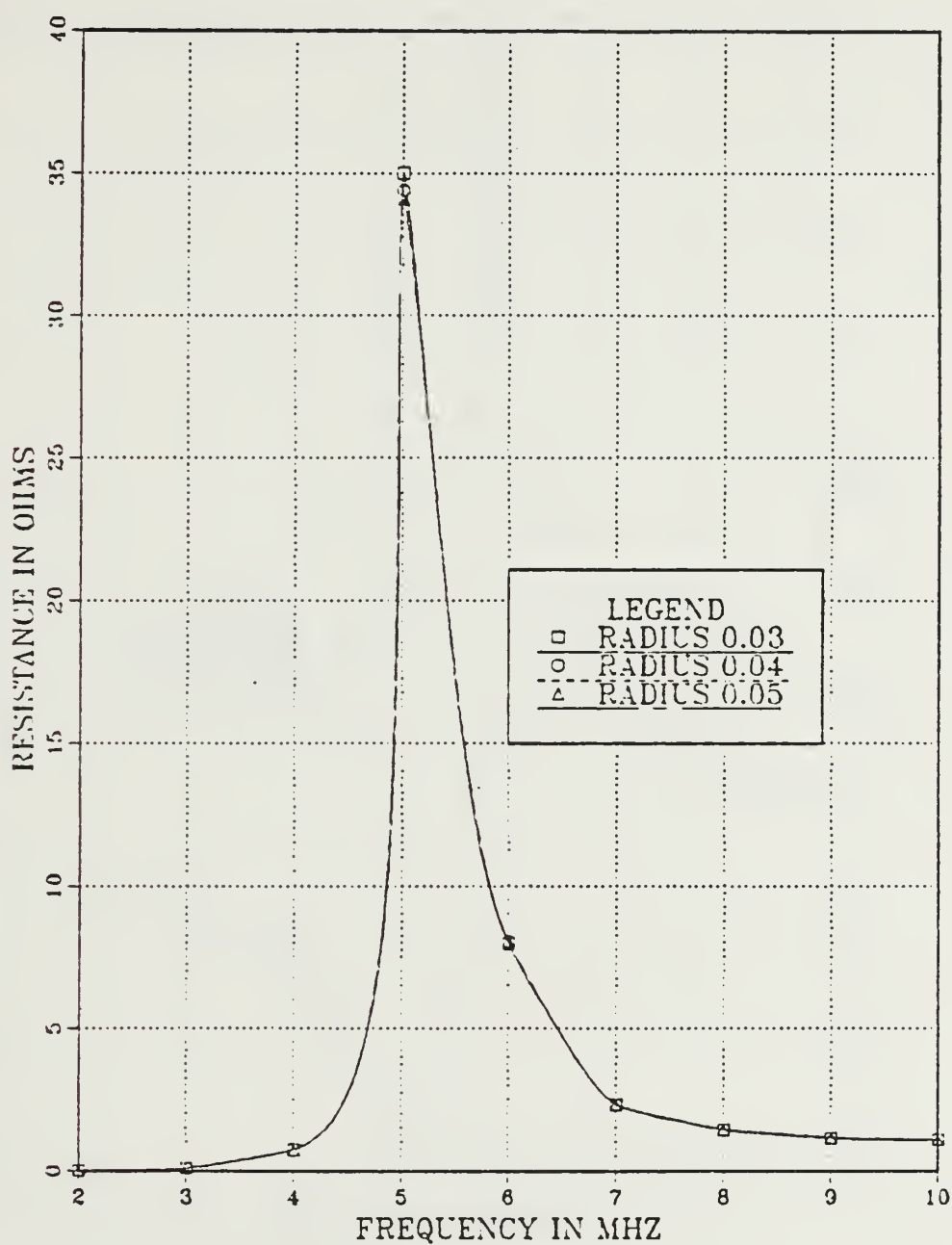


Figure 2.2 Resistance vs Frequency for a 9 Segment EF-TLA with Three Different Wire Radii.

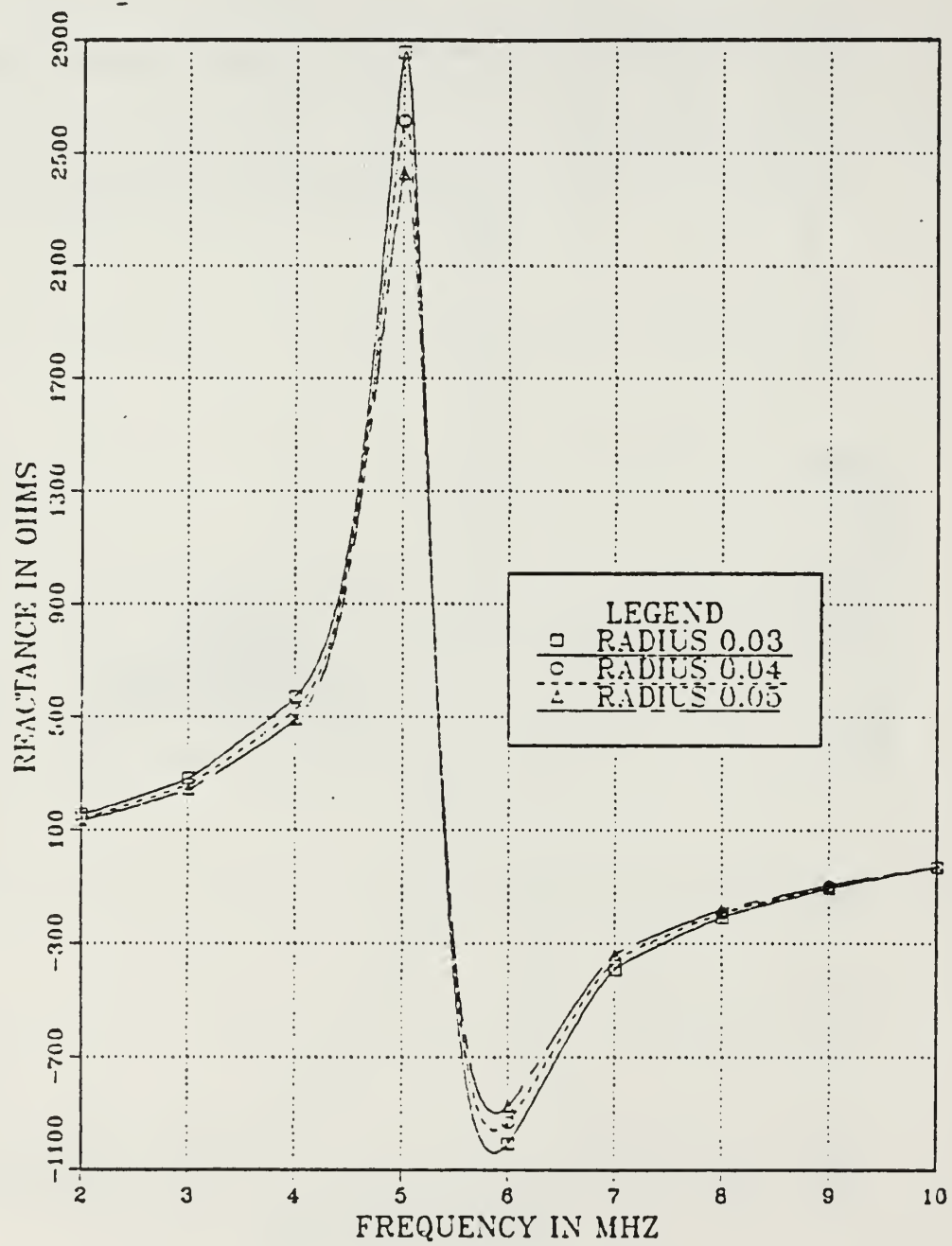


Figure 2.3 Reactance vs Frequency for a 9 Segment EF-TLA with Three Different Wire Radii.

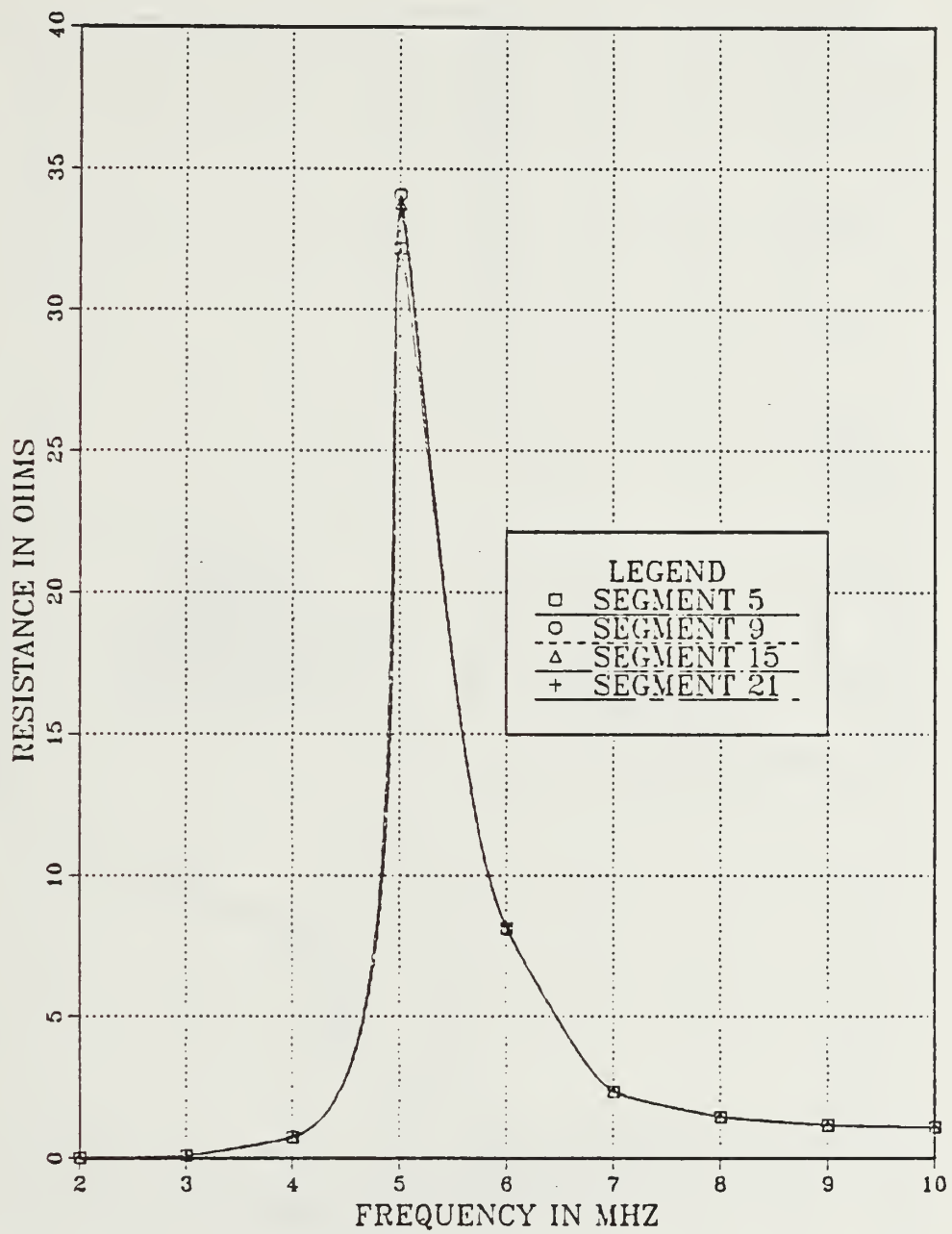


Figure 2.4 Resistance vs Frequency for EF-TLA with Four Different Segmentations.

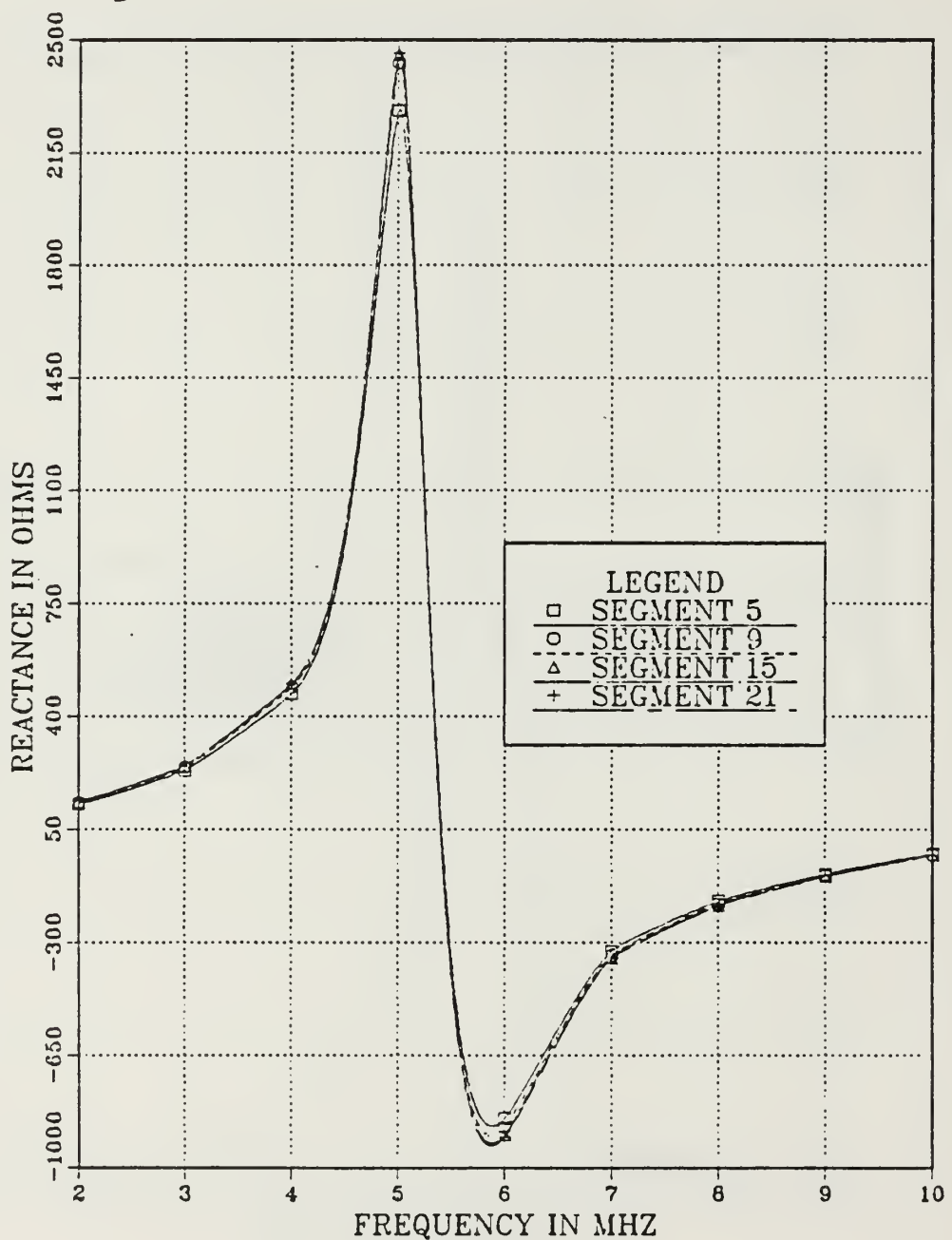


Figure 2.5 Reactance vs Frequency for EF-TLA
with Four Different Segmentations.

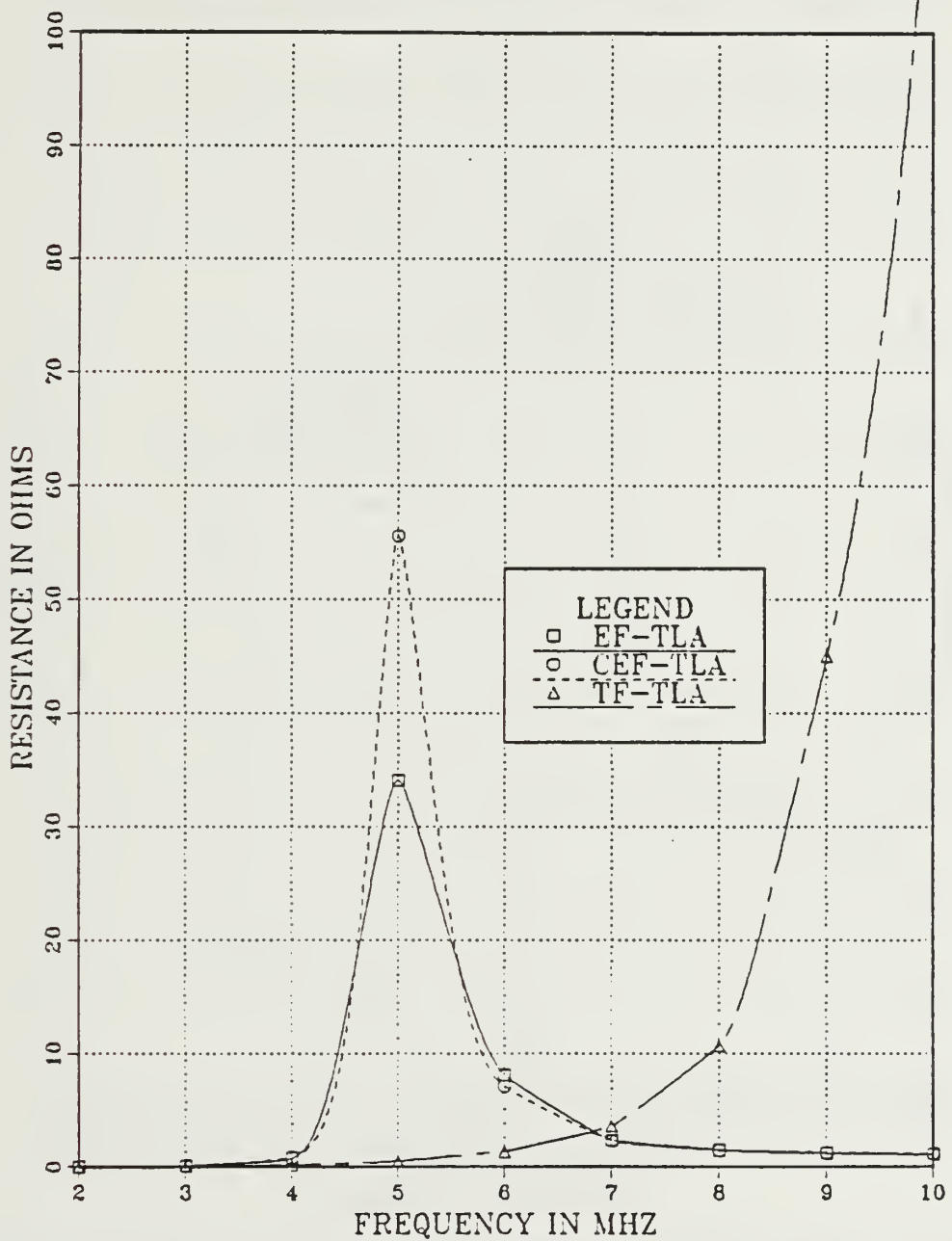


Figure 2.6 Resistance vs Frequency for TLA
with Three Different Feed Points.

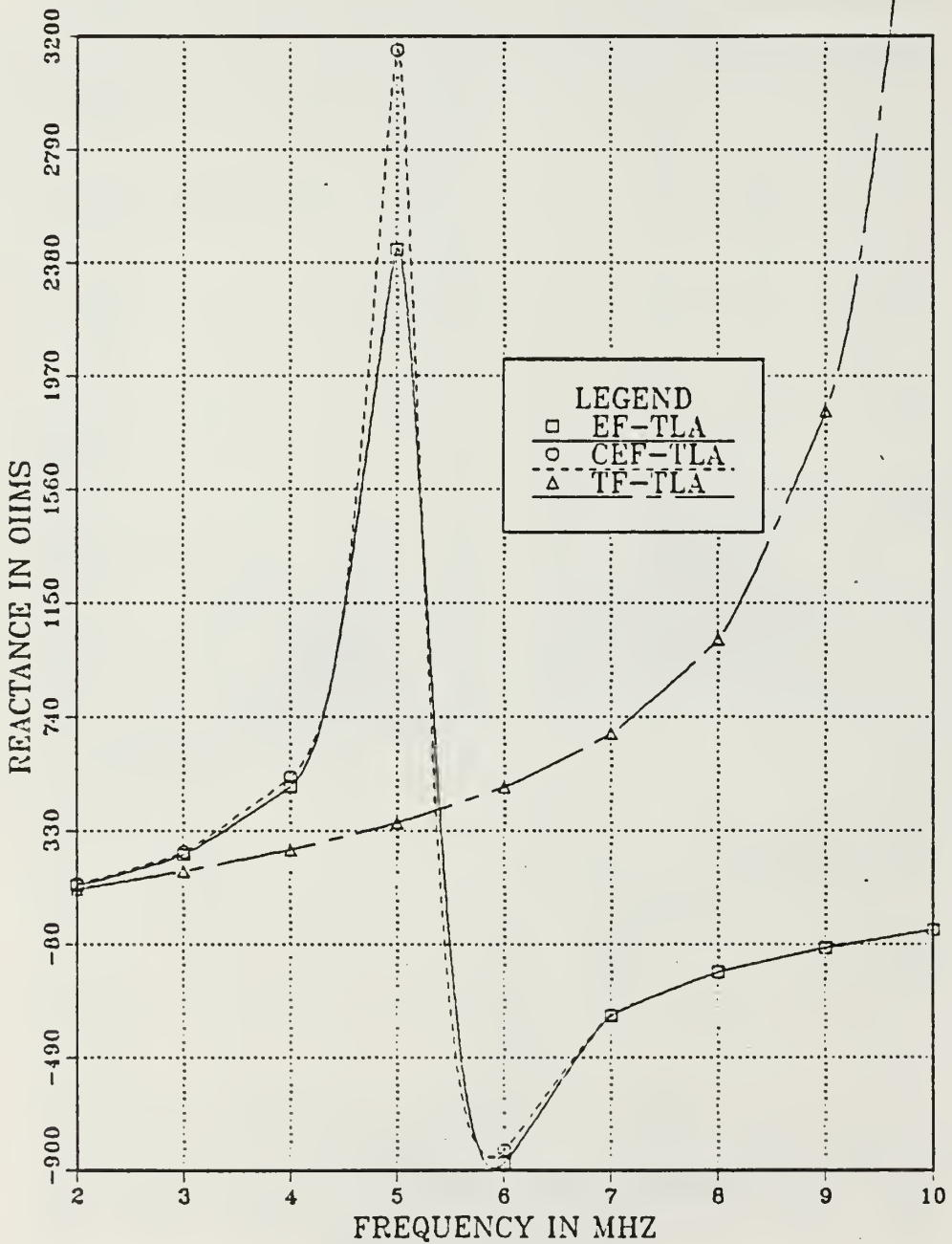


Figure 2.7 Reactance vs Frequency for TLA
with Three Different Feed Points.

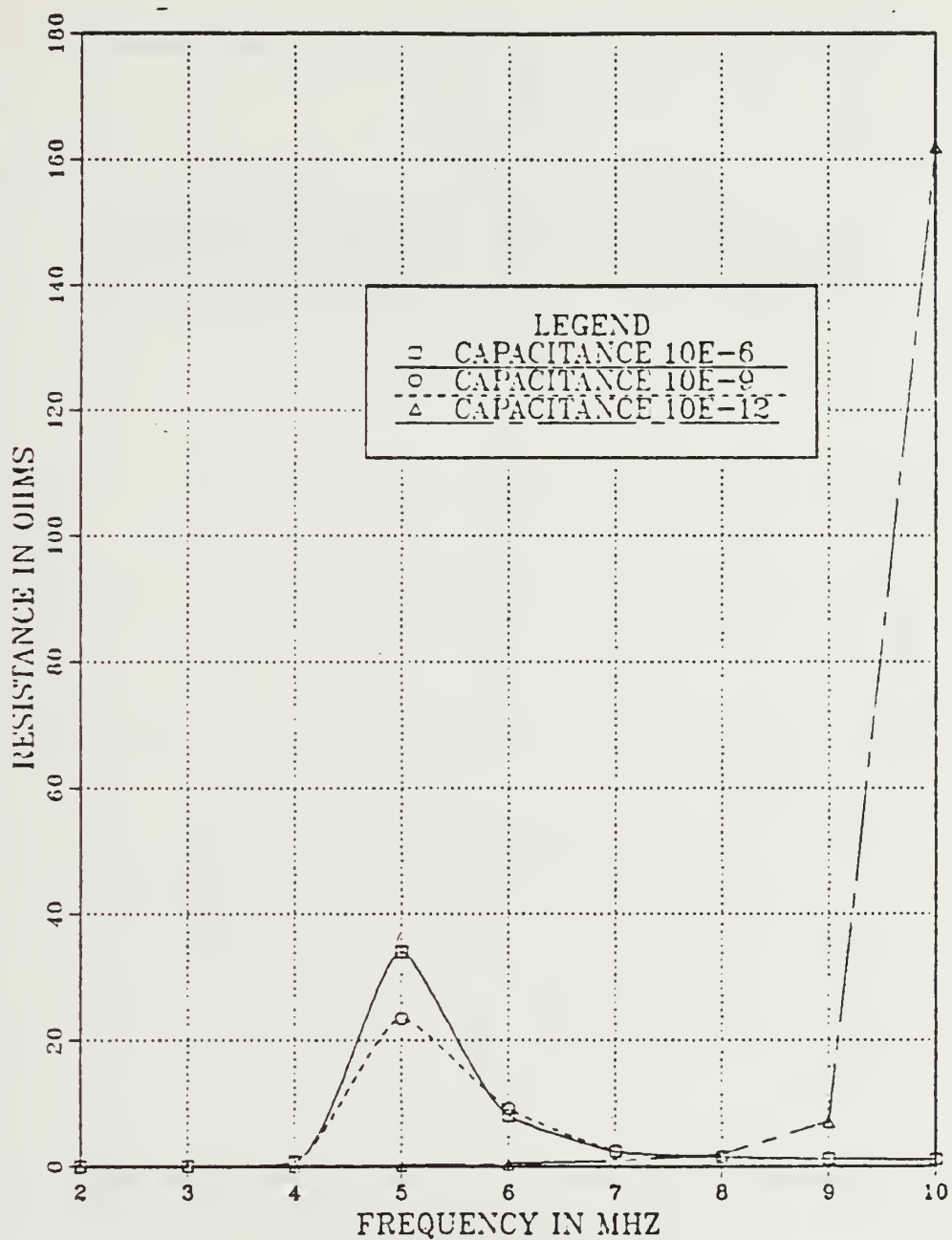


Figure 2.8 Resistance vs Frequency for EF-TLA with Three Different Capacitive Loads.

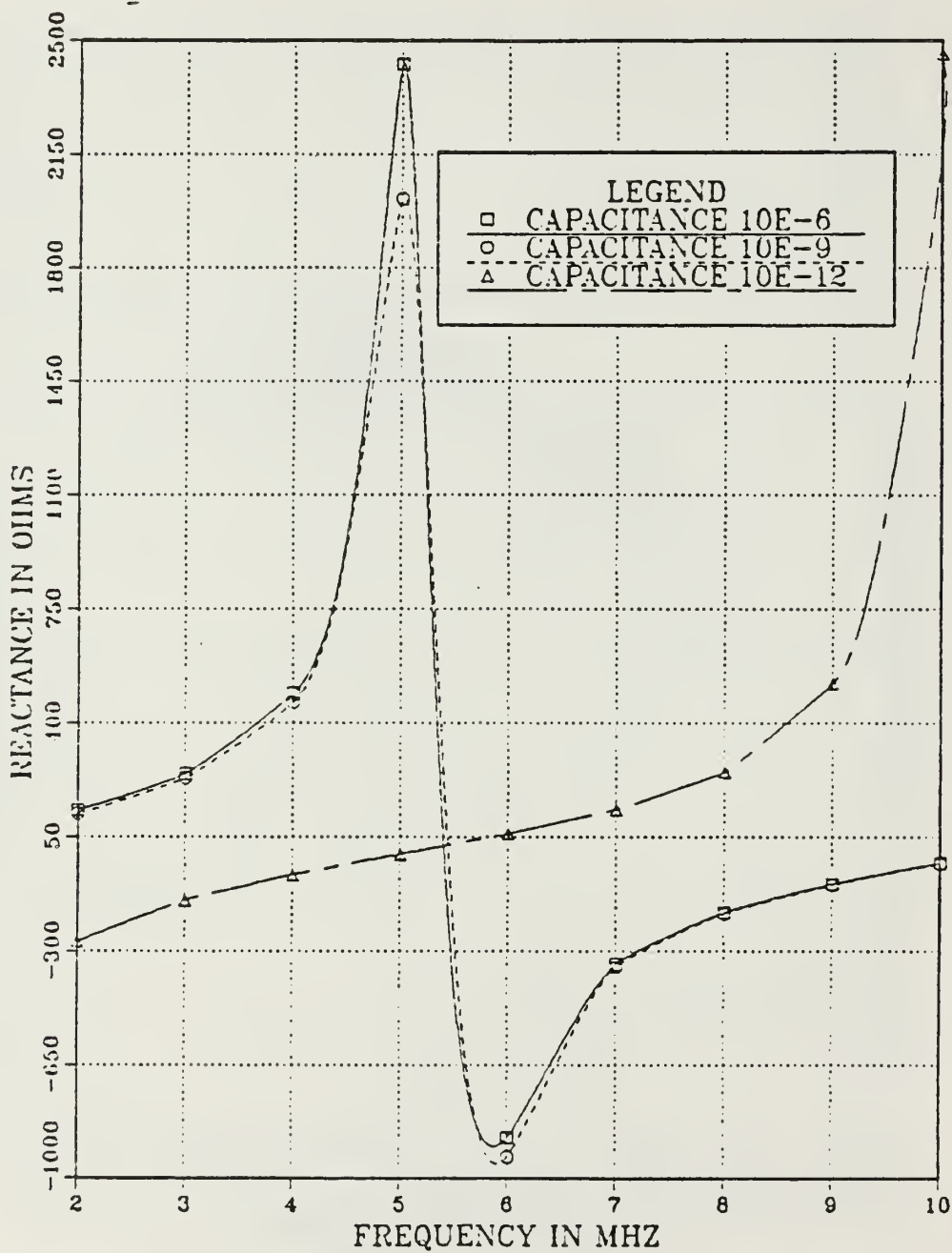


Figure 2.9 Reactance vs Frequency for EF-TLA
with Three Different Capacitive Loads.

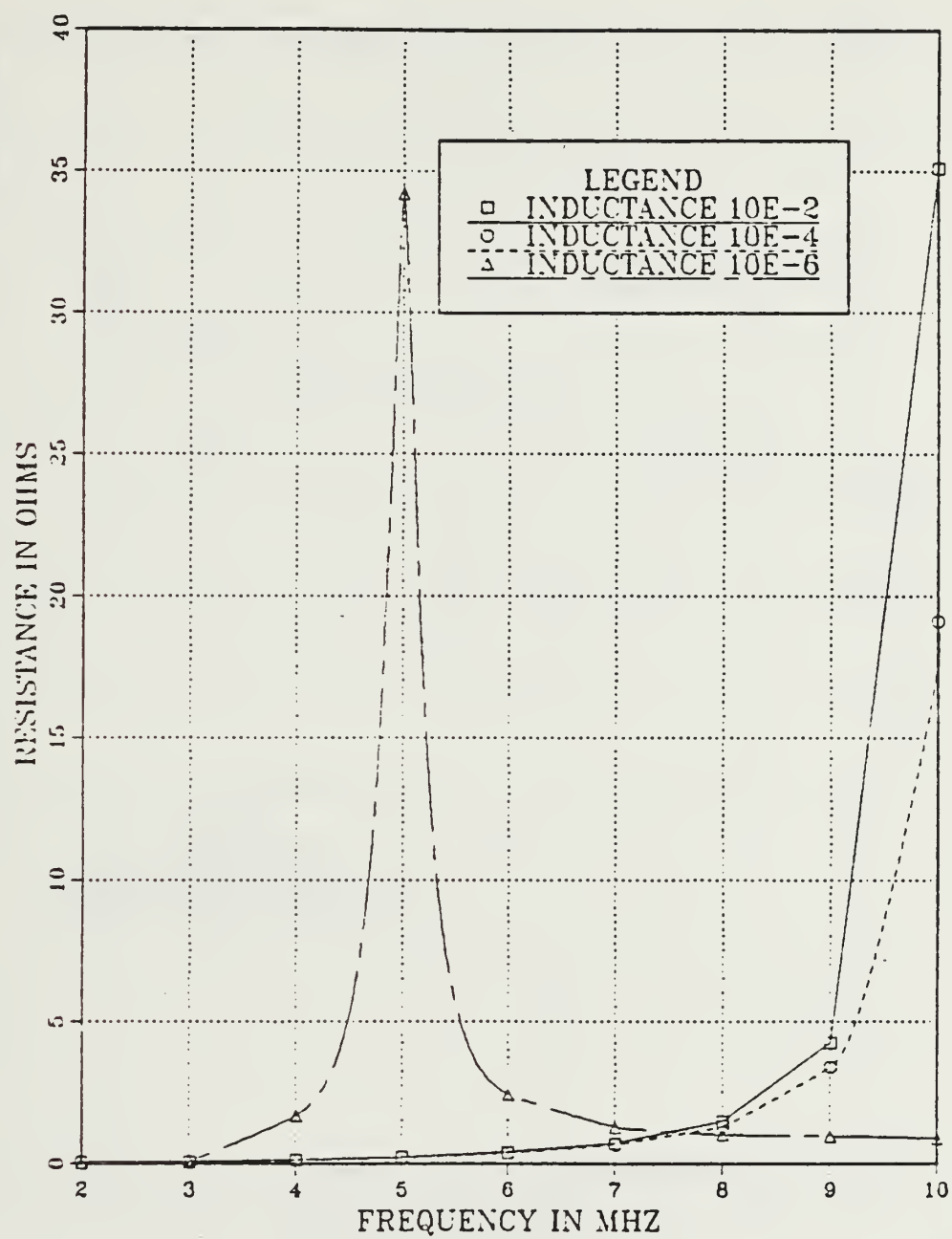


Figure 2.10 Resistance vs Frequency for EF-TLA with Three Different Inductive Loads.

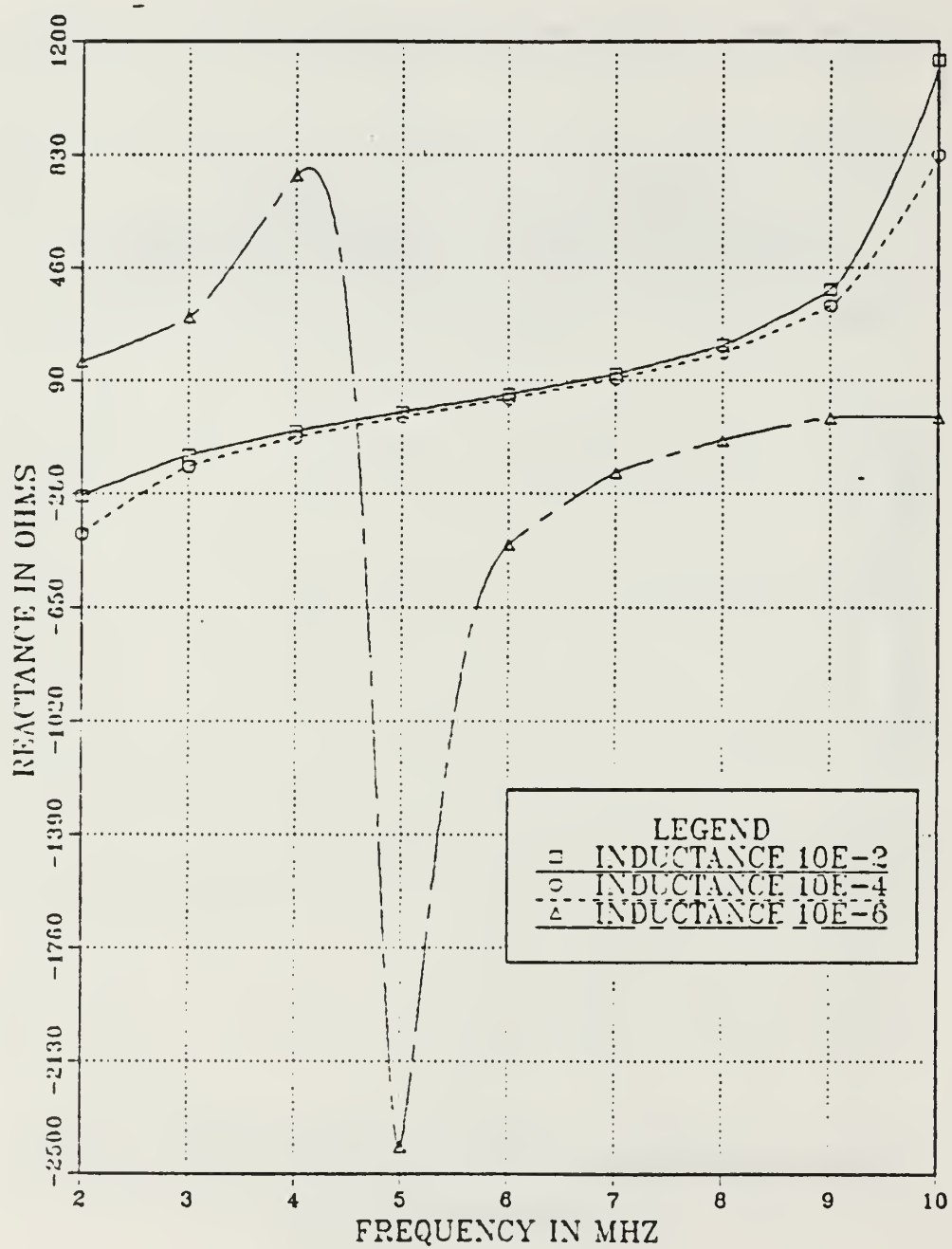


Figure 2.11 Reactance vs Frequency for EF-TLA with Three Different Inductive Loads.

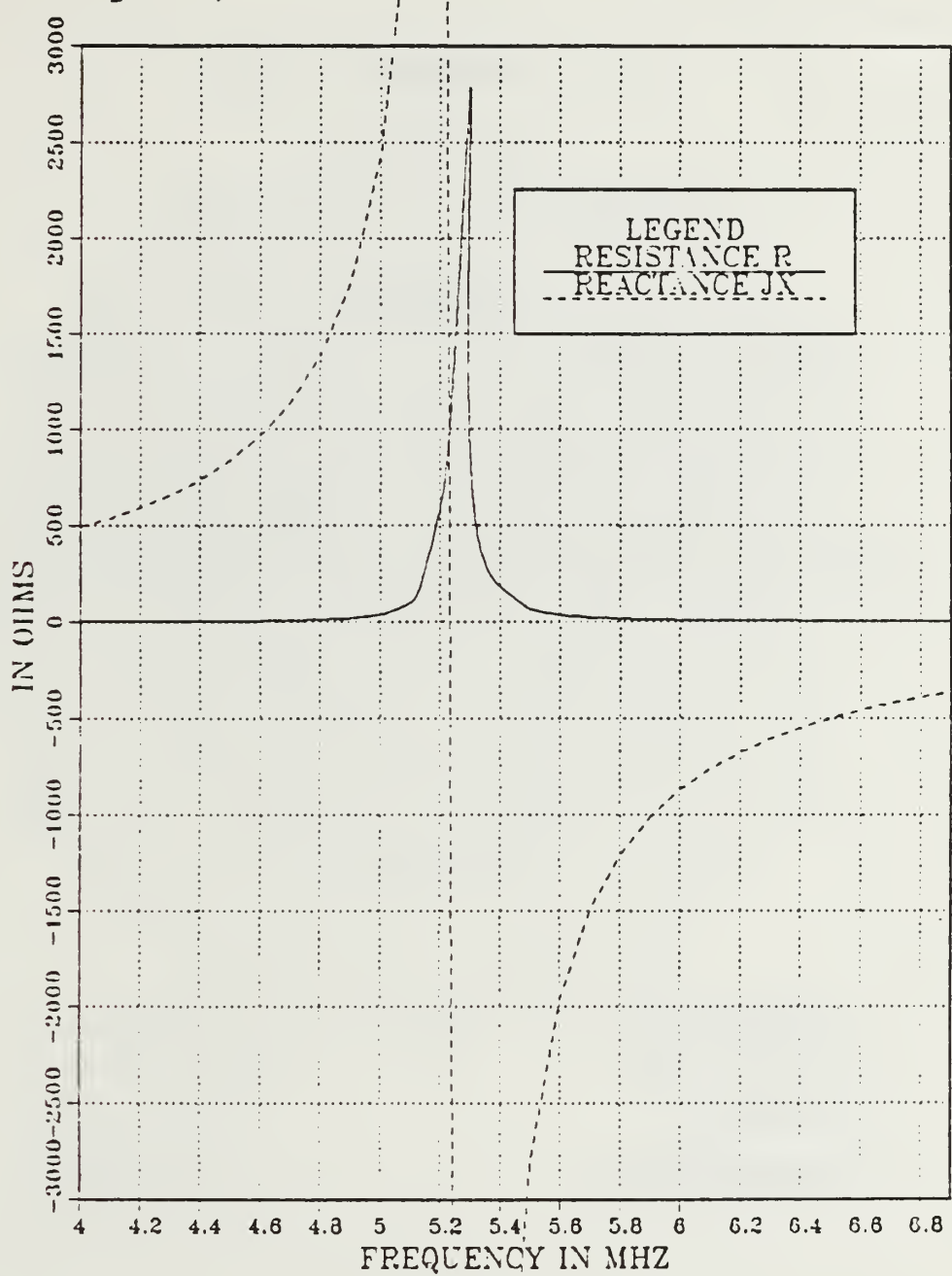


Figure 2.12 Impedance Plot of EF-TLA from 4.0 - 6.9 MHz with 9 Segments and a 0.05 Meter Radius.

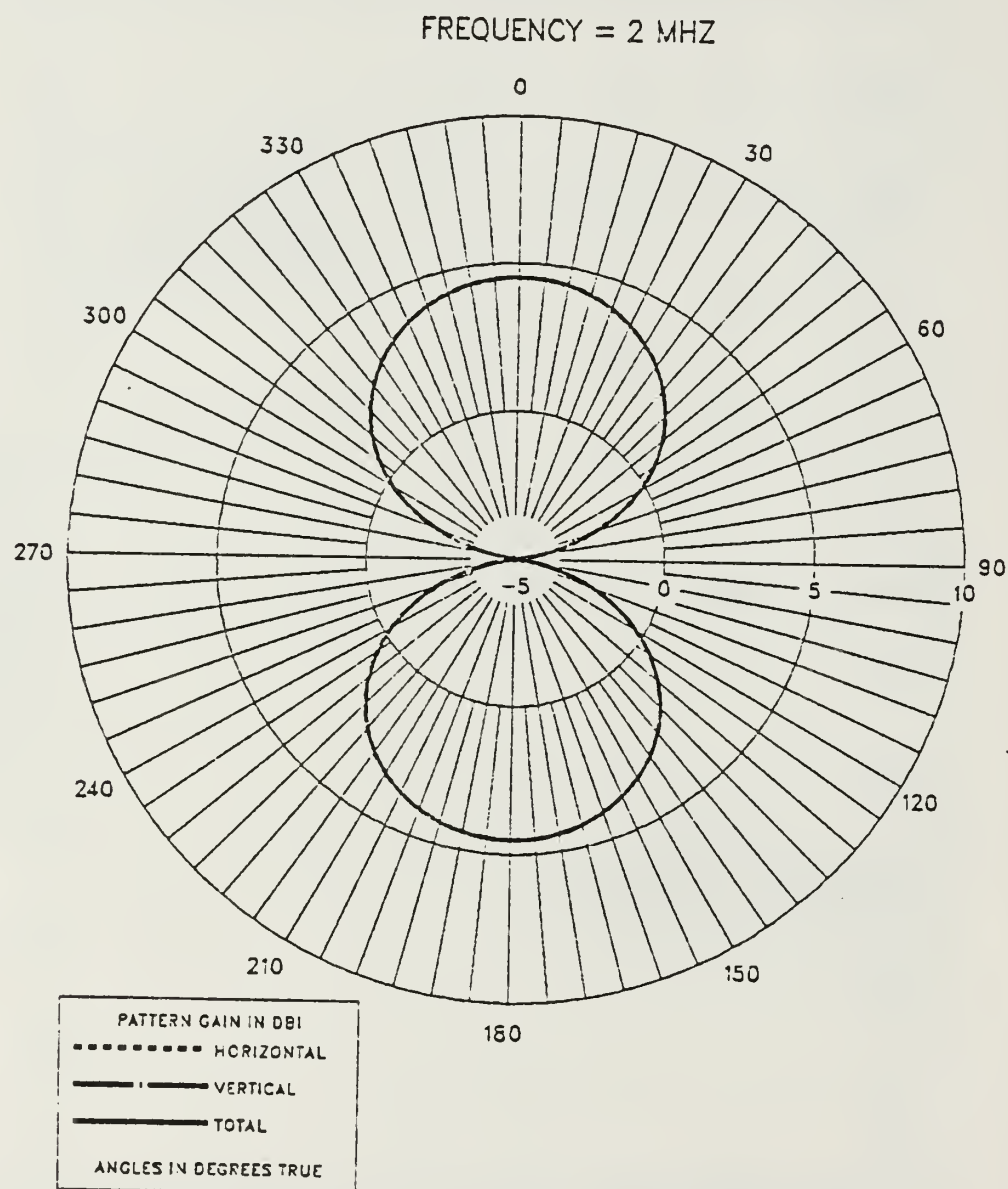


Figure 2.13 E-Field Azimuth Pattern at 2 MHz for EF-TLA.

FREQUENCY = 2 MHZ

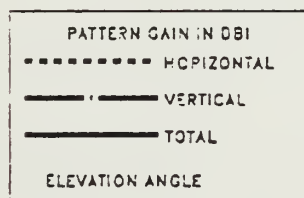
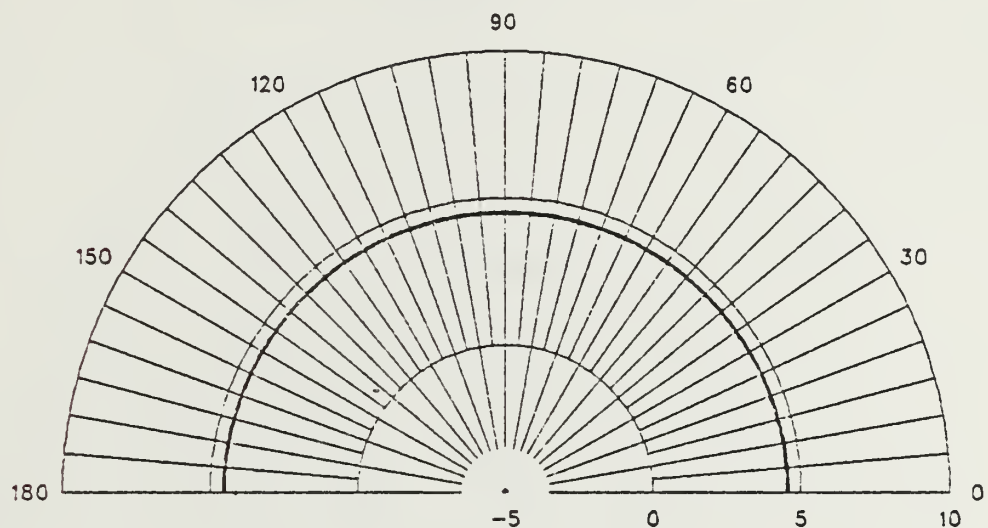


Figure 2.14 E-Field Elevation Pattern at 2 MHz for EF-TLA.

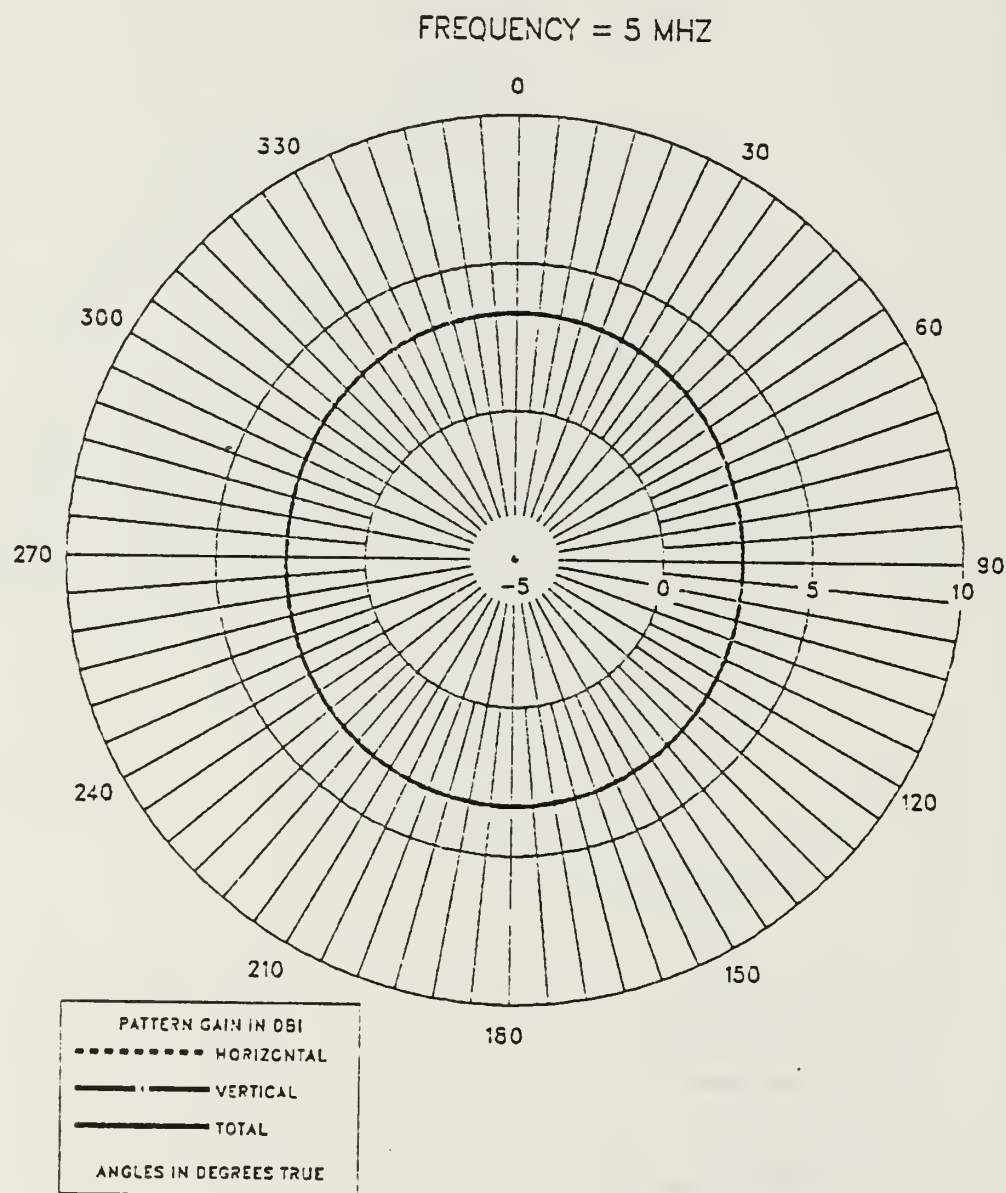


Figure 2.15 E-Field Azimuth Pattern at 5 MHz for EF-TLA.

FREQUENCY = 5 MHZ

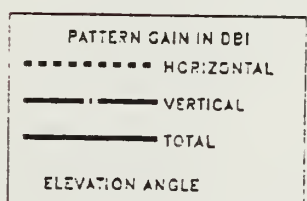
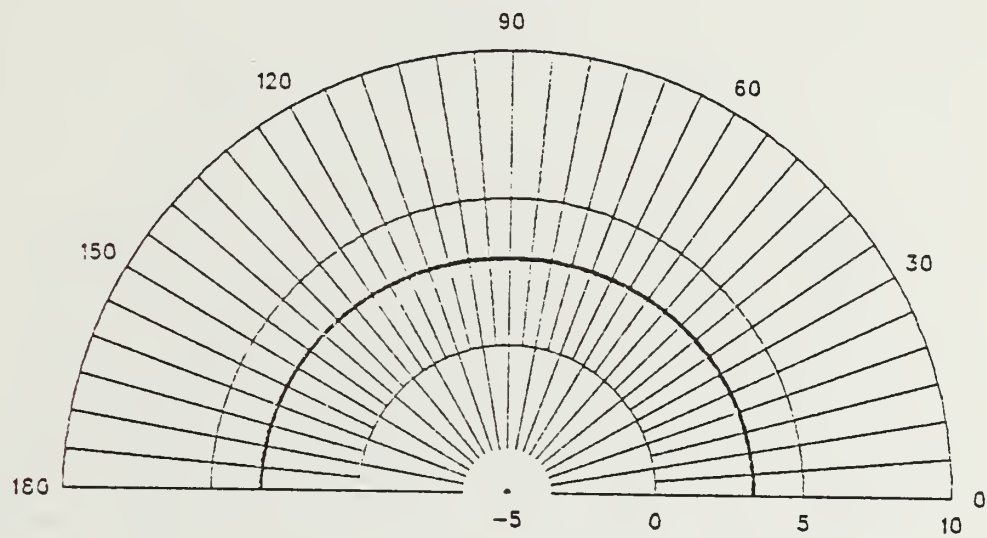


Figure 2.16 E-Field Elevation Pattern at 5 MHz for EF-TLA.

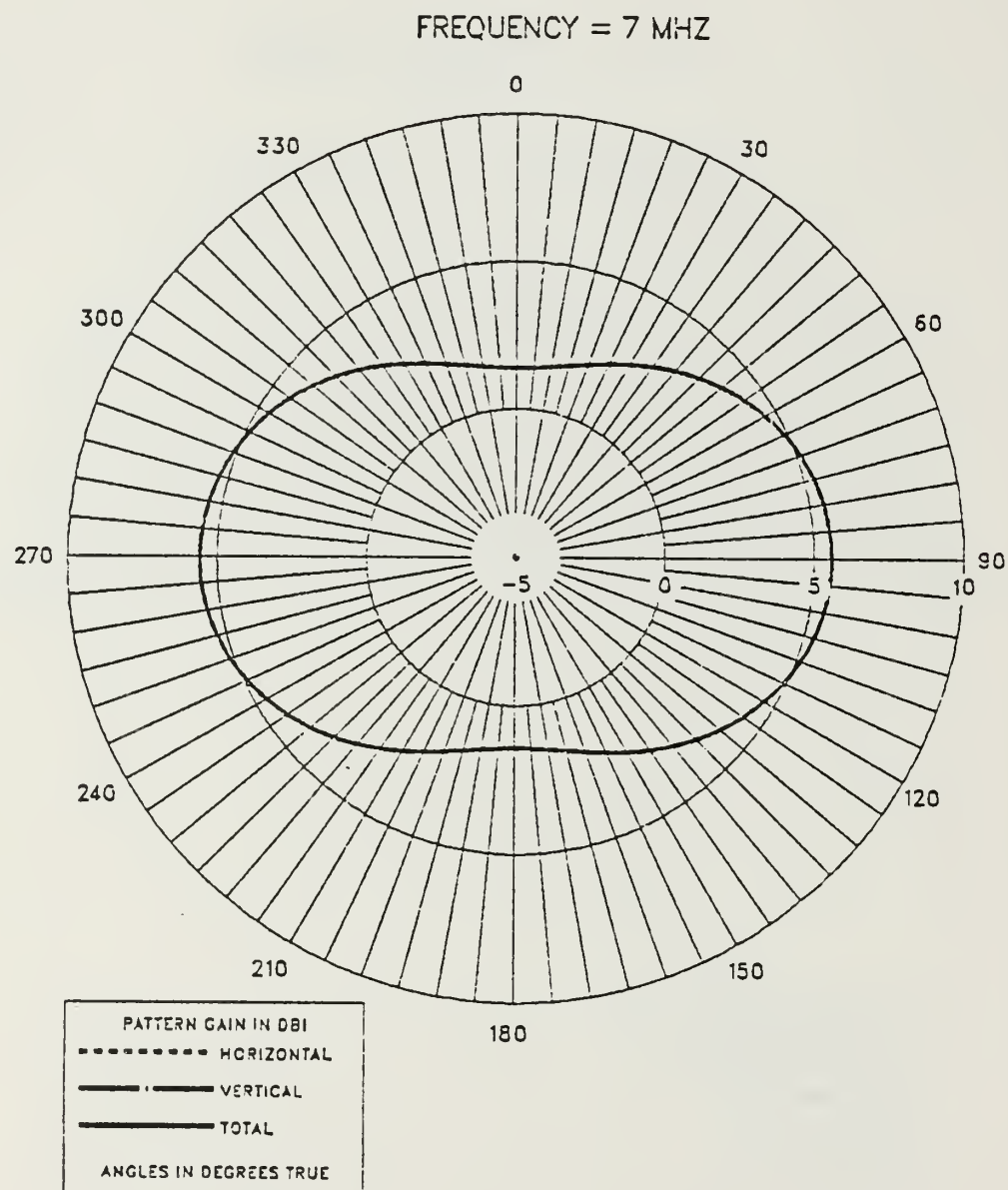


Figure 2.17 E-Field Azimuth Pattern at 7 MHz for EF-TLA.

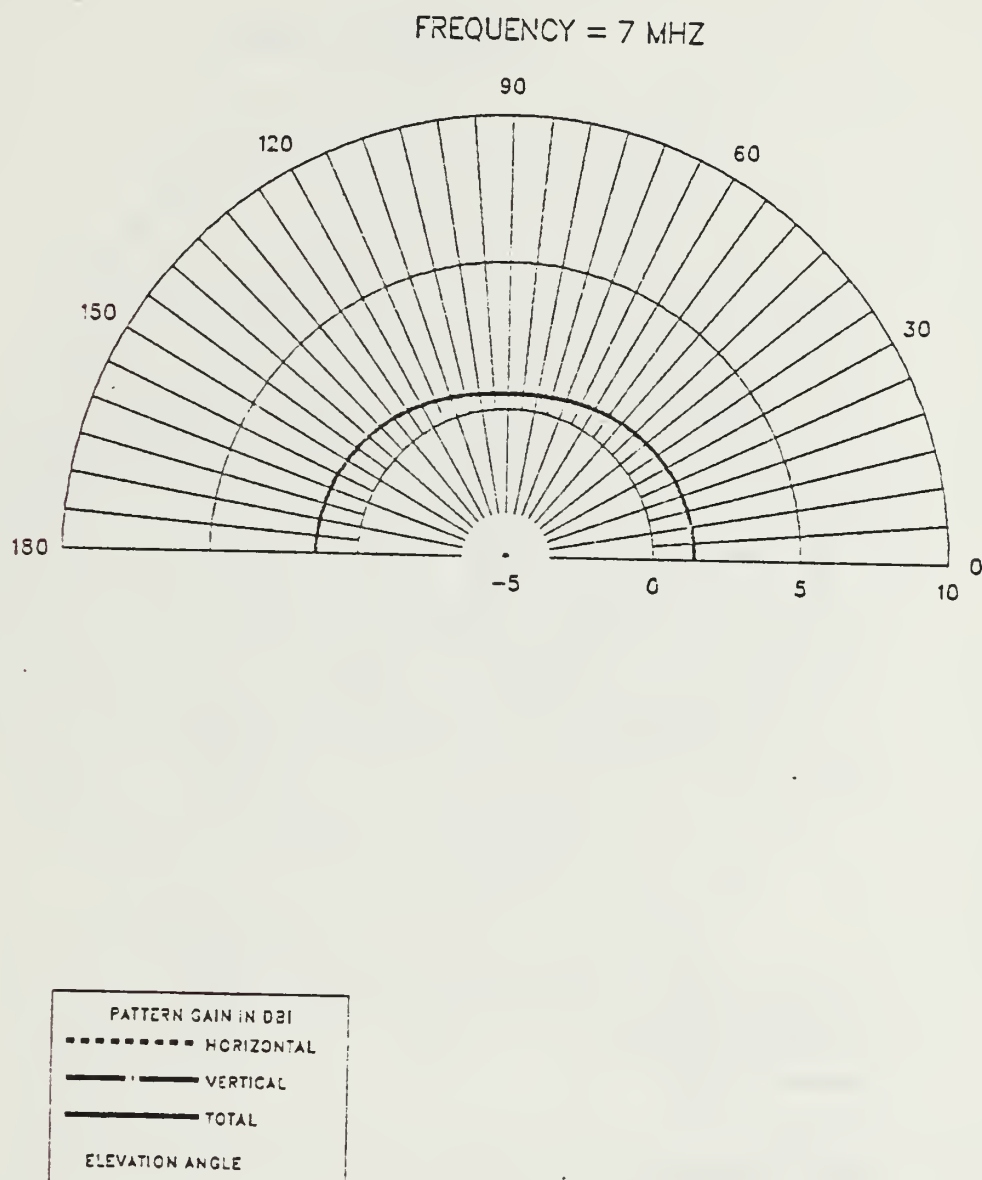


Figure 2.18 E-Field Elevation Pattern at 7 MHz for EF-TLA.

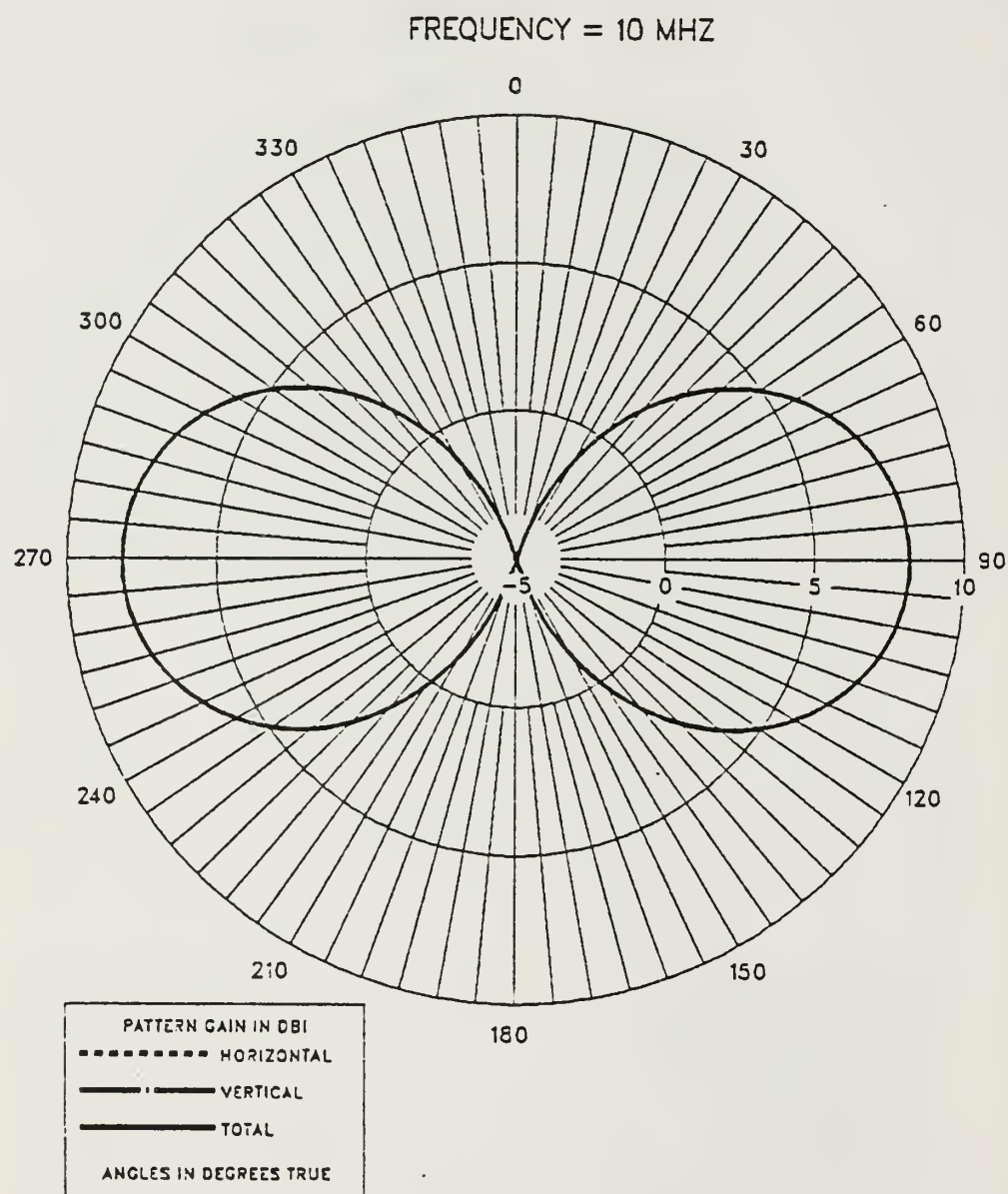


Figure 2.19 E-Field Azimuth Pattern at 10 MHz for EF-TLA.

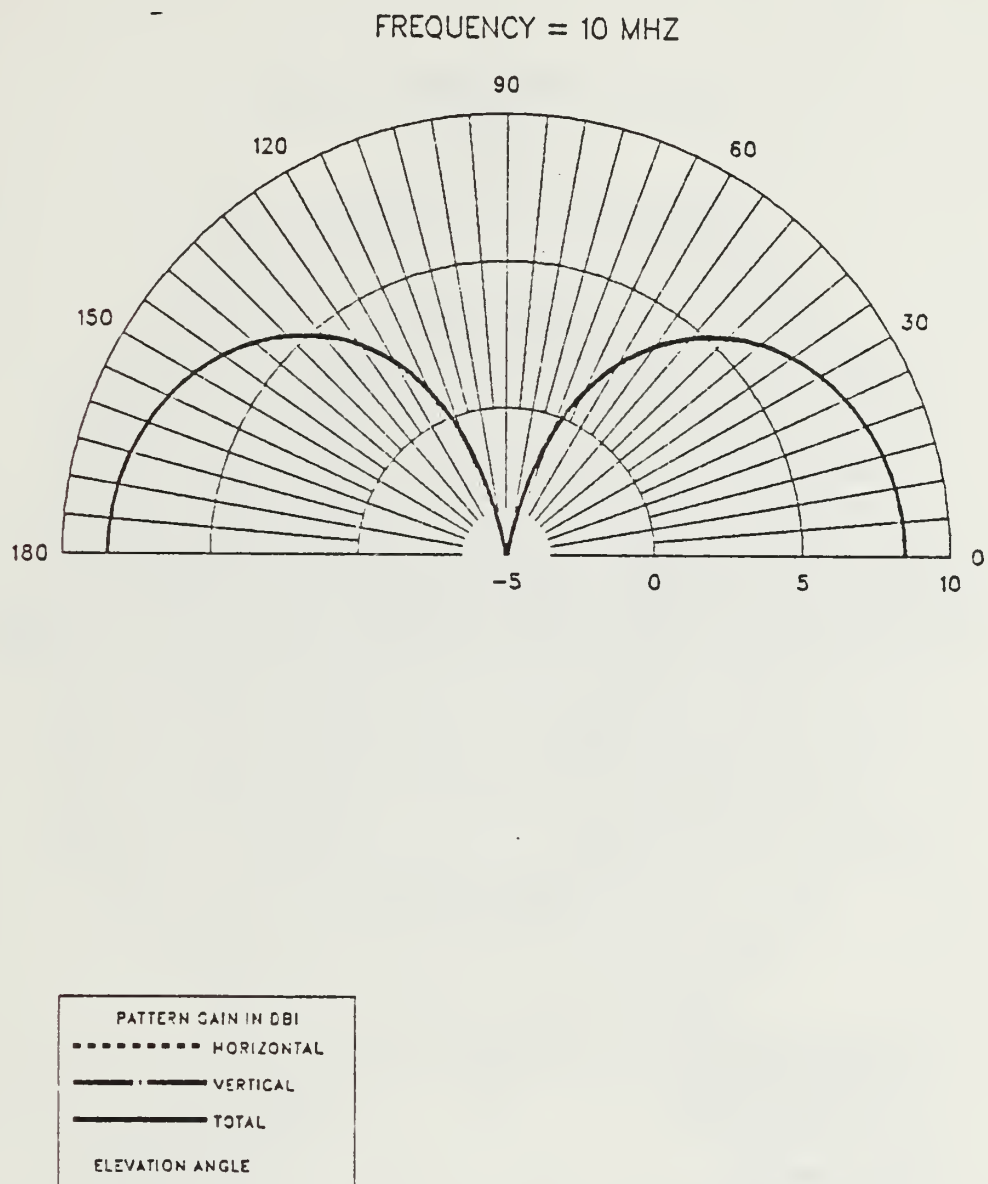


Figure 2.20 E-Field Elevation Pattern at 10 MHz for EF-TLA.

FREQUENCY = 2 MHZ

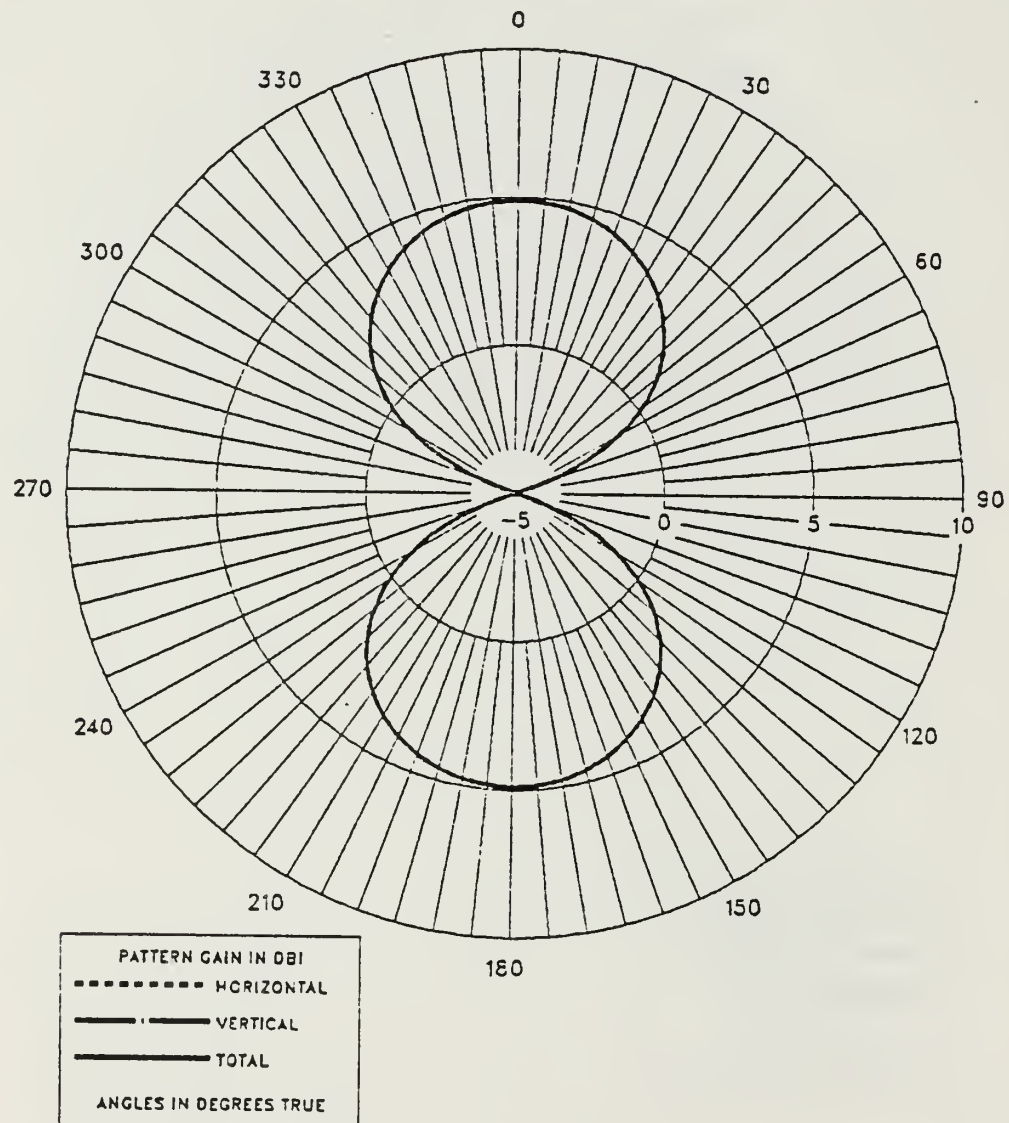


Figure 2.21 E-Field Azimuth Pattern at 2 MHz for TF-TLA.

FREQUENCY = 2 MHZ

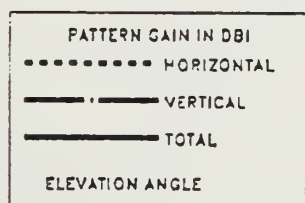
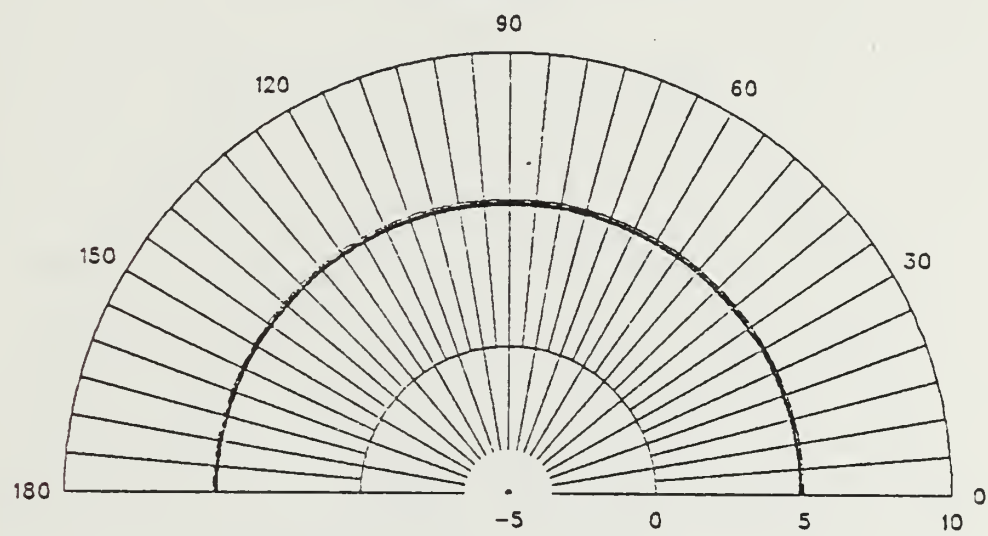


Figure 2.22 E-Field Elevation Pattern at 2 MHz for TF-TLA.

FREQUENCY = 6 MHZ

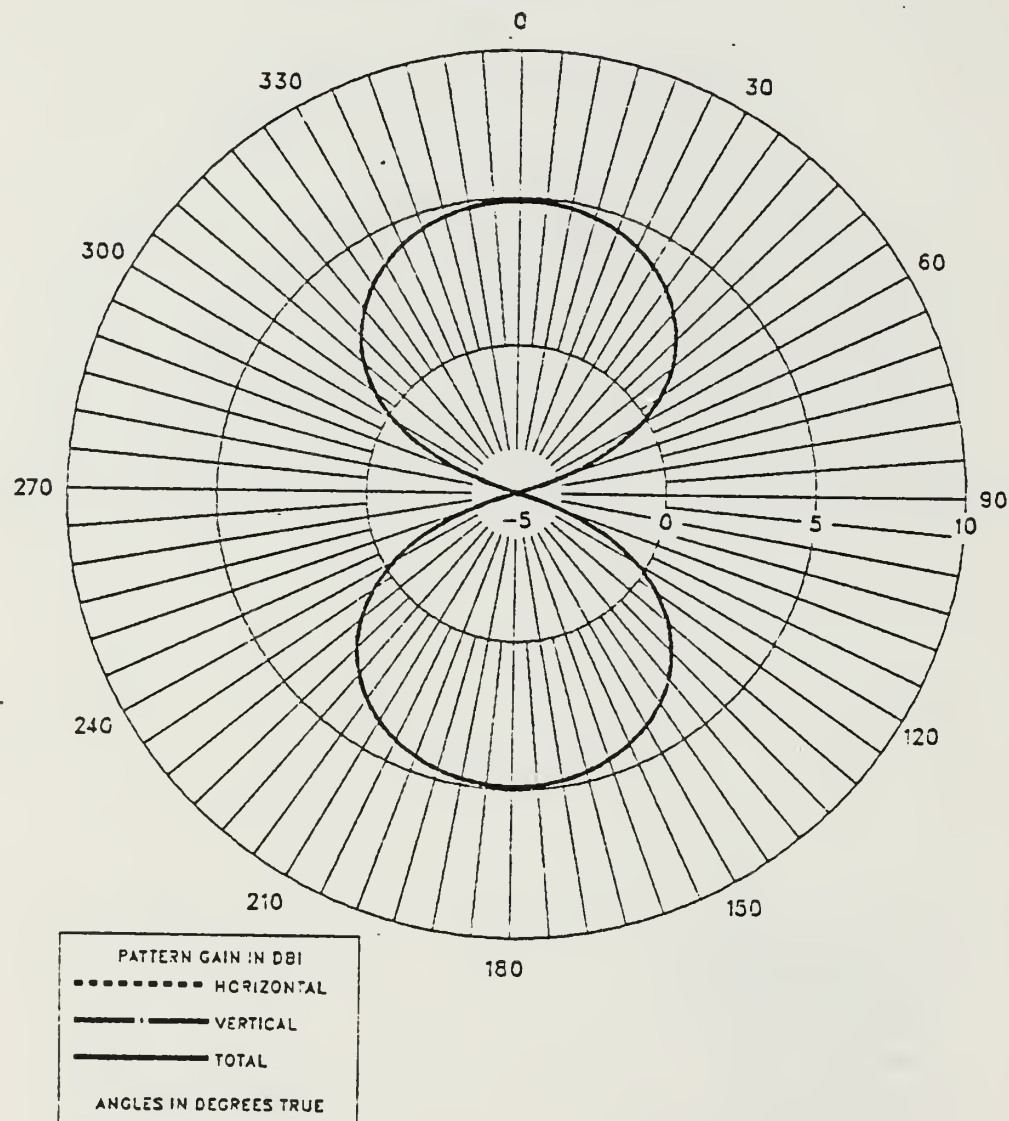


Figure 2.23 E-Field Azimuth Pattern at 6 MHz for TF-TLA.

FREQUENCY = 6 MHZ

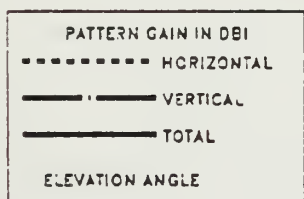
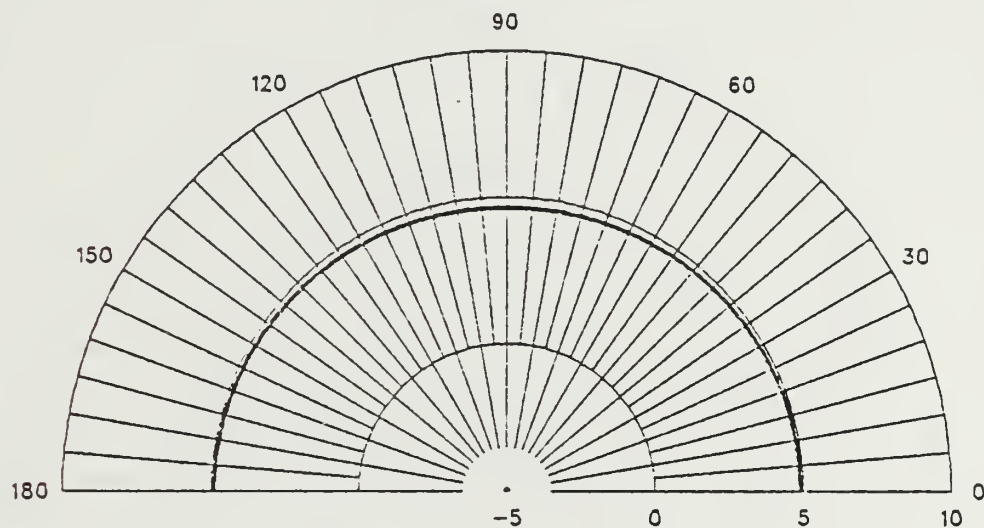


Figure 2.24 E-Field Elevation Pattern at 6 MHz for TF-TLA.

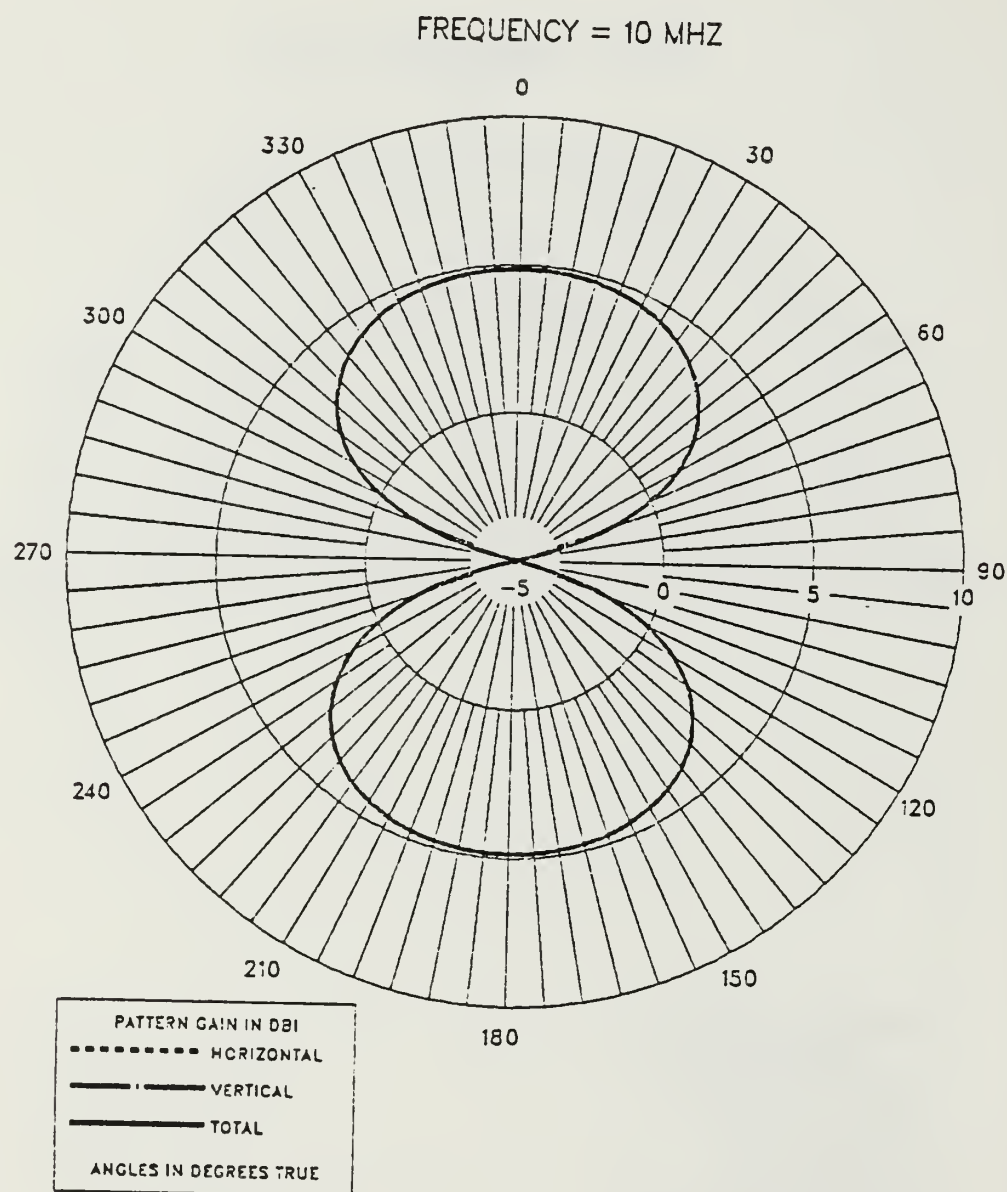


Figure 2.25 E-Field Azimuth Pattern at 10 MHz for TF-TLA.

FREQUENCY = 10 MHZ

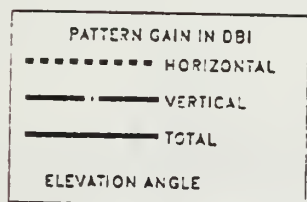
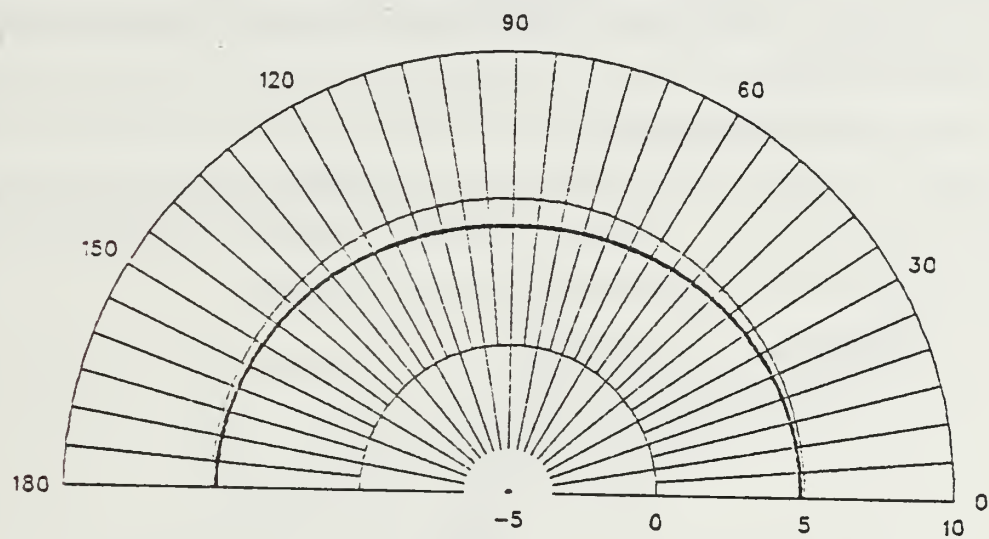


Figure 2.26 E-Field Elevation Pattern at 10 MHz for TF-TLA.

III. SHIP - ANTENNA COMPUTER MODELS AND RESULTS

This chapter presents the ship computer models used in this thesis and the results of mounting TLA structures on the ship. The models are for an FFG-45 frigate which has the transmission line antenna on the bow and the stern of the ship and is operating over a perfect ground.

A. SHIP COMPUTER MODELS

Figure 3.1, from Naval Electronic Systems Command [Ref. 4], illustrate the bow and stern area of an FFG - 45 frigate. As shown in Chapter II, the computer models are the transmission line with dimensions of 13.5 x 0.6 meters.

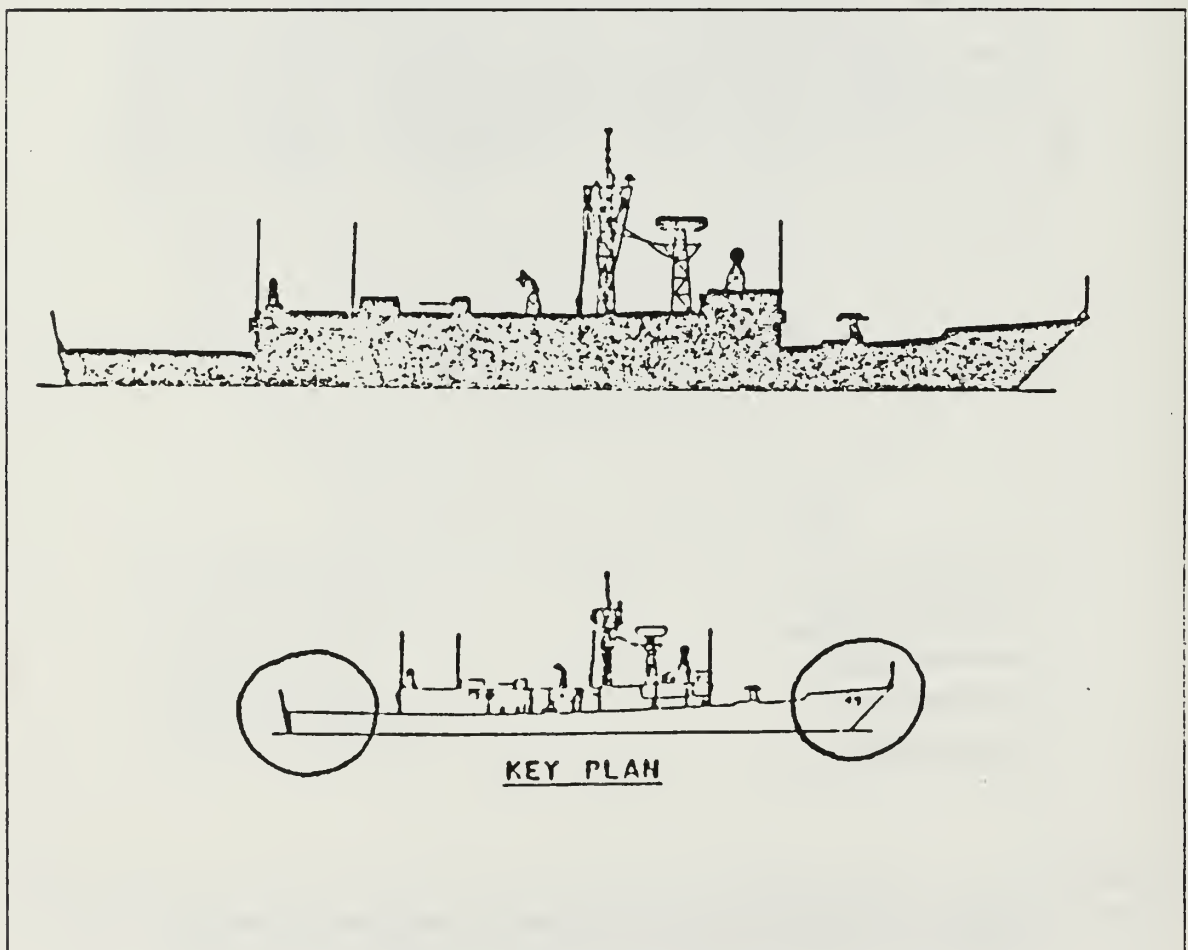


Figure 3.1 FFG-45 Frigate.

Figures 3.2 - 3.5 show the wire-grid of the FFG-45 frigate model used. Using NEC geometry cards, an FFG-45 frigate was modeled with wires of 0.05 meter radius for 2, 4.5, 7.5, and 10 MHz. It was noted by G.J Burke that the NEC code had some limitations in modeling electrically small antennas in the vicinity of loops [Ref. 5]. In the case cited, the loops were formed by the wire grid making up the ship body. The loop currents at low frequencies became proportional to $1/f$ while the antenna current was proportional to f , which was clearly wrong. The interaction matrix for the loops became ill-conditioned at the lower frequencies. Mr. Burke observed that this problem could be minimized by spacing the antenna further from the loops.

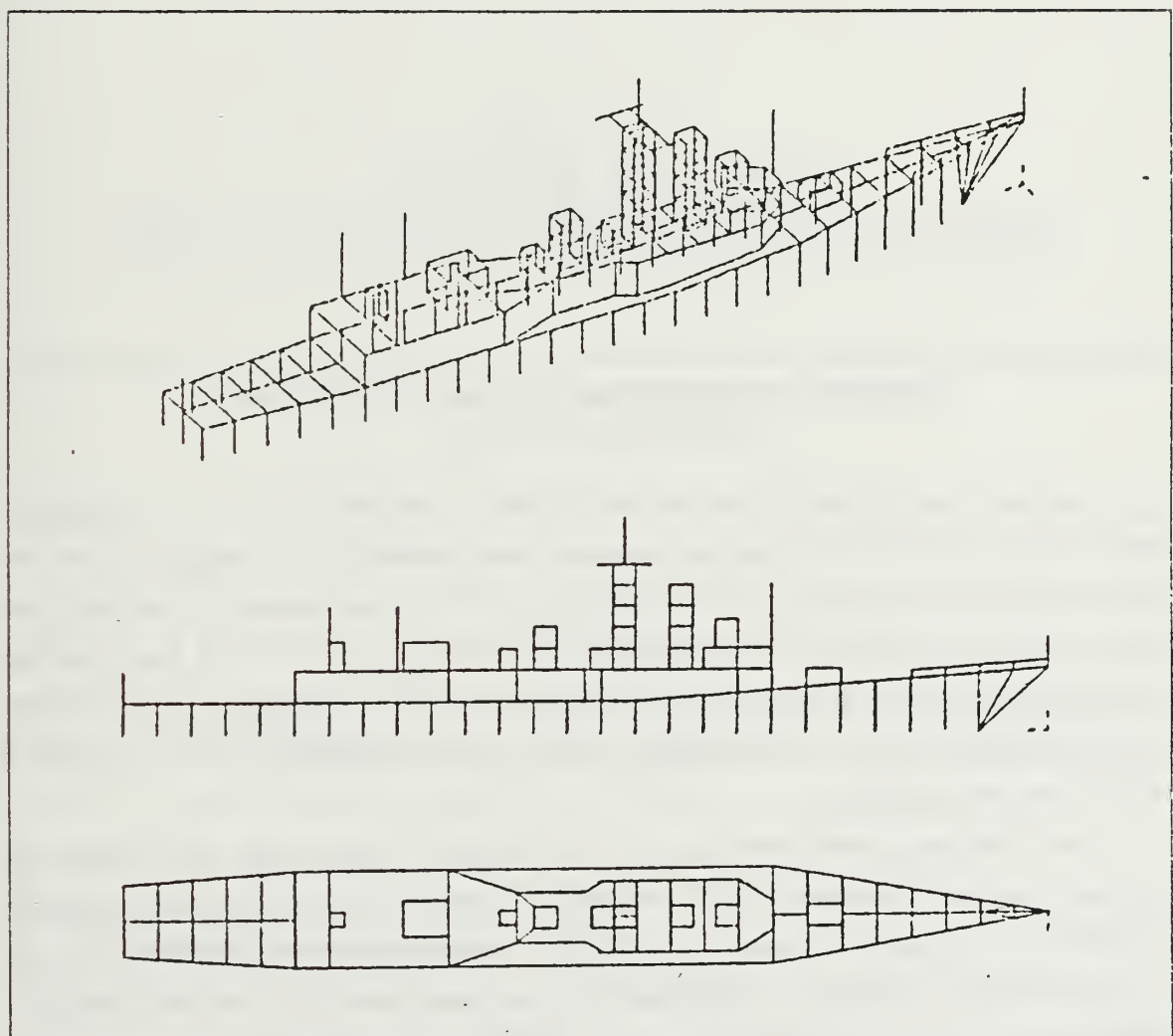


Figure 3.2 Wire Grid Model of an FFG-45 Frigate without Antenna.

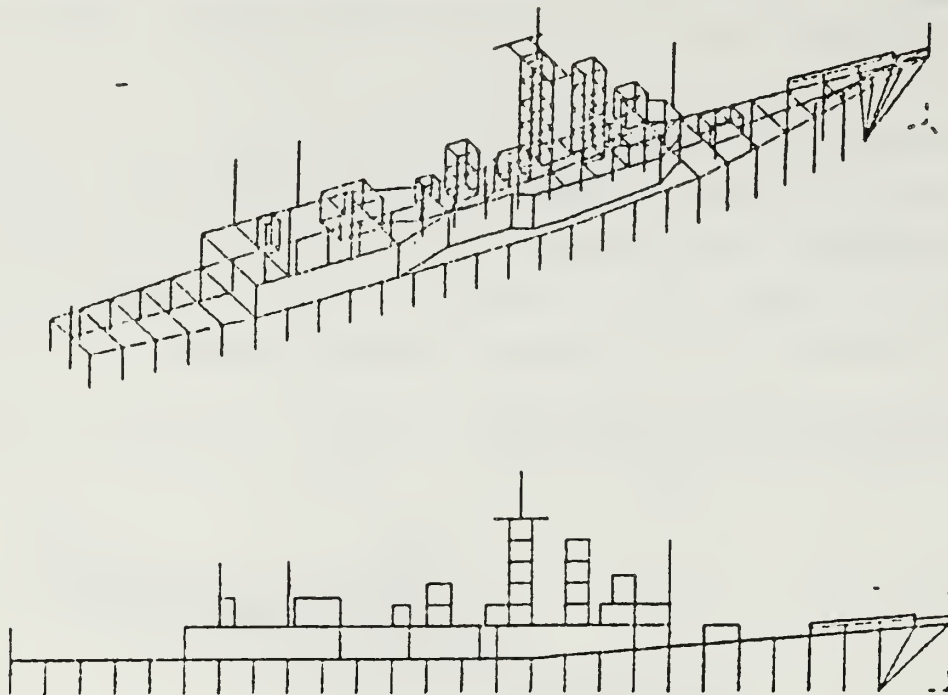


Figure 3.3 Wire Grid Model of an FFG-45 Frigate with Antenna on the Bow.

As shown in Chapter II, the important design considerations required to develop these computer models were the segmentation size, the radii of the segments, and the proper geometrical model. For wire modeling, the main electrical consideration was segment length, Δ , relative to the wavelength, λ . For accurate results, Δ should be less than approximately 0.1λ at the desired frequency. The wire radius, a , relative to the wavelength, was limited to the approximation, that the relationship $2\pi a \lambda \ll 1$ must hold for the configuration.

The wire-grid model was run at four different frequencies to produce the Numerical Green's Function (NGF). Appendix A shows the geometry data cards for the NGF and the EF-TLA and/or the TF-TLA at three different positions at 2, 4.5, 7.5, and 10 MHz. With the Numerical Green's Function (NGF) option [Ref. 6], a fixed structure and its environment may be modeled and the factored interaction matrix saved on a file. The main purpose of the NGF is to avoid unnecessary repetition of calculations when most of a model, such as the ship's structure in a complex



Figure 3.4 Wire Grid Model of an FFG-45 Frigate with Antenna on the Stern.

environment, remains fixed. When modeling antennas on ships, several antenna designs or locations may be considered on an otherwise unchanged ship. With the NGF, the self-interaction matrix for the fixed environment may be computed, factored for solution, and saved on a tape or disk file. The solution for a new antenna then requires only the evaluation of the self-interaction matrix for the antenna, the mutual antenna-to-environment interactions, and matrix manipulations for a partitioned-matrix solution. Another reason for using the NGF option is to exploit partial symmetry in a structure. In a single run, a structure must be perfectly symmetric for NEC to use symmetry in the solution. Such partial symmetry may be exploited to reduce solution time by running the symmetric part of the model first and writing a NGF file. The unsymmetric parts may then be added in a second run. Use of the NGF option may also be warranted for large, time-consuming models to save an expensive result for further use. Without adding new antennas, it may be used with a new excitation or to compute new radiation, nearfield, or coupling data not computed in the original run.

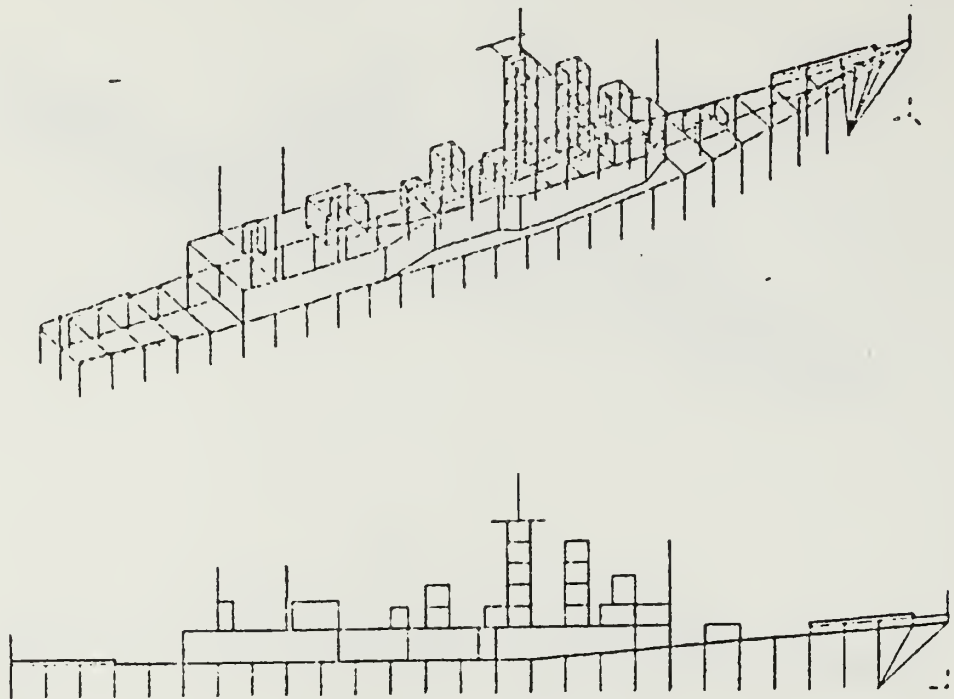


Figure 3.5 Wire Grid Model of an FFG-45 Frigate with Antenna on the Bow and the Stern.

Since this model had over 600 segments, when using NEC, the NGF file 'FILE FT20F001 B4' was produced by running a program. Each frequency run required two to two and one-half hours of CPU time (IBM 370/3033).

B. COMPUTER RESULTS

This section represents the computer results of the EF-TLA and the TF-TLA on the bow and the stern of an FFG-45 frigate which were run over a perfect ground.

1. Average Power Gain

Over a perfectly conducting ground the average power gain should be 2.0. The computed result differed by about 1.5 %, probably due to the 10-degree steps used in integrating the radiated power. For a more complex structure, the average gain can provide a check on the accuracy of the computed input impedance over a perfect ground where it should equal 2.0 or in free space where it should equal 1.0. If the average power gain is less than 1.8 or more than 2.2, this indicates that the input impedance is inaccurate.

Table 4 shows the average power gain of the EF-TLA for three different positions of the transmission line antenna on an FFG-45 frigate. Table 5 shows the average power gain of the TF-TLA for three different positions of the transmission line antenna on an FFG-45 frigate.

TABLE 4
AVERAGE POWER GAIN FOR END FEED-TLA

Frequency in MHz	EF-TLA on Bow	EF-TLA on Stern	EF-TLA on Bow & Stern
2	0.94	1.74	1.19
4.5	1.56	2.04	1.87
7.5	1.47	2.44	1.90
10	1.96	2.43	2.76

TABLE 5
AVERAGE POWER GAIN FOR TOP FEED-TLA

Frequency in MHz	TF-TLA on Bow	TF-TLA on Stern	TF-TLA on Bow & Stern
2	1.18	1.98	1.88
4.5	2.13	1.71	2.07
7.5	2.93	2.85	1.81
10	1.38	2.96	2.12

For the EF-TLA (see Table 4), the average power gains are acceptable in the case of 4.5 and 7.5 MHz with the transmission line on the bow and the stern, 4.5 MHz with the transmission line on the stern, and 10 MHz with the transmission line on the bow. The average power gain of the transmission line on the stern shows higher value than that on the bow, and in the case of the transmission line on the bow and the stern, increased as the frequency increased.

For the TF-TLA (see Table 5), the average power gains are acceptable in the case of 2, 4.5 and 7.5 MHz with the transmission line on the bow and the stern, 4.5 MHz with the transmission line on the bow, and 2 MHz with the transmission line on the stern. The average power gains are high values for the transmission line on the bow at 4.5 and 7.5 MHz, and for the transmission line on the stern at 7.5 and 10 MHz.

2. Input Impedance

Tables 6 - 9 show the input impedance for the three different positions of the transmission line antenna on an FFG-45 frigate. In the case of the antenna on the bow and on the stern, the resistance and the reactance had almost the same values as the antenna on the bow and the stern but differ from the resistance at 7.5 MHz and from the reactance at 10 MHz in the EF-TLA case.

Figures 3.6 - 3.8 show that the resistance and reactance increased at 4.5 MHz, and decreased as the frequency increased. The EF-TLA on the stern has low resistance at 2 and 10 MHz, and high reactance at 4.5 MHz.

Figures 3.9 - 3.11 show that the resistance increased as the frequency increased but the reactance decreased at 10 MHz. The TF-TLA on the bow and the stern has low resistance at 2 and 4.5 MHz, and high resistance and reactance at 7.5 and 10 MHz. The EF-TLA on the bow has a large difference between resistance and reactance except at 10 MHz and at 4.5 MHz. For the TF-TLA on the bow and/or the stern, the resistance has a very low value compared with the reactance.

A SWR of 3:1 was considered as a reasonable criterion for practical operation. Even though many antennas satisfy this criterion over an operating band of frequencies, many of them can be brought into this region of the Smith chart by the use of a series inductance or capacitance [Ref. 7]. Figures 3.12 - 3.15 presents the 3:1 SWR circle. The shaded region represents the impedance region of the Smith chart which may be moved into the 3:1 SWR by the use of series reactances. Any impedance that falls in the 3:1 SWR circle or in the shaded region of the Smith chart, will be considered as acceptable. Two kinds of Smith chart plots were presented at the

TABLE 6
RESISTANCE FOR END FEED-TLA

Frequency in MHz	EF-TLA on Bow	EF-TLA on Stern	EF-TLA on Bow & Stern	
2	0.6	0.2	0.7	0.3
4.5	620.6	259.6	630.9	260.7
7.5	29.9	42.1	28.1	45.7
10	9.3	13.2	9.1	14.7

TABLE 7
REACTANCE FOR END FEED-TLA

Frequency in MHz	EF-TLA on Bow	EF-TLA on Stern	EF-TLA on Bow & Stern	
2	177.5	180.8	177.5	180.7
4.5	789.1	1589.4	796.1	1591.2
7.5	-262.2	-244.4	-261.3	-246.9
10	-13.6	-41.1	-13.5	-52.8

designed frequency range for each feed location. One was the Smith chart plot using the 50 Ohm characteristic impedance of typical HF whip antennas; the other was the Smith chart plot using a characteristic impedance of 500 Ohms. Usually, the characteristic impedance (Z_0) can be shifted for an HF shipboard antenna system. For the 50 Ohm characteristic impedance, the range of frequencies satisfying the 3:1 SWR is limited at 7.5 MHz in the EF-TLA case, and at 4.5 MHz in the TF-TLA. When a characteristic impedance of 500 Ohms was used, it is shown to be the opposite case.

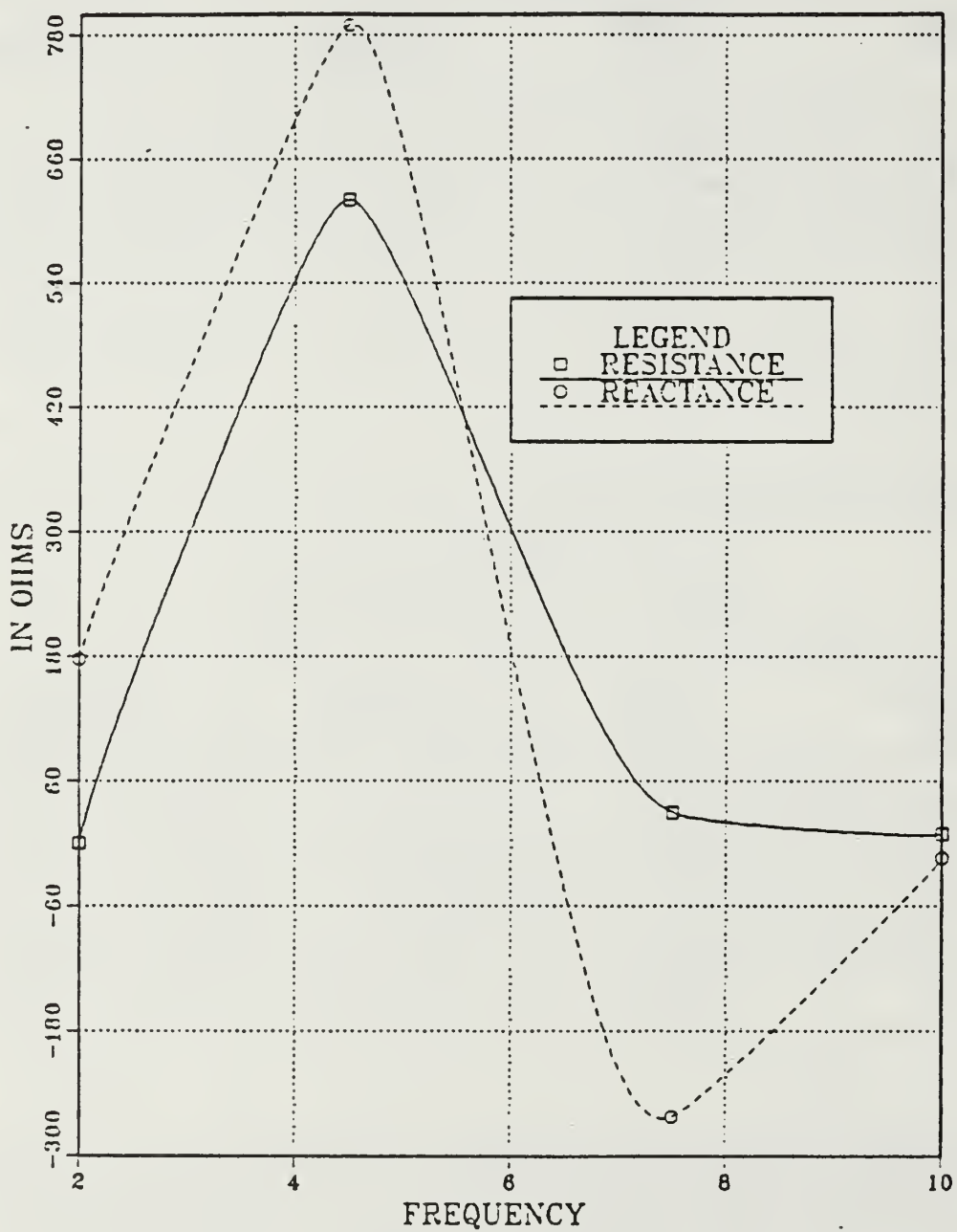


Figure 3.6 Input Impedance vs Frequency for EF-TLA on the Bow.

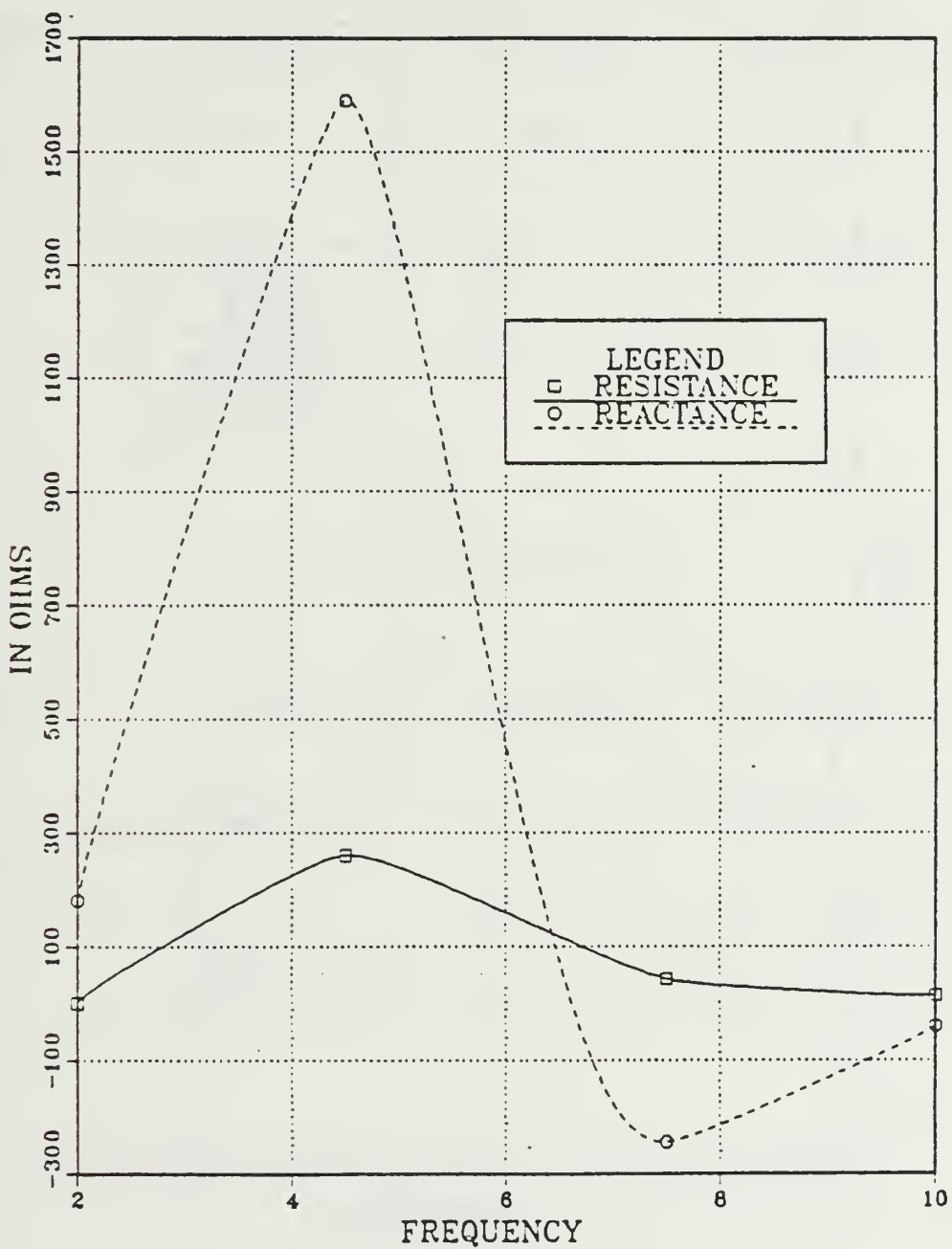


Figure 3.7 Input Impedance vs Frequency for EF-TLA on the Stern.

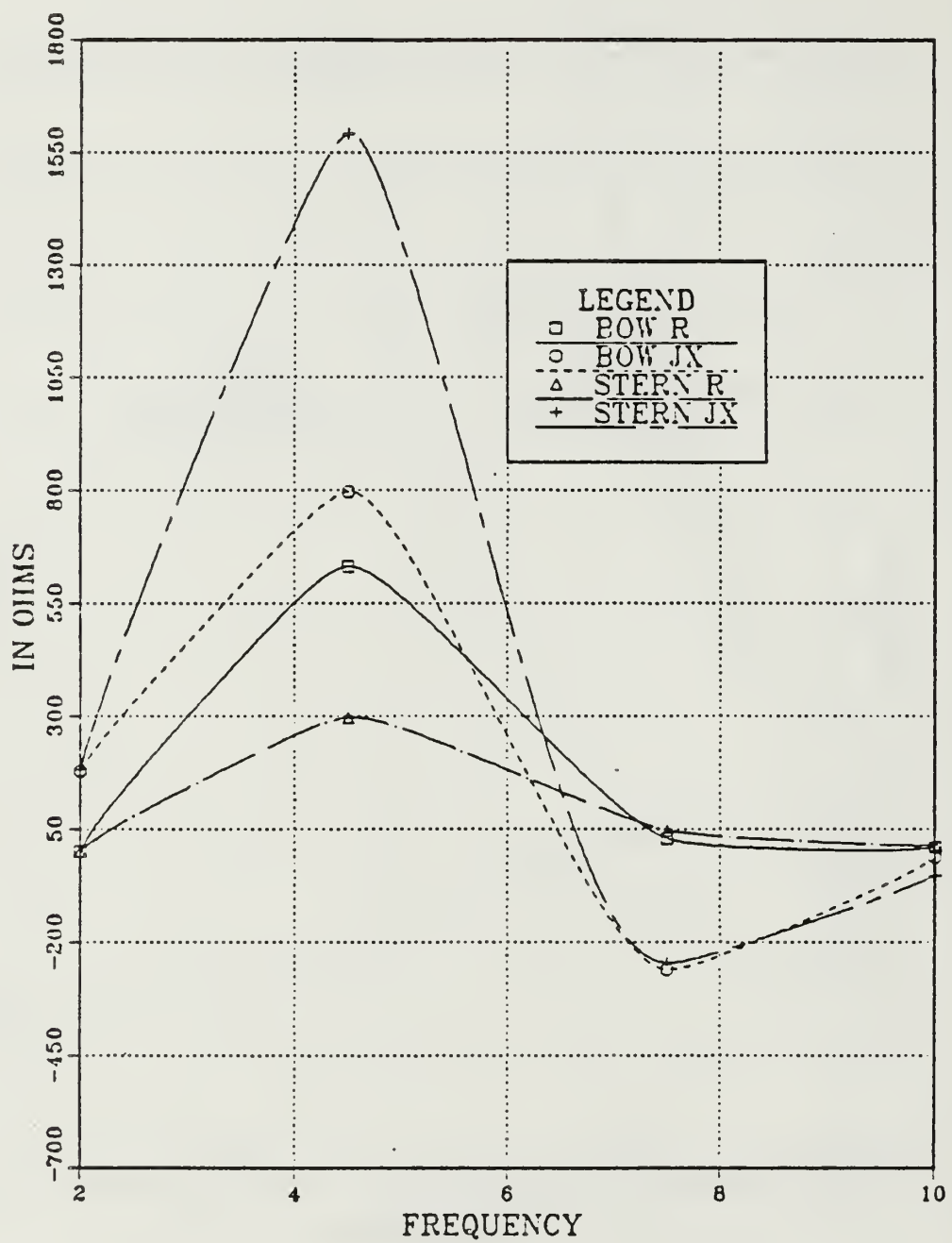


Figure 3.8 Input Impedance vs Frequency for EF-TLA on the Bow and the Stern.

TABLE 8
RESISTANCE FOR TOP FEED-TLA

Frequency in MHz	TF-TLA on Bow	TF-TLA on Stern	TF-TLA on Bow & Stern	
2	0.3	0.2	0.3	0.2
4.5	32.6	5.2	33.5	5.8
7.5	622.4	634.3	583.1	830.1
10	2012.1	3249.9	1999.7	3447.4

TABLE 9
REACTANCE FOR TOP FEED-TLA

Frequency in MHz	TF-TLA on Bow	TF-TLA on Stern	TF-TLA on Bow & Stern	
2	175.5	154.7	175.6	154.8
4.5	526.9	437.5	527.6	436.9
7.5	1640.1	2447.0	1654.4	2234.1
10	-1790.5	-169.2	-1783.3	-350.2

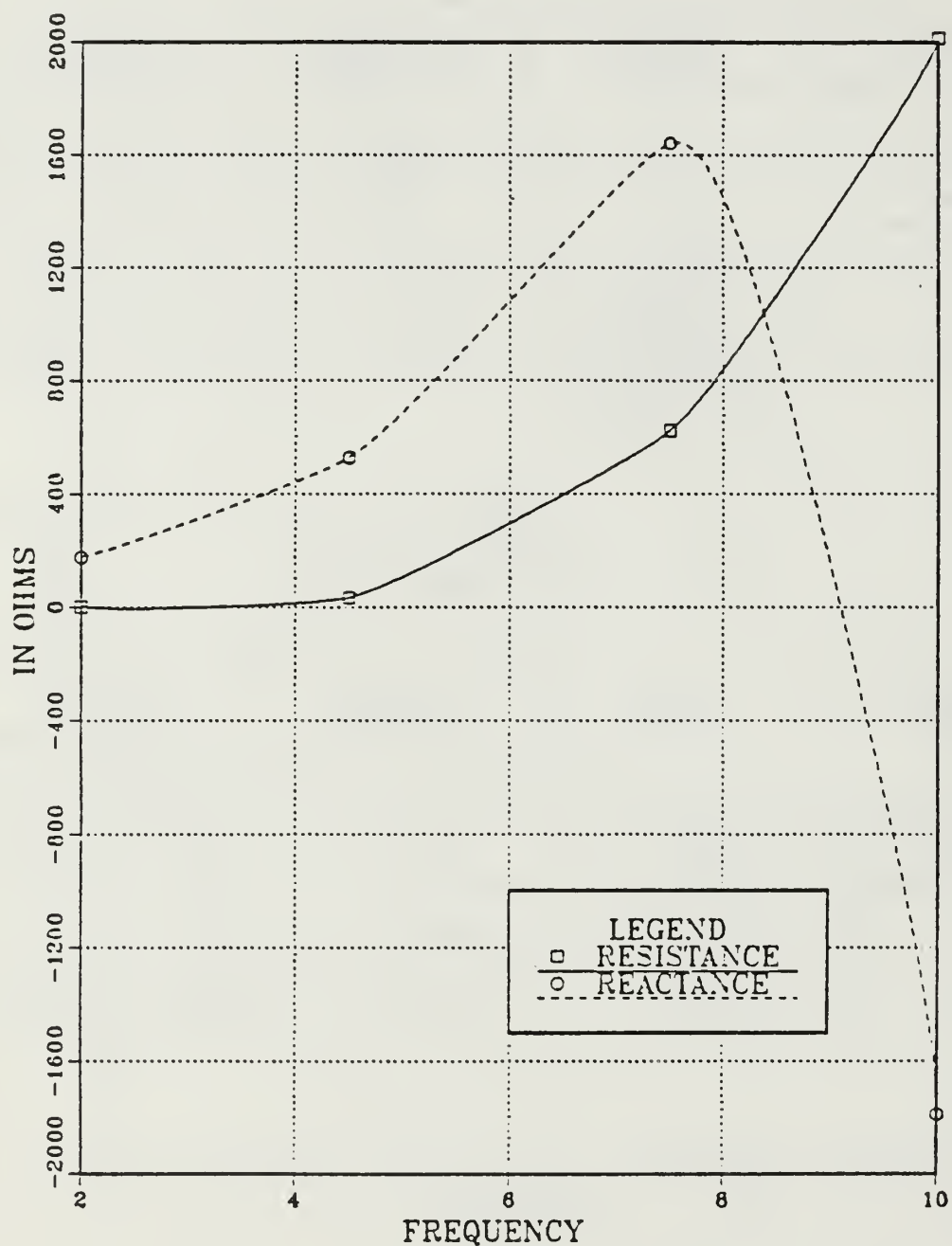


Figure 3.9 Input Impedance vs Frequency for TF-TLA on the Bow.

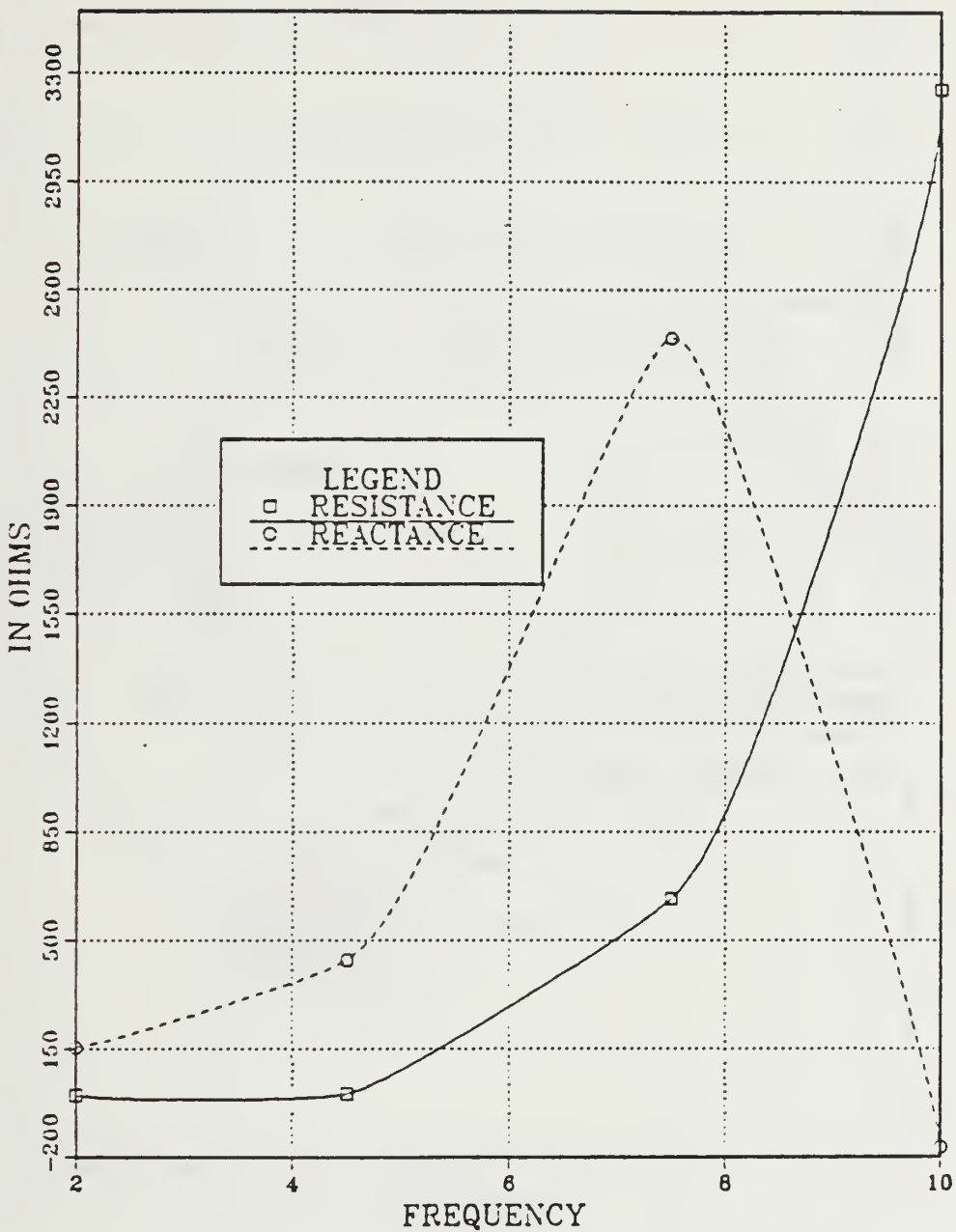


Figure 3.10 Input Impedance vs Frequency for TF-TLA on the Stern.

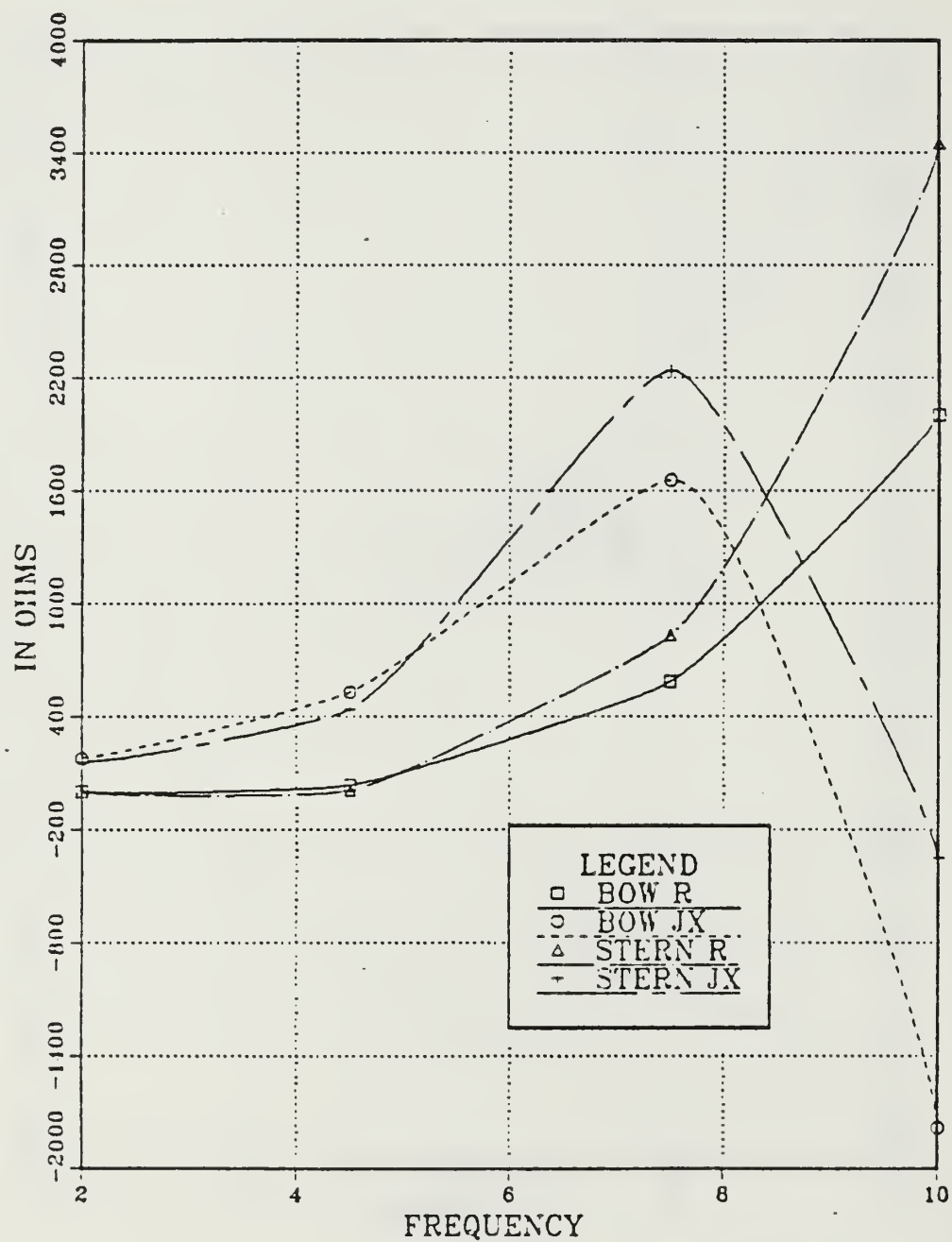


Figure 3.11 Input Impedance vs Frequency for TF-TLA on the Bow and the Stern.

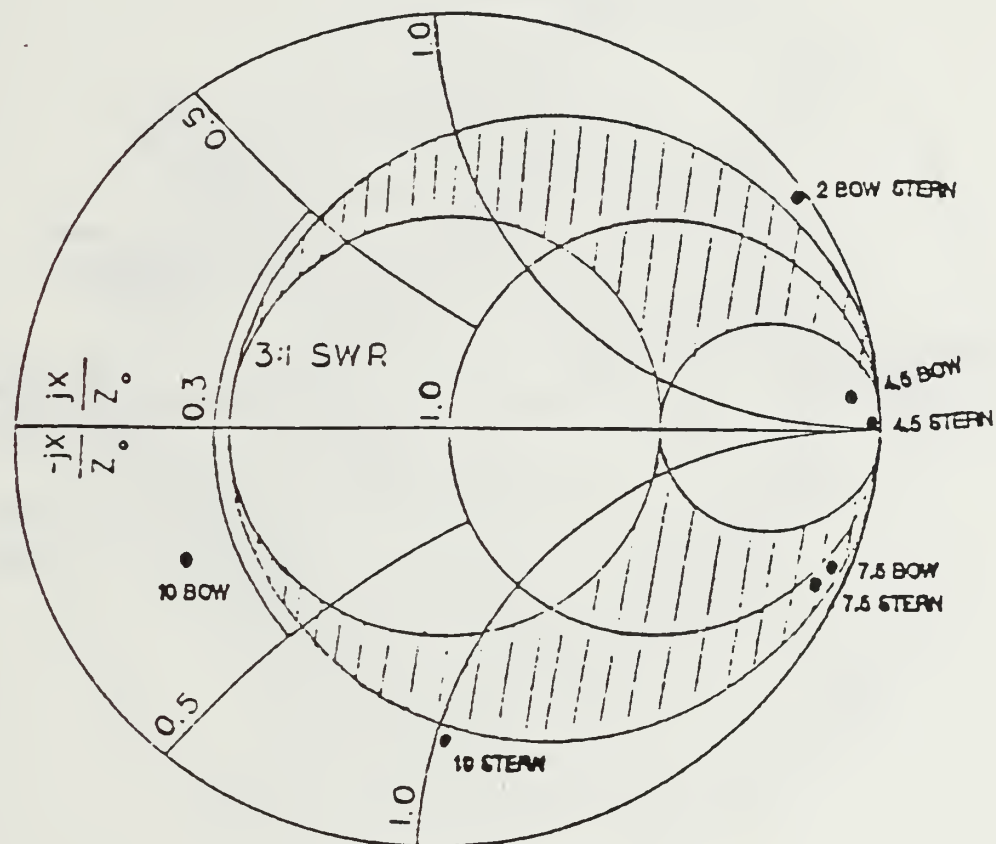


Figure 3.12 Smith Chart Showing 3:1 VSWR
Impedance Plot of EF-TLA : $Z_0 = 50 \text{ Ohm}$.

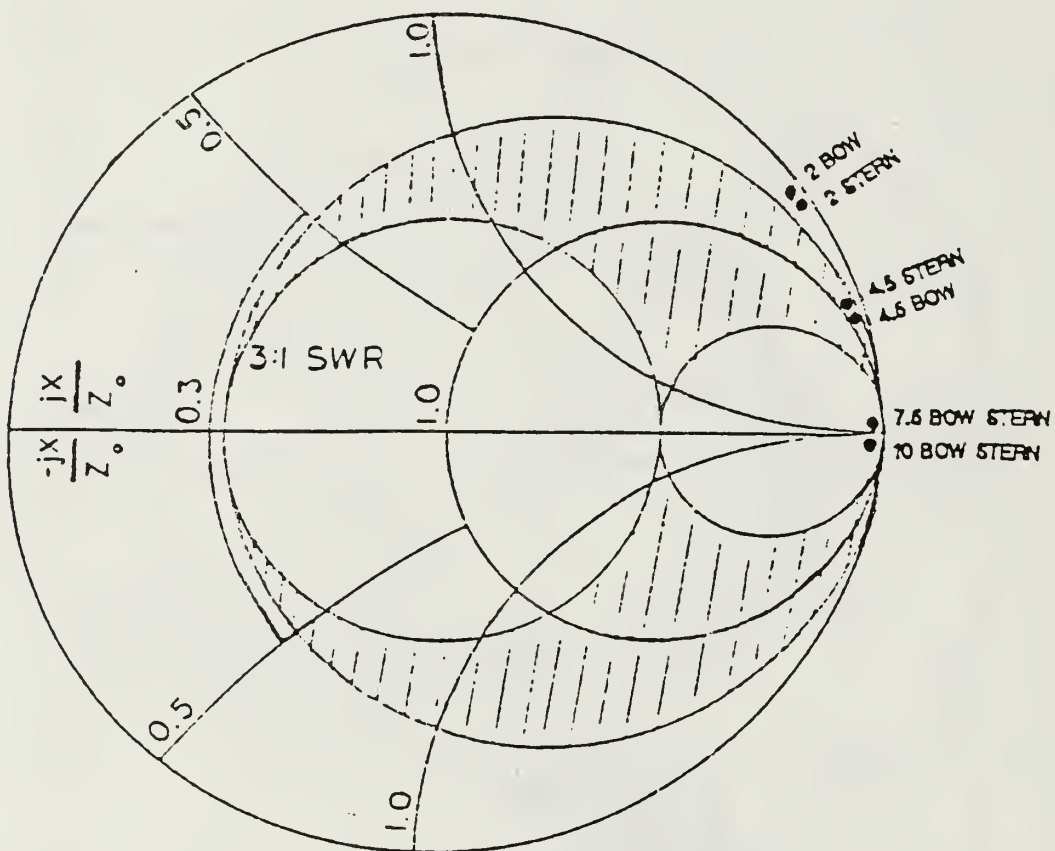


Figure 3.13 Smith Chart Showing 3:1 VSWR
Impedance Plot of TF-TLA : $Z_0 = 50 \text{ Ohm}$.

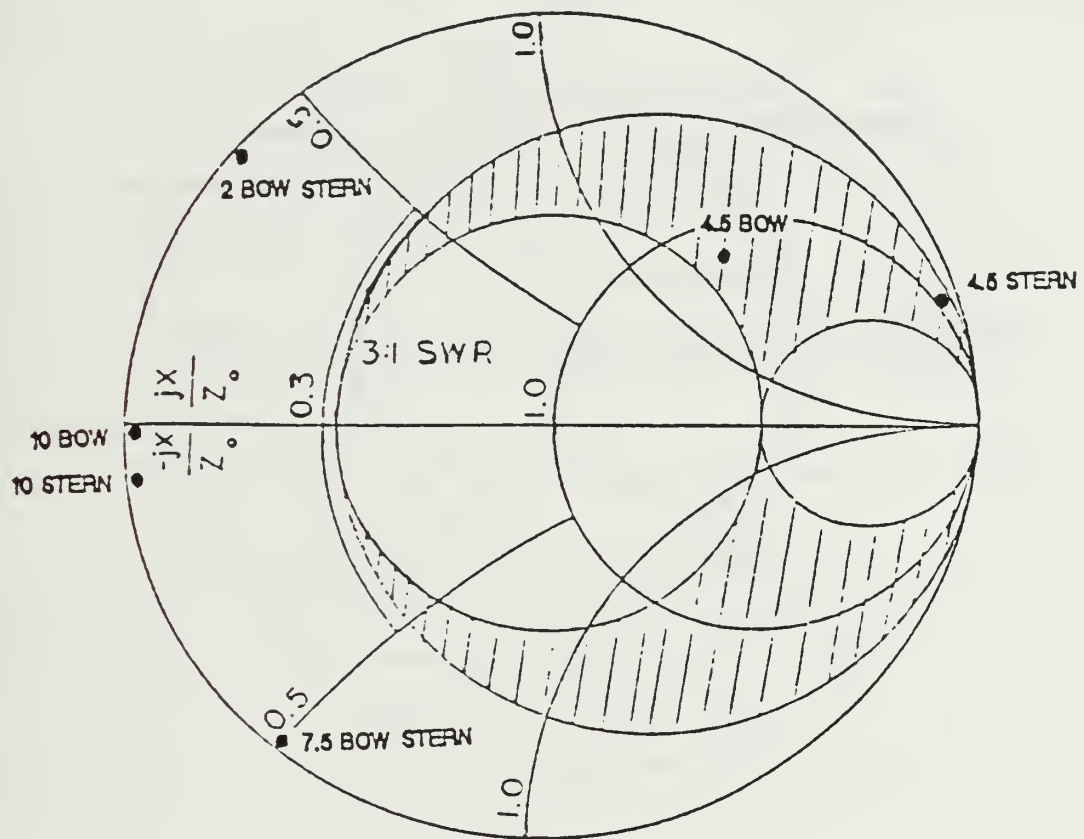


Figure 3.14 Smith Chart Showing 3:1 VSWR
Impedance Plot of EF-TLA : $Z_0 = 500$ Ohm.

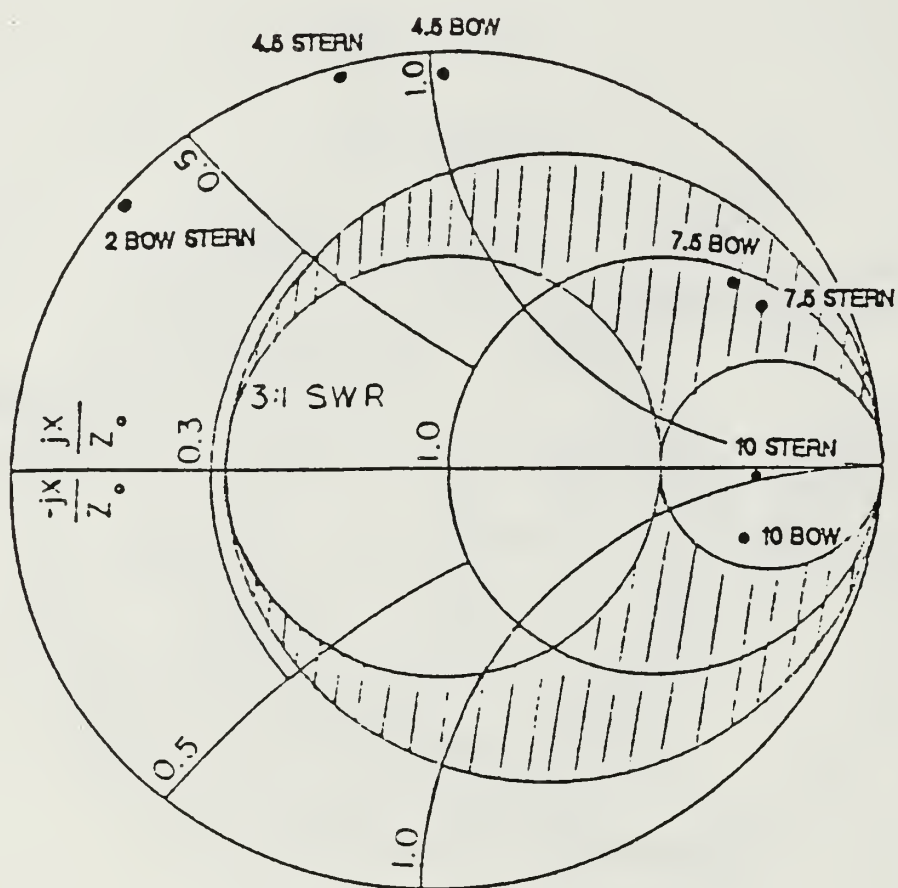


Figure 3.15 Smith Chart Showing 3:1 VSWR Impedance Plot of TF-TLA : $Z_0 = 500 \text{ Ohm}$.

3. Radiation Patterns

a. *EF-TLA on the Ship's Bow or Stern (Appendix E)*

Azimuth patterns of the transmission line on the bow are directed backward at 2 and 4.5 MHz, with two broadside lobes and one back lobe at 7.5 MHz. At 10 MHz, the pattern is more complex. Elevation patterns of the antenna on the bow are fairly uniform with good high angle coverage for lower frequencies. Azimuth patterns of the transmission line on the stern show the opposite effect in which the forward lobe is larger than the backward lobe at 4.5 and 7.5 MHz, but the backward lobe dominates at 10 MHz. Elevation patterns for stern mounting are similar in coverage to the bow ones.

b. *TF-TLA on the Ship's Bow or Stern (Appendix E)*

Azimuth and elevation gains are lower than those in the EF-TLA case over the entire frequency, but elevation patterns are higher gain than in the EF-TLA case, favoring Near Vertical Incidence Skywave (NVIS) coverage. Azimuth patterns of the antenna on the bow show that the forward lobe is larger than the backward lobe at 2, 4.5, and 7.5 MHz but differ at 10 MHz. In the case of the azimuth patterns of the antenna on the stern, the forward and backward lobe is large at 2 MHz and the side lobe is large at 4.5 and 7.5 MHz.

c. *EF-TLA and TF-TLA Mounted on Both the Bow and the Stern (Figure 3.16 - 3.31)*

In the case of the transmission line on both the bow and the stern, the azimuth patterns show that the backward lobe is larger than the forward lobe but indicate almost the same forward and backward lobes at 7.5 MHz. Elevation patterns for dual mounting have a large forward lobe, with slightly more vertical pattern than the case of the antenna on the bow or on the stern. Large azimuth side lobes provide more uniform coverage than for single location mounting.

- EF-TLA ON THE BOW AND THE STERN

FREQUENCY = 2 MHZ

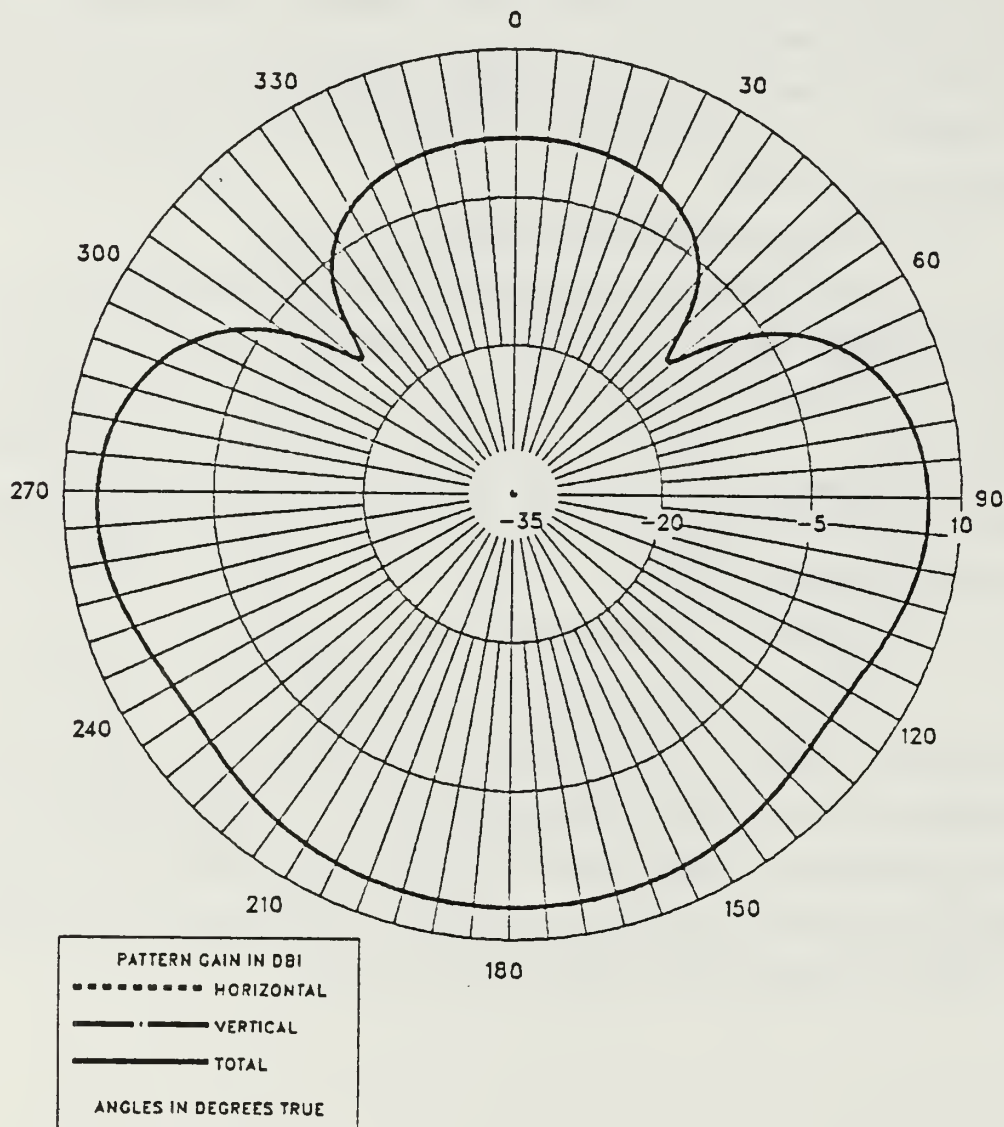
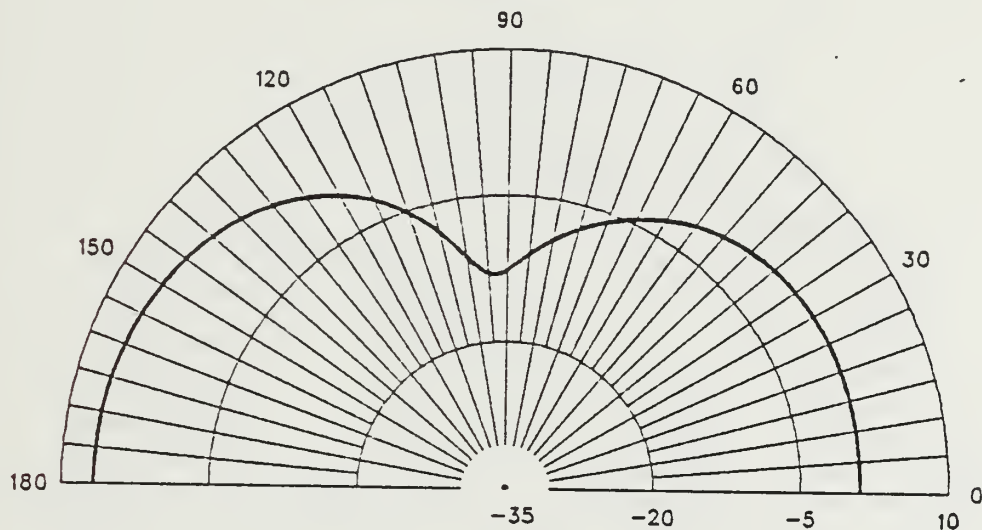


Figure 3.16 E-Field Azimuth Pattern at 2.0 MHz
for EF-TLA on the Bow and the Stern.

- EF-TLA ON THE BOW AND THE STERN

FREQUENCY = 2 MHZ



PATTERN GAIN IN DBI
----- HORIZONTAL
— VERTICAL
— TOTAL
ELEVATION ANGLE

Figure 3.17 E-Field Elevation Pattern at 2.0 MHz
for EF-TLA on the Bow and the Stern.

EF-TLA ON THE BOW AND THE STERN

FREQUENCY = 4.5 MHZ

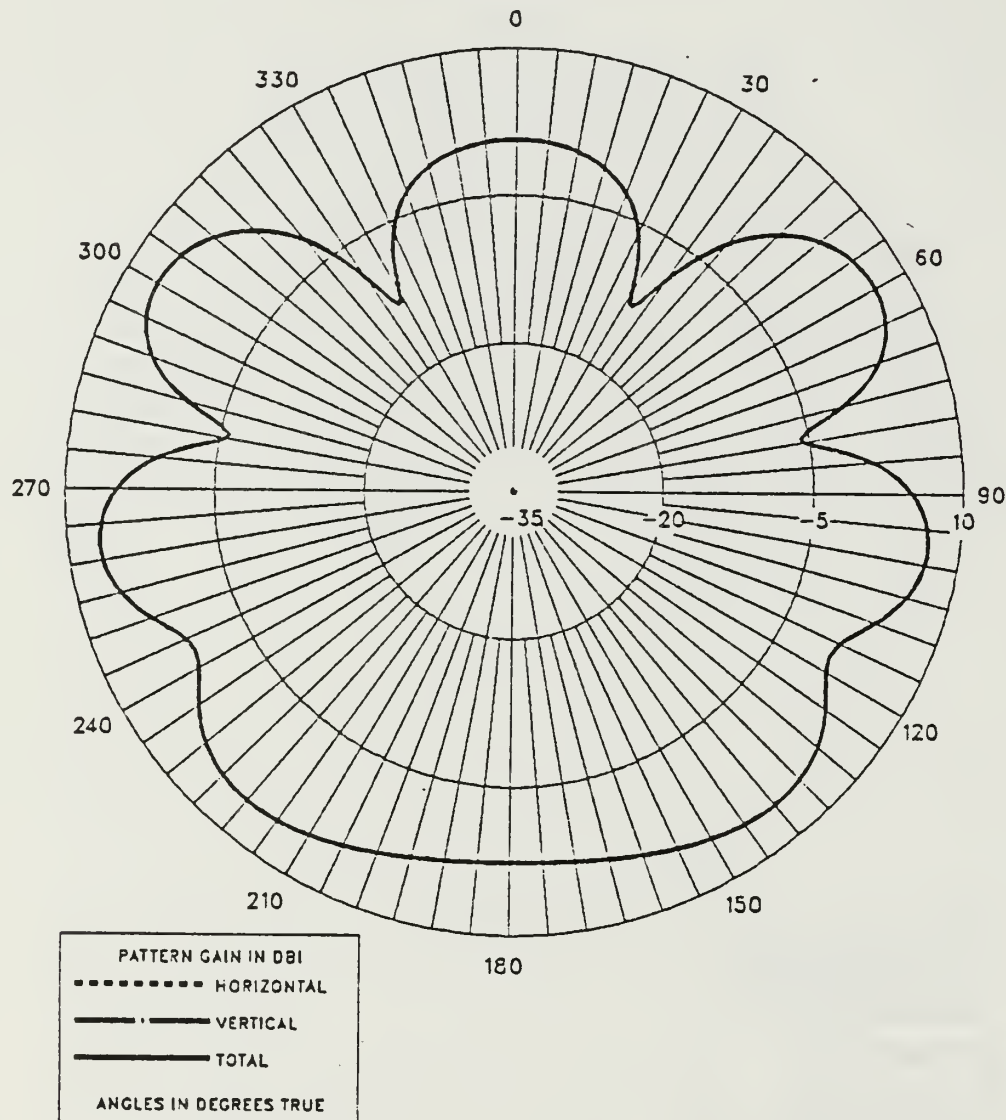
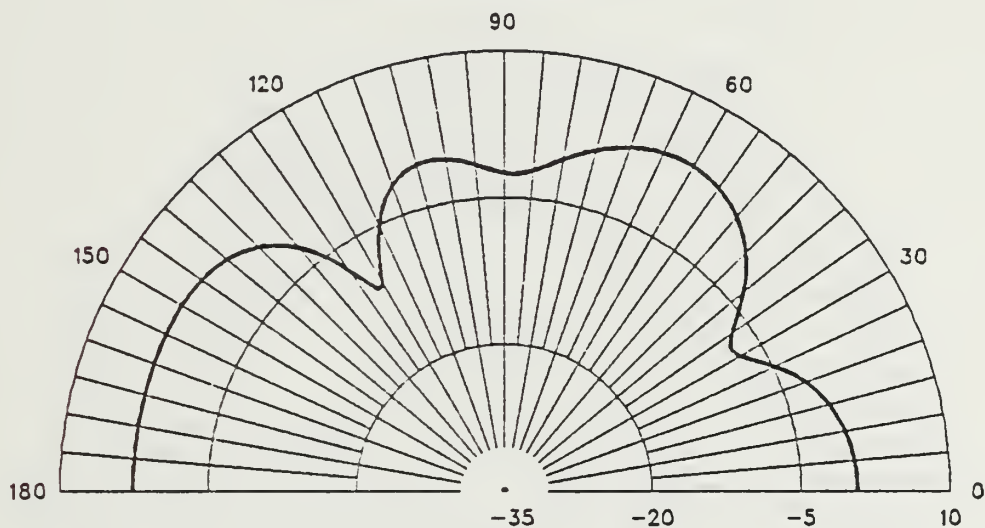


Figure 3.18 E-Field Azimuth Pattern at 4.5 MHz
for EF-TLA on the Bow and the Stern.

- EF-TLA ON THE BOW AND THE STERN

FREQUENCY = 4.5 MHZ



PATTERN GAIN IN DBI	
-----	HORIZONTAL
-----	VERTICAL
-----	TOTAL
ELEVATION ANGLE	

Figure 3.19 E-Field Elevation Pattern at 4.5 MHz
for EF-TLA on the Bow and the Stern.

EF-TLA ON THE BOW AND THE STERN

FREQUENCY = 7.5 MHZ

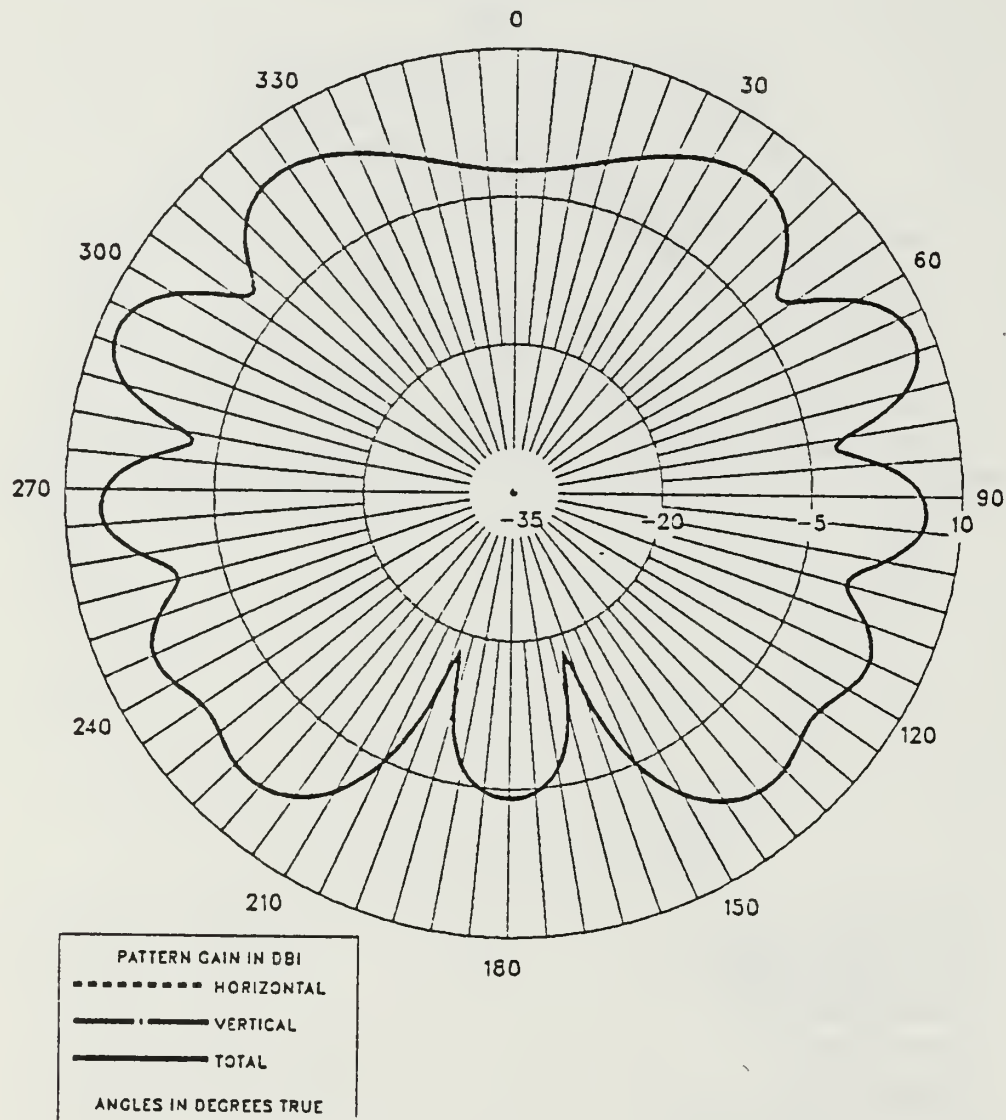
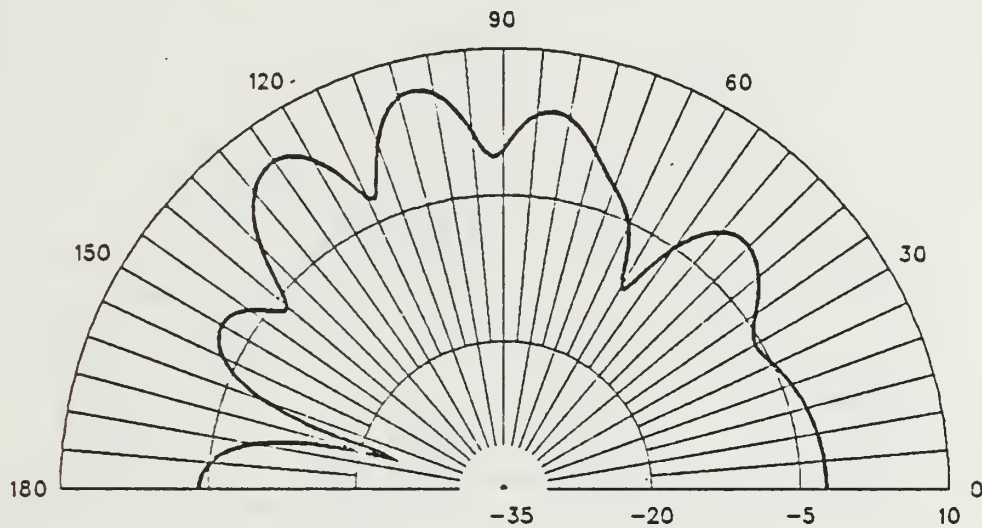


Figure 3.20 E-Field Azimuth Pattern at 7.5 MHz for EF-TLA on the Bow and the Stern.

- EF-TLA ON THE BOW AND THE STERN

FREQUENCY = 7.5 MHZ



PATTERN GAIN IN DBI
----- HORIZONTAL
— VERTICAL
— TOTAL
ELEVATION ANGLE

Figure 3.21 E-Field Elevation Pattern at 7.5 MHz
for EF-TLA on the Bow and the Stern.

- EF-TLA ON THE BOW AND THE STERN

FREQUENCY = 10 MHZ

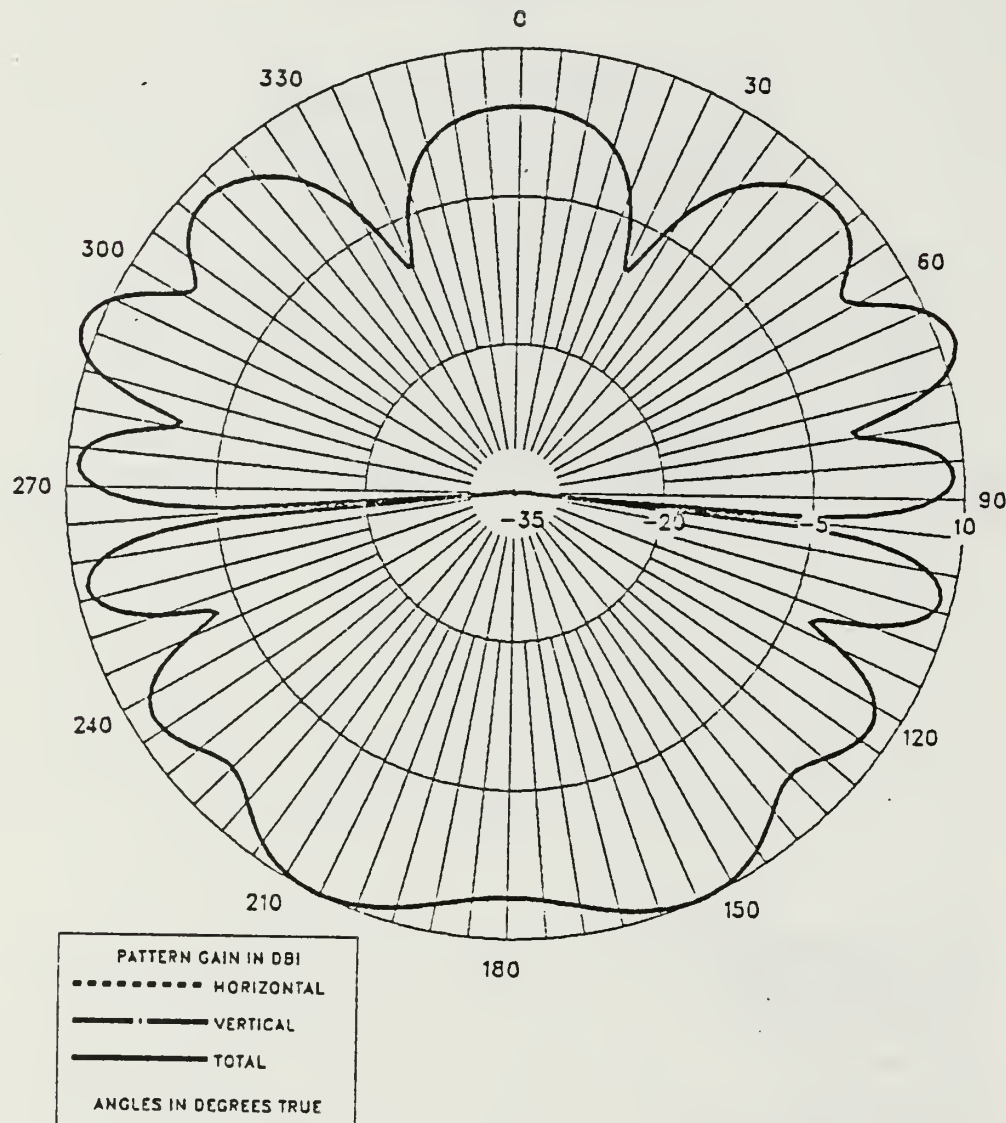


Figure 3.22 E-Field Azimuth Pattern at 10.0 MHz
for EF-TLA on the Bow and the Stern.

- EF-TLA ON THE BOW AND THE STERN

FREQUENCY = 10 MHZ

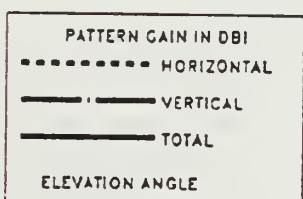
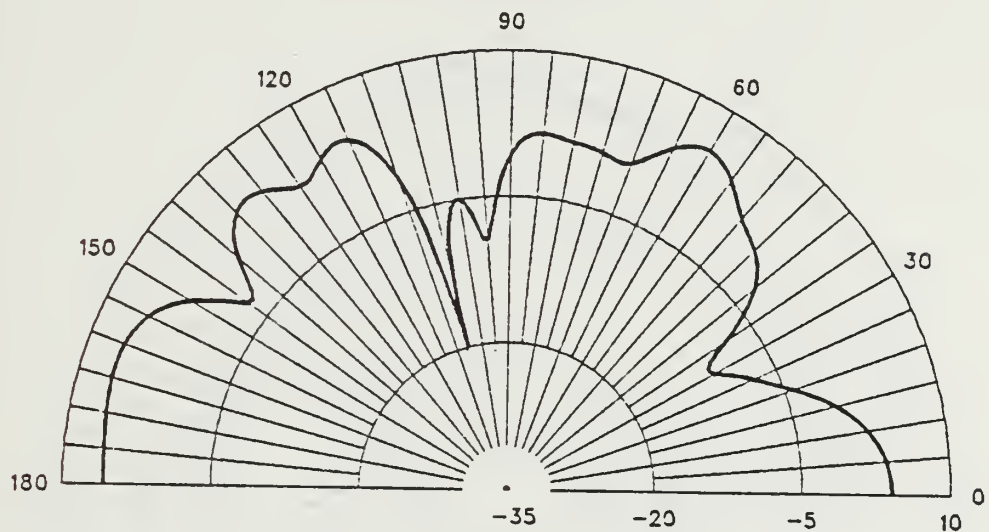


Figure 3.23 E-Field Elevation Pattern at 10.0 MHz
for EF-TLA on the Bow and the Stern.

TF-TLA ON THE BOW AND THE STERN

FREQUENCY = 2 MHZ

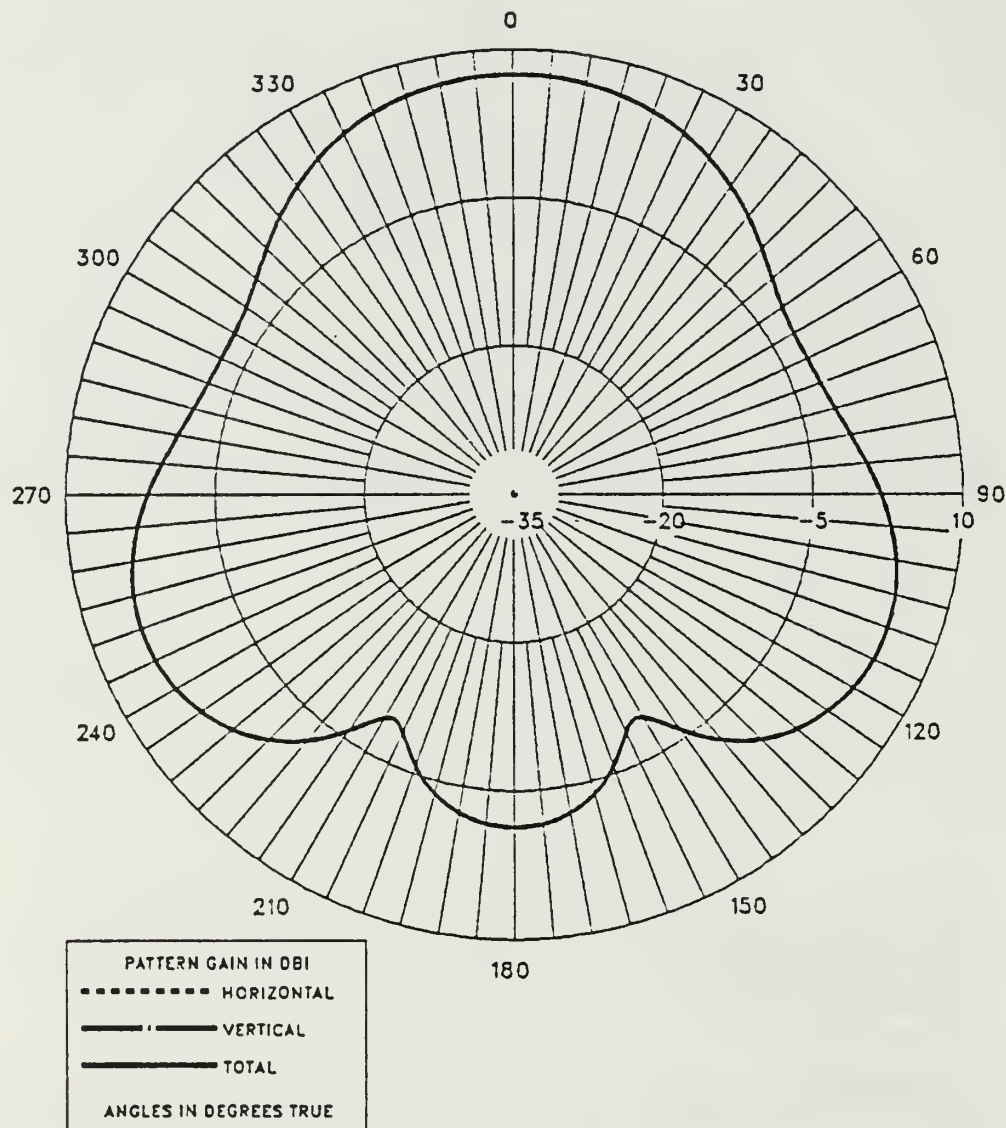


Figure 3.24 E-Field Azimuth Pattern at 2.0 MHz
for TF-TLA on the Bow and the Stern.

TF-TLA ON THE BOW AND THE STERN

FREQUENCY = 2 MHZ

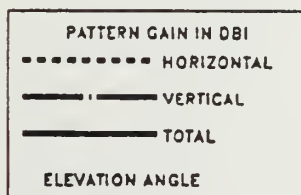
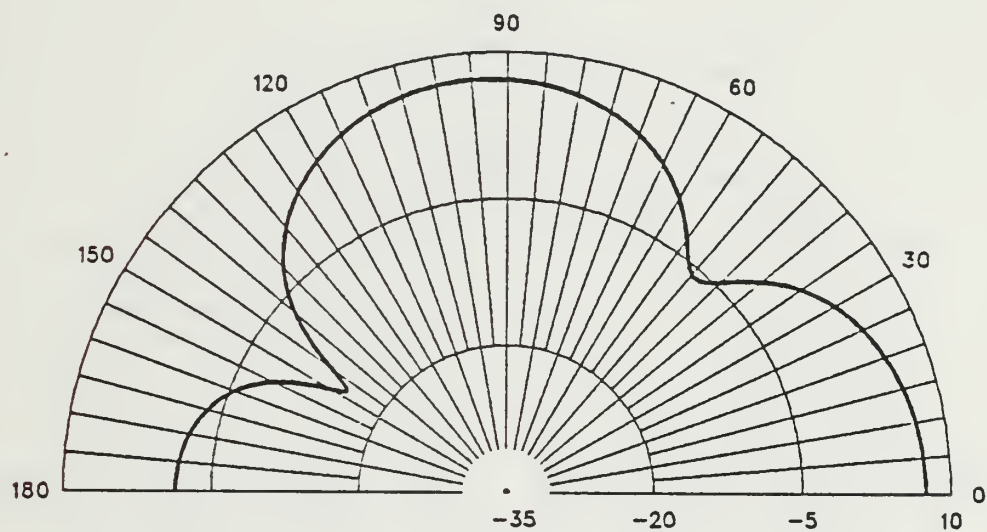


Figure 3.25 E-Field Elevation Pattern at 2.0 MHz
for TF-TLA on the Bow and the Stern.

TF-TLA ON THE BOW AND THE STERN

FREQUENCY = 4.5 MHZ

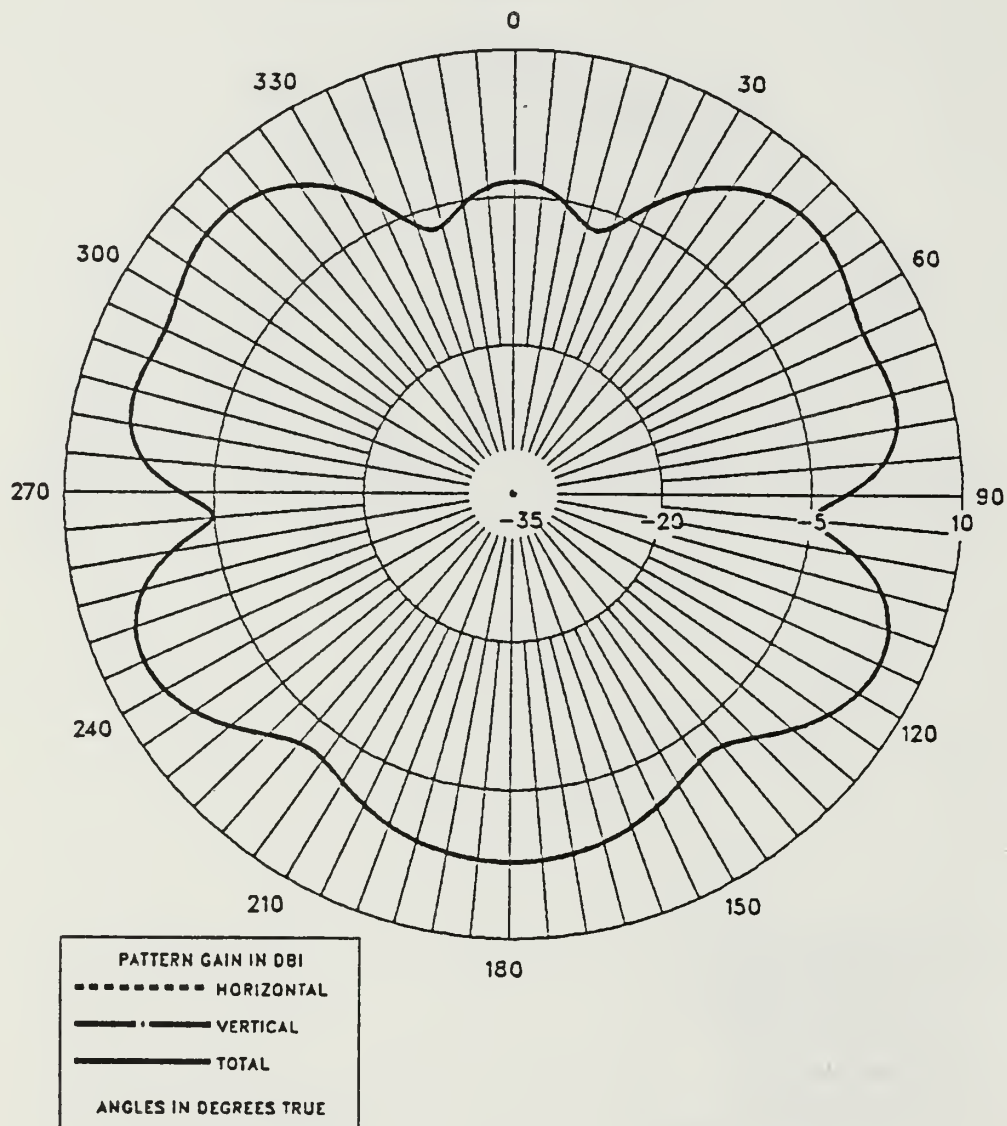
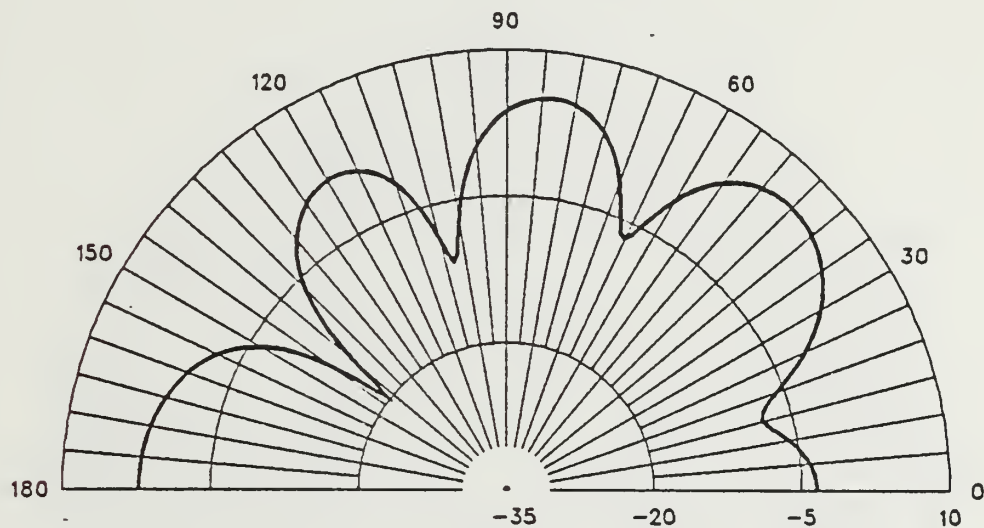


Figure 3.26 E-Field Azimuth Pattern at 4.5 MHz
for TF-TLA on the Bow and the Stern.

TF-TLA ON THE BOW AND THE STERN

FREQUENCY = 4.5 MHZ



PATTERN GAIN IN DBI
----- HORIZONTAL
— VERTICAL
— TOTAL
ELEVATION ANGLE

Figure 3.27 E-Field Elevation Pattern at 4.5 MHz
for TF-TLA on the Bow and the Stern.

TF-TLA ON THE BOW AND THE STERN

FREQUENCY = 7.5 MHZ

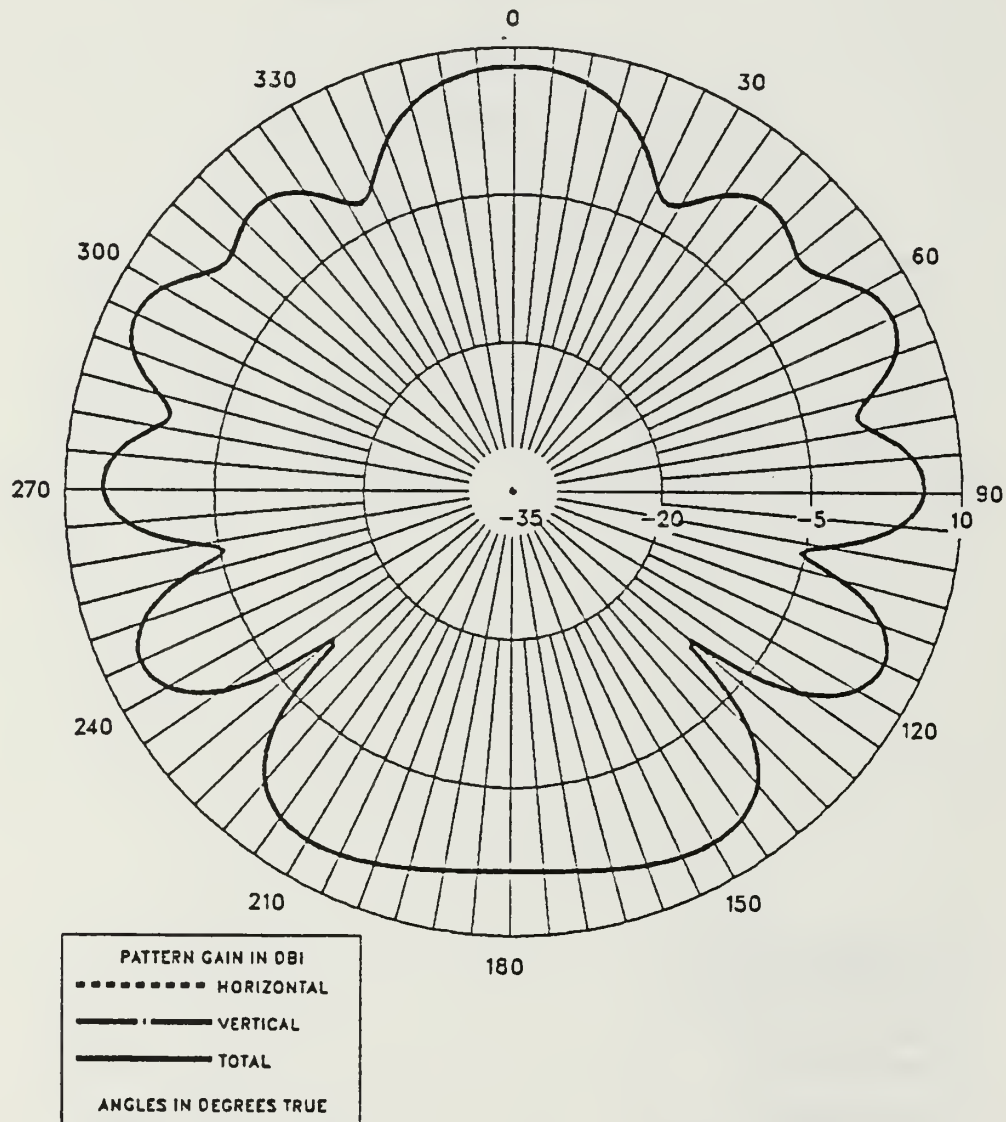


Figure 3.28 E-Field Azimuth Pattern at 7.5 MHz
for TF-TLA on the Bow and the Stern.

TF-TLA ON THE BOW AND THE STERN

FREQUENCY = 7.5 MHZ

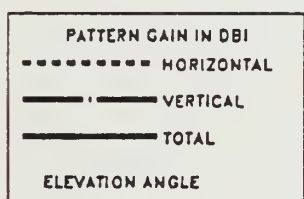
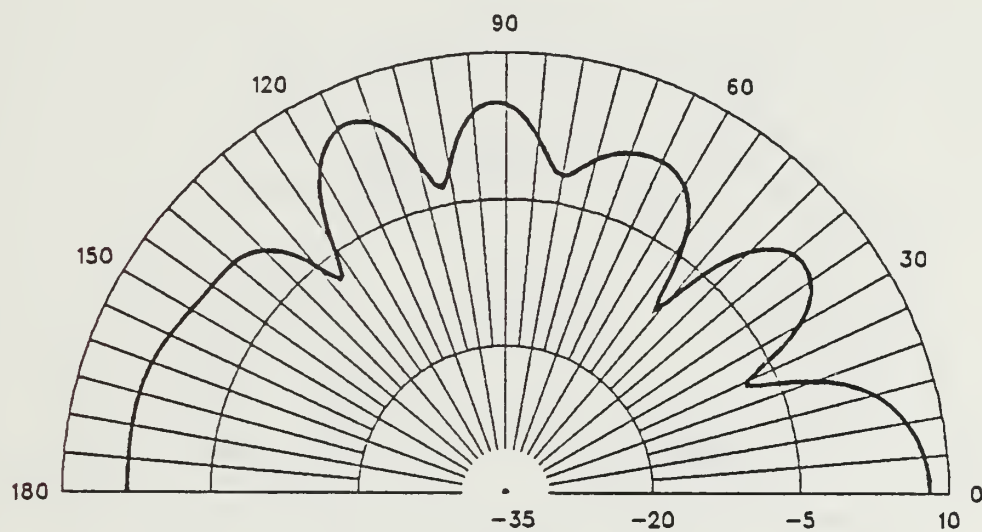


Figure 3.29 E-Field Elevation Pattern at 7.5 MHz
for TF-TLA on the Bow and the Stern.

TF-TLA ON THE BOW AND THE STERN

FREQUENCY = 10 MHZ

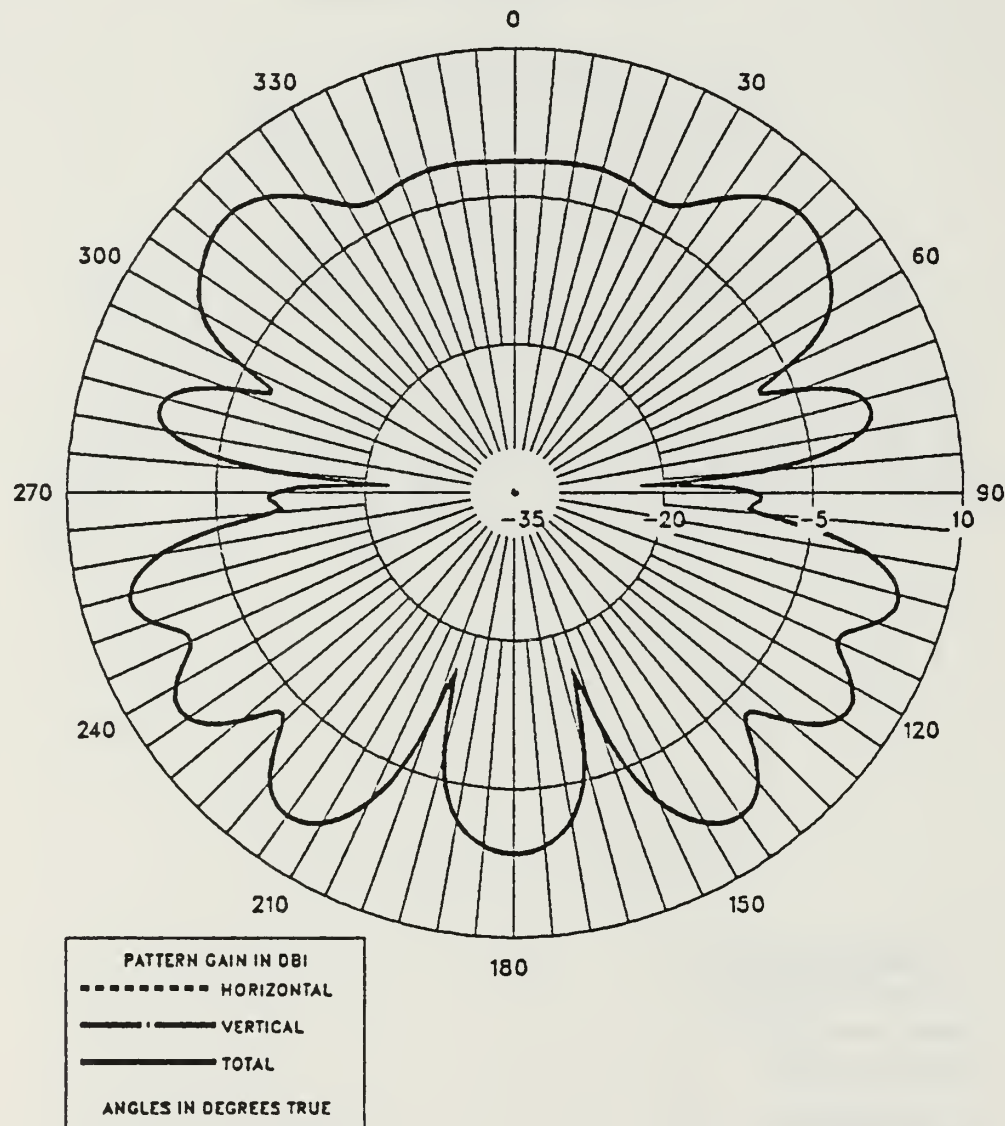


Figure 3.30 E-Field Azimuth Pattern at 10.0 MHz
for TF-TLA on the Bow and the Stern.

TF-TLA ON THE BOW AND THE STERN

FREQUENCY = 10 MHZ

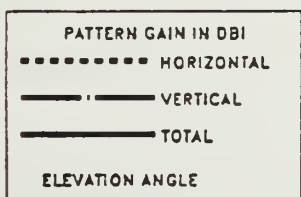
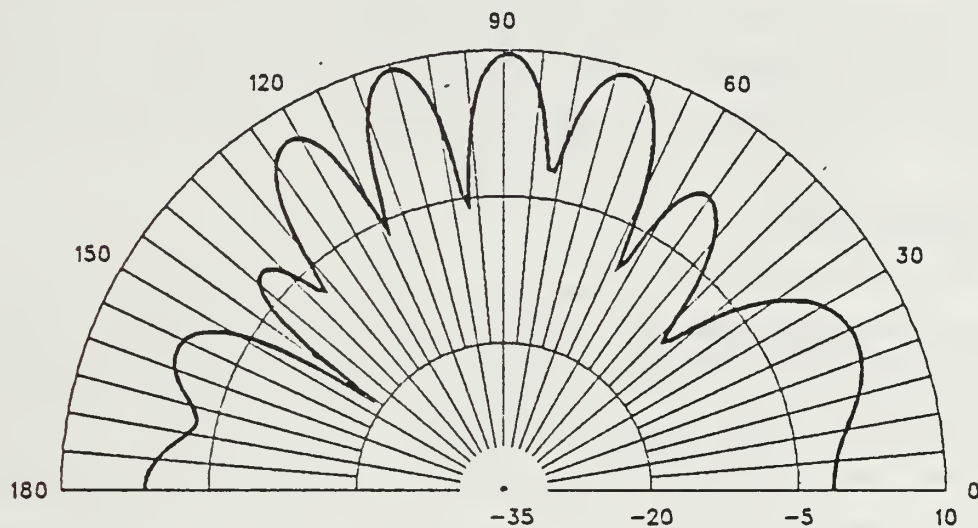


Figure 3.31 E-Field Elevation Pattern at 10.0 MHz
for TF-TLA on the Bow and the Stern.

IV. CONCLUSIONS AND RECOMMENDATIONS

This thesis describes a survivable antenna design and a ship-antenna computer model. The transmission line antenna was modeled for the HF frequency range of 2 - 10 MHz and performance parameters were calculated and presented. A wire grid was used to model the surface of a small frigate. The transmission line antenna was placed on the bow and the stern of the ship and performance for the system was calculated using the NEC program over a perfect ground.

A. CONCLUSIONS

Wire radius changes and increasing the number of segments made virtually no difference in average power gain. The EF-TLA and the TF-TLA had stable average power gains, and the TF-TLA produced more useable radiation patterns for the isolated antenna. The feed location caused different input impedance versus frequency. The resistance was generally low compared with the reactance, particularly in the EF-TLA, which had very high resistance and reactance at 5.2 - 5.4 MHz a resonance frequency. A capacitor and an inductor were used as a load at the far end of the transmission line for the purpose of improving the impedance, but they had no appreciable effect.

For a transmission line antenna on the bow and the stern of the ship, the average power gain of the EF-TLA was acceptable at 4.5 and 7.5 MHz, and the TF-TLA at 2, 4.5, 7.5, and 10 MHz. This identifies the TF-TLA NEC model as more acceptable than the EF-TLA, at the present time. The EF-TLA and the TF-TLA on the bow and the stern had a large difference between resistance and reactance. The elevation pattern of the EF-TLA had a forward lobe that was slightly larger than the backward lobe, and the TF-TLA displayed the opposite effect. Azimuth patterns of the EF-TLA and the TF-TLA show more pronounced lobing at higher frequencies, as can be expected. The patterns are considered useable for shipboard communications for either feed location.

The results of this investigation revealed that transmission line antennas on the bow and the stern of the ship have the common characteristic of requiring equal segment length in the vicinity of the excitation source. The antennas are matchable to 3:1 VSWR at 7.5 MHz in the EF-TLA case and at 4.5 MHz in the TF-TLA case with

a 50 Ohm characteristic impedance. If 500 Ohms is chosen as the normalizing impedance, the above characteristics for matchability reverse with frequency. Thus, the characteristic impedances of 50 Ohms or 500 Ohms yield very limited frequency range for matchable impedance.

B. RECOMMENDATIONS

Many aspects of this study warrant further investigation:

- Since the input impedance was generally high for 50 Ohm normalization, investigate impedance transformation methods or switchable feed points, locating feed at intermediate points between the end and the top, varying the location with frequency to obtain useful results.
- Run additional frequencies for a better impedance definition. Only four frequencies were investigated during this thesis due to time and computer resource limitations.
- Try an increased number of segments on the ship model, in the vicinity of the transmission antenna. This may help improve the accuracy of current definition and improve the average power gain, especially for the end-feed antennas.
- Seek methods to reduce the Q (increase the bandwidth) of the antenna to stabilize the wild impedance variations observed in this study.

APPENDIX A

GEOMETRY DATA SETS

a. Ship NGF Geometry

CM NGF : Wire Grid Model without Antenna
 CM WIRE RADIUS = 0.05 METRES
 CM FREQUENCY = 2, 4.5, 7.5, 10 MHz
 CE

GW 1,1,78.75,2.5,9,78.75,6.8,9,0.05
 GW 2,1,92.5,-1,9,92.5,1,9,0.05
 GW 3,1,92.5,1,9,94.5,1,9,0.05
 GW 4,1,94.5,1,9,94.5,-1,9,0.05
 GW 5,1,94.5,-1,9,92.5,-1,9,0.05
 GW 6,1,92.5,-1,13,92.5,1,13,0.05
 GW 7,3,4.5,0.85,8.625,9,0,0,0.05
 GW 8,3,9,1,7,8.25,9,0,0,0.05
 GW 9,3,13.5,2.55,7.875,13.5,2.55,0,0.05
 GW 10,3,18,3.4,7.5,18,3.4,0,0.05
 GW 11,3,22.5,4.25,7.125,22.5,4.25,0,0.05
 GW 12,2,27,5.1,6.75,27,5.1,0,0.05
 GW 13,2,31.5,5.95,6.375,31.5,5.95,0,0.05
 GW 14,2,36,6.8,6,36,6.8,0,0.05
 GW 15,2,40.5,6.8,5.625,40.5,6.8,0,0.05
 GW 16,2,45,6.8,5.25,45,6.8,0,0.05
 GW 17,2,49.5,6.8,4.875,49.5,6.8,0,0.05
 GW 18,1,54,6.8,4.5,54,6.8,0,0.05
 GW 19,1,58.5,6.8,4.5,58.5,6.8,0,0.05
 GW 20,1,63,6.8,4.5,63,6.8,0,0.05
 GW 21,1,67.5,6.8,4.5,67.5,6.8,0,0.05
 GW 22,1,72,6.8,4.5,72,6.8,0,0.05
 GW 23,1,76.5,6.8,4.5,76.5,6.8,0,0.05
 GW 24,1,81,6.8,4.5,81,6.8,0,0.05
 GW 25,1,85.5,6.8,4.5,85.5,6.8,0,0.05
 GW 26,1,90,6.8,4.5,90,6.8,0,0.05
 GW 27,1,94.5,6.8,4.5,94.5,6.8,0,0.05
 GW 28,1,99,6.8,4.5,99,6.8,0,0.05
 GW 29,3,103.5,6.44,4.5,103.5,6.44,0,0.05
 GW 30,5,108,6.08,4.5,108,6.08,0,0.05
 GW 31,3,112.5,5.72,4.5,112.5,5.72,0,0.05
 GW 32,3,117,5.36,4.5,117,5.36,0,0.05
 GW 33,5,121.5,5,4.5,121.5,5,0,0.05
 GW 34,1,92.5,1,13,94.5,1,13,0.05
 GW 35,1,94.5,1,13,94.5,-1,13,0.05
 GW 36,1,94.5,-1,13,92.5,-1,13,0.05
 GW 37,1,92.5,-1,9,92.5,-1,13,0.05
 GW 38,1,92.5,1,9,92.5,1,13,0.05
 GW 39,1,94.5,-1,9,94.5,-1,13,0.05
 GW 40,3,4.5,-0.85,8.625,9,0,0,0.05
 GW 41,3,9,-1.7,8.25,9,0,0,0.05
 GW 42,3,13.5,-2.55,7.875,13.5,-2.55,0,0.05
 GW 43,3,18,-3.4,7.5,18,-3.4,0,0.05
 GW 44,3,22.5,-4.25,7.125,22.5,-4.25,0,0.05
 GW 45,2,27,-5.1,6.75,27,-5.1,0,0.05
 GW 46,2,31.5,-5.95,6.375,31.5,-5.95,0,0.05
 GW 47,2,36,-6.8,6,36,-6.8,0,0.05
 GW 48,2,40.5,-6.8,5.625,40.5,-6.8,0,0.05
 GW 49,2,45,-6.8,5.25,45,-6.8,0,0.05
 GW 50,2,49.5,-6.8,4.875,49.5,-6.8,0,0.05
 GW 51,1,54,-6.8,4.5,54,-6.8,0,0.05
 GW 52,1,58.5,-6.8,4.5,58.5,-6.8,0,0.05
 GW 53,1,63,-6.8,4.5,63,-6.8,0,0.05
 GW 54,1,67.5,-6.8,4.5,67.5,-6.8,0,0.05
 GW 55,1,72,-6.8,4.5,72,-6.8,0,0.05

GW 56,1,76.5,-6.8,4.5,76.5,-6.8,0,0.05
 GW 57,1,81,-6.8,4.5,81,-6.8,0,0.05
 GW 58,1,85.5,-6.8,4.5,85.5,-6.8,0,0.05
 GW 59,1,90,-6.8,4.5,90,-6.8,0,0.05
 GW 60,1,94.5,-6.8,4.5,94.5,-6.8,0,0.05
 GW 61,1,99,-6.8,4.5,99,-6.8,0,0.05
 GW 62,3,103.5,-6.44,4.5,103.5,-6.44,0,0.05
 GW 63,5,108,-6.08,4.5,108,-6.08,0,0.05
 GW 64,3,112.5,-5.72,4.5,112.5,-5.72,0,0.05
 GW 65,3,117,-5.36,4.5,117,-5.36,0,0.05
 GW 66,5,121.5,-5.45,121.5,-5.0,0.05
 GW 67,1,36,0,6,36,2,6,0.05
 GW 68,1,36,2,6,40.5,5,5.625,0.05
 GW 69,3,40.5,5,5.625,54,5,4.5,0.05
 GW 70,1,54,5,4.5,58.5,5,4.5,0.05
 GW 71,1,58.5,5,4.5,60.75,3.5,4.5,0.05
 GW 72,3,60.75,3.5,4.5,69.75,3.5,4.5,0.05
 GW 73,2,69.75,3.5,4.5,78.75,6.8,4.5,0.05
 GW 74,6,22.5,4.25,7.125,36,6.8,6,0.05
 GW 75,6,22.5,-4.25,7.125,36,-6.8,6,0.05
 GW 76,1,36,2,9,40.5,5,9,0.05
 GW 77,3,40.5,5,9,54,5,9,0.05
 GW 78,1,54,5,9,58.5,5,9,0.05
 GW 79,1,58.5,5,9,60.75,3.5,9,0.05
 GW 80,3,60.75,3.5,9,69.75,3.5,9,0.05
 GW 81,2,69.75,3.5,9,78.75,6.8,9,0.05
 GW 82,1,36,0,6,36,-2,6,0.05
 GW 83,1,36,-2,6,40.5,-5,5.625,0.05
 GW 84,3,40.5,-5,5.625,54,-5,4.5,0.05
 GW 85,1,54,-5,4.5,58.5,-5,4.5,0.05
 GW 86,1,58.5,-5,4.5,60.75,-3.5,4.5,0.05
 GW 87,3,60.75,-3.5,4.5,69.75,-3.5,4.5,0.05
 GW 88,2,69.75,-3.5,4.5,78.75,-6.8,4.5,0.05
 GW 89,1,36,-2,9,40.5,-5,9,0.05
 GW 90,3,40.5,-5,9,54,-5,9,0.05
 GW 91,1,54,-5,9,58.5,-5,9,0.05
 GW 92,1,58.5,-5,9,60.75,-3.5,9,0.05
 GW 93,3,60.75,-3.5,9,69.75,-3.5,9,0.05
 GW 94,2,69.75,-3.5,9,78.75,-6.8,9,0.05
 GW 95,1,36,2,6,36,2,9,0.05
 GW 96,1,40.5,5,5.625,40.5,5,9,0.05
 GW 97,1,58.5,5,4.5,58.5,5,9,0.05
 GW 98,1,60.75,3.5,4.5,60.75,3.5,9,0.05
 GW 99,1,69.75,3.5,4.5,69.75,3.5,9,0.05
 GW 100,1,78.75,6.8,4.5,78.75,6.8,9,0.05
 GW 101,1,99,6.8,4.5,99,6.8,9,0.05
 GW 102,2,99,0,4.5,99,6.8,4.5,0.05
 GW 103,2,99,0,9,99,6.8,9,0.05
 GW 104,1,36,-2,6,36,-2,9,0.05
 GW 105,1,40.5,-5,5.625,40.5,-5,9,0.05
 GW 106,1,58.5,-5,4.5,58.5,-5,9,0.05
 GW 107,1,60.75,-3.5,4.5,60.75,-3.5,9,0.05
 GW 108,1,69.75,-3.5,4.5,69.75,-3.5,9,0.05
 GW 109,1,78.75,-6.8,4.5,78.75,-6.8,9,0.05
 GW 110,1,99,-6.8,4.5,99,-6.8,9,0.05
 GW 111,2,99,0,4.5,99,-6.8,4.5,0.05
 GW 112,2,99,0,9,99,-6.8,9,0.05
 GW 113,2,27,-1.5,6.75,27,1.5,6.75,0.05
 GW 114,2,27,1.5,6.75,31.5,1.5,6.375,0.05
 GW 115,2,31.5,1.5,6.375,31.5,-1.5,6.375,0.05
 GW 116,2,31.5,-1.5,6.375,27,-1.5,6.75,0.05
 GW 117,2,27,-1.5,9,27,1.5,9,0.05
 GW 118,1,27,1.5,9,31.5,1.5,9,0.05
 GW 119,2,31.5,1.5,9,31.5,-1.5,9,0.05
 GW 120,1,31.5,-1.5,9,27,-1.5,9,0.05
 GW 121,1,27,-1.5,6.75,27,-1.5,9,0.05
 GW 122,1,27,1.5,6.75,27,1.5,9,0.05
 GW 123,1,31.5,1.5,6.375,31.5,1.5,9,0.05
 GW 124,1,31.5,-1.5,6.375,31.5,-1.5,9,0.05
 GW 125,10,0,0,9,22.5,4.25,7.125,0.05

GW 126,4,36,6.8,6,54,6.8,4.5,0.05
 GW 127,10,54,6.8,4.5,99,6.8,4.5,0.05
 GW 128,20,99,6.8,4.5,121.5,5,4.5,0.05
 GW 129,10,0,0,9,22.5,-4.25,7.125,0.05
 GW 130,4,36,-6.8,6,54,-6.8,4.5,0.05
 GW 131,10,54,-6.8,4.5,99,-6.8,4.5,0.05
 GW 132,20,99,-6.8,4.5,121.5,-5,4.5,0.05
 GW 133,6,0,0,9,9,0,0,0,0.05
 GW 134,4,0,0,9,0,0,13.5,0.05
 GW 135,3,121.5,0,4.5,121.5,0,0,0.05
 GW 136,3,121.5,0,4.5,121.5,0,9,0.05
 GW 137,12,0,0,9,27,0,6.75,0.05
 GW 138,2,31.5,0,6.375,36,0,6,0.05
 GW 139,15,121.5,0,4.5,99,0,4.5,0.05
 GW 140,2,4.5,-0.85,8.625,4.5,0.85,8.625,0.05
 GW 141,2,9,-1.70,8.25,9,1,7.8.25,0.05
 GW 142,4,13.5,-2.550,7.875,13.5,2.55,7.875,0.05
 GW 143,4,18,-3.40,7.5,18,3.4,7.5,0.05
 GW 144,4,22.5,-4.250,7.125,22.5,4.25,7.125,0.05
 GW 145,8,81,6.8,9,99,6.8,9,0.05
 GW 146,8,81,-6.8,9,99,-6.8,9,0.05
 GW 147,2,85.5,6.8,9,85.5,6.8,18,0.05
 GW 148,4,121.5,0,4.5,121.5,5,4.5,0.05
 GW 149,4,117,0,4.5,117,5.36,4.5,0.05
 GW 150,4,112.5,0,4.5,112.5,5.72,4.5,0.05
 GW 151,4,108,0,4.5,108,6.08,4.5,0.05
 GW 152,4,103.5,0,4.5,103.5,6.44,4.5,0.05
 GW 153,4,121.5,0,4.5,121.5,-5,4.5,0.05
 GW 154,4,117,0,4.5,117,-5.36,4.5,0.05
 GW 155,4,112.5,0,4.5,112.5,-5.72,4.5,0.05
 GW 156,4,108,0,4.5,108,-6.08,4.5,0.05
 GW 157,4,103.5,0,4.5,103.5,-6.44,4.5,0.05
 GW 158,1,78.75,6.8,9,81,6.8,9,0.05
 GW 159,1,78.75,-6.8,9,81,-6.8,9,0.05
 GW 160,1,36,0,12,36,2,12,0.05
 GW 161,2,36,2,12,40.5,5,12,0.05
 GW 162,1,40.5,5,12,45,5,12,0.05
 GW 163,2,45,5,12,45,0,12,0.05
 GW 164,1,36,0,12,36,-2,12,0.05
 GW 165,2,36,-2,12,40.5,-5,12,0.05
 GW 166,1,40.5,-5,12,45,-5,12,0.05
 GW 167,2,45,-5,12,45,0,12,0.05
 GW 168,1,40.5,-1.5,12,40.5,1.5,12,0.05
 GW 169,1,40.5,1.5,12,43.5,1.5,12,0.05
 GW 170,1,43.5,1.5,12,43.5,-1.5,12,0.05
 GW 171,1,43.5,-1.5,12,40.5,-1.5,12,0.05
 GW 172,1,40.5,-1.5,16,40.5,1.5,16,0.05
 GW 173,1,40.5,1.5,16,43.5,1.5,16,0.05
 GW 174,1,43.5,1.5,16,43.5,-1.5,16,0.05
 GW 175,1,43.5,-1.5,16,40.5,-1.5,16,0.05
 GW 176,1,40.5,-1.5,12,40.5,-1.5,16,0.05
 GW 177,1,40.5,1.5,12,40.5,1.5,16,0.05
 GW 178,1,43.5,-1.5,12,43.5,-1.5,16,0.05
 GW 179,1,43.5,1.5,12,43.5,1.5,16,0.05
 GW 180,1,36,2,9,36,-2,9,0.05
 GW 181,1,45,0,9,45,0,12,0.05
 GW 182,2,36,0,12,36,0,21,0.05
 GW 183,1,36,2,9,36,2,12,0.05
 GW 184,1,40.5,5,9,40.5,5,12,0.05
 GW 185,1,45,5,9,45,5,12,0.05
 GW 186,1,36,-2,9,36,-2,12,0.05
 GW 187,1,40.5,-5,9,40.5,-5,12,0.05
 GW 188,1,45,-5,9,45,-5,12,0.05
 GW 189,2,45,5,9,45,0,9,0.05
 GW 190,2,45,-5,9,45,0,9,0.05
 GW 191,1,40.5,1.5,12,40.5,5,12,0.05
 GW 192,1,40.5,-1.5,12,40.5,-5,12,0.05
 GW 193,1,46.5,1.5,9,46.5,-1.5,9,0.05
 GW 194,1,46.5,1.5,9,49.5,1.5,9,0.05
 GW 195,1,49.5,1.5,9,49.5,-1.5,9,0.05

GW 196,1,46.5,-1.5,9,49.5,-1.5,9,0.05
 GW 197,1,46.5,1.5,9,46.5,1.5,12,0.05
 GW 198,1,46.5,-1.5,9,46.5,-1.5,12,0.05
 GW 199,1,49.5,1.5,9,49.5,1.5,12,0.05
 GW 200,1,49.5,-1.5,9,49.5,-1.5,12,0.05
 GW 201,1,46.5,1.5,12,46.5,-1.5,12,0.05
 GW 202,1,46.5,1.5,12,49.5,1.5,12,0.05
 GW 203,1,49.5,1.5,12,49.5,-1.5,12,0.05
 GW 204,1,46.5,-1.5,12,49.5,-1.5,12,0.05
 GW 205,1,46.5,1.5,12,46.5,1.5,15,0.05
 GW 206,1,46.5,-1.5,12,46.5,-1.5,15,0.05
 GW 207,1,49.5,1.5,12,49.5,1.5,15,0.05
 GW 208,1,49.5,-1.5,12,49.5,-1.5,15,0.05
 GW 209,1,46.5,1.5,15,46.5,-1.5,15,0.05
 GW 210,1,46.5,1.5,15,49.5,1.5,15,0.05
 GW 211,1,49.5,1.5,15,49.5,-1.5,15,0.05
 GW 212,1,46.5,-1.5,15,49.5,-1.5,15,0.05
 GW 213,1,46.5,1.5,15,46.5,1.5,18,0.05
 GW 214,1,46.5,-1.5,15,46.5,-1.5,18,0.05
 GW 215,1,49.5,1.5,15,49.5,1.5,18,0.05
 GW 216,1,49.5,-1.5,15,49.5,-1.5,18,0.05
 GW 217,1,46.5,1.5,18,46.5,-1.5,18,0.05
 GW 218,1,46.5,1.5,18,49.5,1.5,18,0.05
 GW 219,1,49.5,1.5,18,49.5,-1.5,18,0.05
 GW 220,1,46.5,-1.5,18,49.5,-1.5,18,0.05
 GW 221,1,46.5,1.5,18,46.5,1.5,21,0.05
 GW 222,1,46.5,-1.5,18,46.5,-1.5,21,0.05
 GW 223,1,49.5,1.5,18,49.5,1.5,21,0.05
 GW 224,1,49.5,-1.5,18,49.5,-1.5,21,0.05
 GW 225,1,46.5,1.5,21,46.5,-1.5,21,0.05
 GW 226,1,46.5,1.5,21,49.5,1.5,21,0.05
 GW 227,1,49.5,1.5,21,49.5,-1.5,21,0.05
 GW 228,1,46.5,-1.5,21,49.5,-1.5,21,0.05
 GW 229,1,49.5,1.5,9,49.5,5,9,0.05
 GW 230,1,49.5,-1.5,9,49.5,-5,9,0.05
 GW 231,1,54,1.5,9,54,-1.5,9,0.05
 GW 232,1,54,1.5,9,57,1.5,9,0.05
 GW 233,1,57,1.5,9,57,-1.5,9,0.05
 GW 234,1,54,-1.5,9,57,-1.5,9,0.05
 GW 235,1,54,1.5,9,54,1.5,12,0.05
 GW 236,1,54,-1.5,9,54,-1.5,12,0.05
 GW 237,1,57,1.5,9,57,1.5,12,0.05
 GW 238,1,57,-1.5,9,57,-1.5,12,0.05
 GW 239,1,54,1.5,12,54,-1.5,12,0.05
 GW 240,1,54,1.5,12,57,1.5,12,0.05
 GW 241,1,57,1.5,12,57,-1.5,12,0.05
 GW 242,1,54,-1.5,12,57,-1.5,12,0.05
 GW 243,1,54,1.5,12,54,1.5,15,0.05
 GW 244,1,54,-1.5,12,54,-1.5,15,0.05
 GW 245,1,57,1.5,12,57,1.5,15,0.05
 GW 246,1,57,-1.5,12,57,-1.5,15,0.05
 GW 247,1,54,1.5,15,54,-1.5,15,0.05
 GW 248,1,54,1.5,15,57,1.5,15,0.05
 GW 249,1,57,1.5,15,57,-1.5,15,0.05
 GW 250,1,54,-1.5,15,57,-1.5,15,0.05
 GW 251,1,54,1.5,15,54,1.5,18,0.05
 GW 252,1,54,-1.5,15,54,-1.5,18,0.05
 GW 253,1,57,1.5,15,57,1.5,18,0.05
 GW 254,1,57,-1.5,15,57,-1.5,18,0.05
 GW 255,1,54,1.5,18,54,-1.5,18,0.05
 GW 256,1,54,1.5,18,57,1.5,18,0.05
 GW 257,1,57,1.5,18,57,-1.5,18,0.05
 GW 258,1,54,-1.5,18,57,-1.5,18,0.05
 GW 259,1,54,1.5,18,54,1.5,21,0.05
 GW 260,1,54,-1.5,18,54,-1.5,21,0.05
 GW 261,1,57,1.5,18,57,1.5,21,0.05
 GW 262,1,57,-1.5,18,57,-1.5,21,0.05
 GW 263,1,54,1.5,21,54,-1.5,21,0.05
 GW 264,1,54,1.5,21,57,1.5,21,0.05
 GW 265,1,57,1.5,21,57,-1.5,21,0.05

GW 266,1,54,-1.5,21,57,-1.5,21,0,05
 GW 267,1,54,1.5,21,54,1.5,24,0,05
 GW 268,1,54,-1.5,21,54,-1.5,24,0,05
 GW 269,1,57,1.5,21,57,1.5,24,0,05
 GW 270,1,57,-1.5,21,57,-1.5,24,0,05
 GW 271,2,54,1.5,24,54,-1.5,24,0,05
 GW 272,1,54,1.5,24,57,1.5,24,0,05
 GW 273,2,57,1.5,24,57,-1.5,24,0,05
 GW 274,1,54,-1.5,24,57,-1.5,24,0,05
 GW 275,1,54,1.5,24,54,5,24,0,05
 GW 276,1,54,5,24,57,5,24,0,05
 GW 277,1,57,5,24,57,1.5,24,0,05
 GW 278,1,54,5,24,52,5,24,0,05
 GW 279,1,57,5,24,59,5,24,0,05
 GW 280,2,31.5,-1.5,6,375,31.5,-5.95,6.375,0,05
 GW 281,2,31.5,1.5,6,375,31.5,5.95,6.375,0,05
 GW 282,1,54,-1.5,24,54,-5,24,0,05
 GW 283,1,54,-5,24,57,-5,24,0,05
 GW 284,1,57,-5,24,57,-1.5,24,0,05
 GW 285,1,54,-5,24,52,-5,24,0,05
 GW 286,1,57,-5,24,59,-5,24,0,05
 GW 287,2,54,0,24,57,0,24,0,05
 GW 288,2,55.5,0,24,55.5,0,31,0,05
 GW 289,1,54,1.5,9,54,5,9,0,05
 GW 290,1,54,-1.5,9,54,-5,9,0,05
 GW 291,1,57,-1.5,9,60,-1.5,9,0,05
 GW 292,1,60,-1.5,9,60,1.5,9,0,05
 GW 293,1,60,1.5,9,57,1.5,9,0,05
 GW 294,1,57,-1.5,12,60,-1.5,12,0,05
 GW 295,1,60,-1.5,12,60,1.5,12,0,05
 GW 296,1,60,1.5,12,57,1.5,12,0,05
 GW 297,1,60,-1.5,9,60,-1.5,12,0,05
 GW 298,1,60,1.5,9,60,1.5,12,0,05
 GW 299,1,64.5,-1.5,9,64.5,1.5,9,0,05
 GW 300,1,64.5,1.5,9,67.5,1.5,9,0,05
 GW 301,1,67.5,1.5,9,67.5,-1.5,9,0,05
 GW 302,1,67.5,-1.5,9,64.5,-1.5,9,0,05
 GW 303,1,64.5,-1.5,9,64.5,-1.5,12,0,05
 GW 304,1,64.5,1.5,9,64.5,1.5,12,0,05
 GW 305,1,67.5,1.5,9,67.5,1.5,12,0,05
 GW 306,1,67.5,-1.5,9,67.5,-1.5,12,0,05
 GW 307,1,64.5,-1.5,12,64.5,1.5,12,0,05
 GW 308,1,64.5,1.5,12,67.5,1.5,12,0,05
 GW 309,1,67.5,1.5,12,67.5,-1.5,12,0,05
 GW 310,1,67.5,-1.5,12,64.5,-1.5,12,0,05
 GW 311,1,64.5,-1.5,12,64.5,-1.5,15,0,05
 GW 312,1,64.5,1.5,12,64.5,1.5,15,0,05
 GW 313,1,67.5,1.5,12,67.5,1.5,15,0,05
 GW 314,1,67.5,-1.5,12,67.5,-1.5,15,0,05
 GW 315,1,64.5,-1.5,15,64.5,1.5,15,0,05
 GW 316,1,64.5,1.5,15,67.5,1.5,15,0,05
 GW 317,1,67.5,1.5,15,67.5,-1.5,15,0,05
 GW 318,1,67.5,-1.5,15,64.5,-1.5,15,0,05
 GW 319,1,67.5,1.5,9,69.75,3.5,9,0,05
 GW 320,1,67.5,-1.5,9,69.75,-3.5,9,0,05
 GW 321,1,69.75,-1,9,69.75,1,9,0,05
 GW 322,1,69.75,1,9,72,1,9,0,05
 GW 323,1,72,1,9,72,-1,9,0,05
 GW 324,1,72,-1,9,69.75,-1,9,0,05
 GW 325,1,69.75,-1,12,69.75,1,12,0,05
 GW 326,1,69.75,1,12,72,1,12,0,05
 GW 327,1,72,1,12,72,-1,12,0,05
 GW 328,1,72,-1,12,69.75,-1,12,0,05
 GW 329,1,69.75,-1,9,69.75,-1,12,0,05
 GW 330,1,69.75,1,9,69.75,1,12,0,05
 GW 331,1,72,-1,9,72,-1,12,0,05
 GW 332,1,72,1,9,72,1,12,0,05
 GW 333,1,27,-1.5,6.75,27,-5.1,6.75,0,05
 GW 334,1,27,1.5,6.75,27,5.1,6.75,0,05
 GW 335,1,69.75,-1,9,69.75,-3.5,9,0,05

GW 336,1,69.75,1,9,69.75,3.5,9,0,05
 GW 337,2,78.75,-2.5,9,78.75,2.5,9,0,05
 GW 338,2,78.75,2.5,9,84.75,2.5,9,0,05
 GW 339,2,84.75,2.5,9,84.75,-2.5,9,0,05
 GW 340,2,84.75,-2.5,9,78.75,-2.5,9,0,05
 GW 341,2,78.75,-2.5,13,78.75,2.5,13,0,05
 GW 342,2,78.75,2.5,13,84.75,2.5,13,0,05
 GW 343,2,84.75,2.5,13,84.75,-2.5,13,0,05
 GW 344,2,84.75,-2.5,13,78.75,-2.5,13,0,05
 GW 345,1,78.75,-2.5,9,78.75,-2.5,13,0,05
 GW 346,1,78.75,2.5,9,78.75,2.5,13,0,05
 GW 347,1,84.75,-2.5,9,84.75,-2.5,13,0,05
 GW 348,1,84.75,2.5,9,84.75,2.5,13,0,05
 GW 349,1,78.75,-2.5,9,78.75,-6.8,9,0,05
 GW 350,1,94.5,1,9,94.5,1,13,0,05
 GW 351,2,94.5,-6.8,9,94.5,-6.8,18,0,05
 GW 352,2,94.5,6.8,9,94.5,6.8,18,0,05
 GW 353,2,94.5,-1,9,94.5,-6.8,9,0,05
 GW 354,2,94.5,1,9,94.5,6.8,9,0,05
 GW 355,2,76.5,6.8,4.5,81,6.8,4.5,0,05
 GW 356,2,76.5,-6.8,4.5,81,-6.8,4.5,0,05
 GW 357,2,36,2,6,36,6.8,6,0,05
 GW 358,2,36,-2,6,36,-6.8,6,0,05
 GW 359,2,85.5,-6.8,9,85.5,-6.8,18,0,05
 GW 360,1,18,3.4,7.5,18,3.4,8.625,0,05
 GW 361,8,18,3.4,8.625,0,0,10.125,0,05
 GW 362,1,18,-3.4,7.5,18,-3.4,8.625,0,05
 GW 363,8,18,-3.4,8.625,0,0,10.125,0,05
 GW 364,1,0,0,10.125,0,0,9,0,05
 GW 365,1,13.5,2.55,7.875,13.5,2.55,9,0,05
 GW 366,1,9,1.7,8.25,9,1.7,9.375,0,05
 GW 367,1,4.5,0.85,8.625,4.5,0.85,9.75,0,05
 GW 368,1,13.5,-2.55,7.875,13.5,-2.55,9,0,05
 GW 369,1,9,-1.7,8.25,9,-1.7,9.375,0,05
 GW 370,1,4.5,-0.85,8.625,4.5,-0.85,9.75,0,05
 GE1
 GN1
 FR 0,0,0,0,2 (4.5, 7.5, 10)
 WG
 EN

b. End Feed Transmission Line Antenna on the Bow

CM EF-TLA WIRE GRID MODEL
 CM HEIGHT = 0.6 METERS
 CM LENGTH = 13.5 METERS
 CM WIRE RADIUS = 0.05 METERS
 CM SOURCE POINT = 2
 CE
 GF
 GW 371,1,4.5,0.85,10.35,4.5,0.85,9.75,0,05
 GW 372,7,4.5,0.85,10.35,18,3.4,9.225,0,05
 GW 373,1,18,3.4,8.625,18,3.4,9.225,0,05
 GW 374,1,4.5,-0.85,10.35,4.5,-0.85,9.75,0,05
 GW 375,7,4.5,-0.85,10.35,18,-3.4,9.225,0,05
 GW 376,1,18,-3.4,8.625,18,-3.4,9.225,0,05
 GE1
 EX 0,373,1,00,1
 EX 0,376,1,00,1
 RP 0,91,10,1501,0,0,1,10
 PL3, 2, 0, 4
 RPO, 1, 361, 1000, 90, 0, 0, 1, 1 STD. HORIZONTAL PATTERN CUT
 PL3, 1, 0, 4
 RPO, 181, 1, 1000, -90, 0, 1, 0 STD. VERTICAL PATTERN CUT
 EN

c. End Feed Transmission Line Antenna on the Stern

```
CM      EF-TLA WIRE GRID MODEL
CM      HEIGHT      = 0.6  METERS
CM      LENGTH      = 13.5 METERS
CM      WIRE RADIUS = 0.05 METERS
CM      - SOURCE POINT = 2
CE
GF
GW 371,1,108,6.08,4.5,108,6.08,5.1,0.05
GW 372,7,108,6.08,5.1,121.5,5,5.1,0.05
GW 373,1,121.5,5,5.1,121.5,5,4.5,0.05
GW 374,1,108,-6.08,4.5,108,-6.08,5.1,0.05
GW 375,7,108,-6.08,5.1,121.5,-5,5.1,0.05
GW 376,1,121.5,-5,5.1,121.5,-5,4.5,0.05
GE1
EX 0,371,1,00,1
EX 0,374,1,00,1
RP 0,91,10,1501,0,0,1,10
PL3, 2, 0, 4
RPO, 1, 361, 1000, 90, 0, 0, 1      STD. HORIZONTAL PATTERN CUT
PL3, 1, 0, 4
RPO, 181, 1, 1000, -90, 0, 1, 0      STD. VERTICAL PATTERN CUT
EN
```

d. End Feed Transmission Line Antenna on the Bow and the Stern

```
CM      EF-TLA WIRE GRID MODEL
CM      HEIGHT      = 0.6  METERS
CM      LENGTH      = 13.5 METERS
CM      WIRE RADIUS = 0.05 METERS
CM      SOURCE POINT = 4
CE
GF
GW 371,1,4.5,0.85,10.35,4.5,0.85,9.75,0.05
GW 372,7,4.5,0.85,10.35,18,3.4,9.225,0.05
GW 373,1,18,3.4,8.625,18,3.4,9.225,0.05
GW 374,1,4.5,-0.85,10.35,4.5,-0.85,9.75,0.05
GW 375,7,4.5,-0.85,10.35,18,-3.4,9.225,0.05
GW 376,1,18,-3.4,8.625,18,-3.4,9.225,0.05
GW 377,1,108,6.08,4.5,108,6.08,5.1,0.05
GW 378,7,108,6.08,5.1,121.5,5,5.1,0.05
GW 379,1,121.5,5,5.1,121.5,5,4.5,0.05
GW 380,1,108,-6.08,4.5,108,-6.08,5.1,0.05
GW 381,7,108,-6.08,5.1,121.5,-5,5.1,0.05
GW 382,1,121.5,-5,5.1,121.5,-5,4.5,0.05
GE1
EX 0,373,1,00,1
EX 0,376,1,00,1
EX 0,377,1,00,1
EX 0,380,1,00,1
RP 0,91,10,1501,0,0,1,10
PL3, 2, 0, 4
RPO, 1, 361, 1000, 90, 0, 0, 1      STD. HORIZONTAL PATTERN CUT
PL3, 1, 0, 4
RPO, 181, 1, 1000, -90, 0, 1, 0      STD. VERTICAL PATTERN CUT
EN
```

e. Top Feed Transmission Line Antenna on the Bow

```
CM      TF-TLA WIRE GRID MODEL
CM      HEIGHT      = 0.6  METERS
CM      LENGTH      = 13.5 METERS
CM      WIRE RADIUS = 0.05 METERS
CM      SOURCE POINT = 2
CE
```

GF
 GW 371,1,4.5,0.85,10.35,4.5,0.85,9.75,0.05
 GW 372,19,4.5,0.85,10.35,18,3.4,9.225,0.05
 GW 373,1,18,3.4,8.625,18,3.4,9.225,0.05
 GW 374,1,4.5,-0.85,10.35,4.5,-0.85,9.75,0.05
 GW 375,19,4.5,-0.85,10.35,18,-3.4,9.225,0.05
 GW 376,1,18,-3.4,8.625,18,-3.4,9.225,0.05
 GE1
 EX 0,372,10,00,1
 EX 0,375,10,00,1
 RP 0,91,10,1501,0,0,1,10
 PL3, 2, 0, 4
 RPO, 1, 361, 1000, 90, 0, 0, 1 STD. HORIZONTAL PATTERN CUT
 PL3, 1, 0, -4
 RPO, 181, 1, 1000, -90, 0, 1, 0 STD. VERTICAL PATTERN CUT
 EN

f. Top Feed Transmission Line Antenna on the Stern

CM TF-TLA WIRE GRID MODEL
 CM HEIGHT = 0.6 METERS
 CM LENGTH = 13.5 METERS
 CM WIRE RADIUS = 0.05 METERS
 CM SOURCE POINT = 2
 CE
 GF
 GW 371,1,108,6.08,4.5,108,6.08,5.1,0.05
 GW 372,19,108,6.08,5.1,121.5,5.5,5.1,0.05
 GW 373,1,121.5,5.5,5.1,121.5,5.5,4.5,0.05
 GW 374,1,108,-6.08,4.5,108,-6.08,5.1,0.05
 GW 375,19,108,-6.08,5.1,121.5,-5.5,5.1,0.05
 GW 376,1,121.5,-5.5,5.1,121.5,-5,4.5,0.05
 GE1
 EX 0,372,10,00,1
 EX 0,375,10,00,1
 RP 0,91,10,1501,0,0,1,10
 PL3, 2, 0, 4
 RPO, 1, 361, 1000, 90, 0, 0, 1 STD. HORIZONTAL PATTERN CUT
 PL3, 1, 0, 4
 RPO, 181, 1, 1000, -90, 0, 1, 0 STD. VERTICAL PATTERN CUT
 EN

g. Top Feed Transmission Line Antenna on the Bow and the Stern

CM TF-TLA WIRE GRID MODEL
 CM HEIGHT = 0.6 METERS
 CM LENGTH = 13.5 METERS
 CM WIRE RADIUS = 0.05 METERS
 CM SOURCE POINT = 4
 CE
 GF
 GW 371,1,4.5,0.85,10.35,4.5,0.85,9.75,0.05
 GW 372,19,4.5,0.85,10.35,18,3.4,9.225,0.05
 GW 373,1,18,3.4,8.625,18,3.4,9.225,0.05
 GW 374,1,4.5,-0.85,10.35,4.5,-0.85,9.75,0.05
 GW 375,19,4.5,-0.85,10.35,18,-3.4,9.225,0.05
 GW 376,1,18,-3.4,8.625,18,-3.4,9.225,0.05
 GW 377,1,108,6.08,4.5,108,6.08,5.1,0.05
 GW 378,19,108,6.08,5.1,121.5,5.5,5.1,0.05
 GW 379,1,121.5,5.5,5.1,121.5,5.5,4.5,0.05
 GW 380,1,108,-6.08,4.5,108,-6.08,5.1,0.05
 GW 381,19,108,-6.08,5.1,121.5,-5.5,5.1,0.05
 GW 382,1,121.5,-5.5,5.1,121.5,-5,4.5,0.05
 GE1
 EX 0,372,10,00,1
 EX 0,375,10,00,1
 EX 0,378,10,00,1

EX 0,381,10,00,1
RP 0,91,10,1501,0,0,1,10
PL3, 2, 0, 4
RPO, 1, 361, 1000, 90, 0, 0, 1 STD. HORIZONTAL PATTERN CUT
PL3, 1, 0, 4
RPO, 181, 1, 1000, -90, 0, 1, 0 STD. VERTICAL PATTERN CUT
EN

APPENDIX B
AVERAGE POWER GAIN FOR REACTIVELY LOADED
TRANSMISSION LINE ANTENNAS VS FREQUENCY

This appendix provides average power gains for end feed transmission line antenna from 2 - 10 MHz with three different capacitors, with three different inductors and from 4.0 - 6.9 MHz with 9 segments and a 0.05 meter radius, showing valid numerical models.

TABLE 10
AVERAGE POWER GAINS OF TLA WITH CAPACITIVE LOADS

Frequency in MHz	$C = 10^{-6}$ in Farads	$C = 10^{-9}$ in Farads	$C = 10^{-12}$ in Farads
2	1.99	1.99	1.99
3	1.99	1.99	1.99
4	1.99	1.99	1.99
5	1.99	1.99	1.99
6	1.99	1.99	1.99
7	1.99	1.99	1.99
8	1.99	1.99	1.98
9	1.99	1.99	1.97
10	1.99	1.99	1.97

TABLE 11
AVERAGE POWER GAINS OF TLA WITH INDUCTIVE LOADS

Frequency in MHz	$L = 10^{-2}$ in Henry	$L = 10^{-4}$ in Henry	$L = 10^{-6}$ in Henry
2	1.99	1.99	1.99
3	1.99	1.99	1.99
4	1.99	1.99	1.99
5	1.99	1.99	1.99
6	1.99	1.99	1.99
7	1.99	1.99	1.99
8	1.98	1.98	1.99
9	1.98	1.98	1.99
10	1.97	1.97	2.00

TABLE 12
AVERAGE POWER GAINS FOR EF-TLA FROM 4.0 - 6.9 MHZ
WITH 9 SEGMENTS AND A 0.05 METER RADIUS

Frequency in MHZ	Gain	Frequency in MHZ	Gain	Frequency in MHZ	Gain
4.0	1.99	5.0	1.99	6.0	1.99
4.1	1.99	5.1	1.99	6.1	1.99
4.2	1.99	5.2	1.99	6.2	1.99
4.3	1.99	5.3	1.99	6.3	1.99
4.4	1.99	5.4	1.99	6.4	1.99
4.5	1.99	5.5	1.99	6.5	1.99
4.6	1.99	5.6	1.99	6.6	1.99
4.7	1.99	5.7	1.99	6.7	1.99
4.8	1.99	5.8	1.99	6.8	1.99
4.9	1.99	5.9	1.99	6.9	1.99

APPENDIX C
INPUT IMPEDANCE FOR AN END FEED TRANSMISSION LINE
ANTENNA WITH DIFFERENT RADII, SEGMENTATION, FEED
LOCATION AND LOADING

TABLE 13
RESISTANCE OF TLA WITH THREE DIFFERENT RADII

Frequency in MHz	$r = 0.03$	$r = 0.04$	$r = 0.05$
2	0.01	0.01	0.01
3	0.09	0.09	0.09
4	0.75	0.75	0.75
5	35.02	34.49	34.08
6	7.97	8.03	8.08
7	2.33	2.34	2.34
8	1.44	1.45	1.45
9	1.16	1.16	1.17
10	1.09	1.09	1.09

TABLE 14
REACTANCE OF TLA WITH THREE DIFFERENT RADII

Frequency in MHz	$r = 0.03$	$r = 0.04$	$r = 0.05$
2	153.9	141.7	132.2
3	282.3	260.0	242.6
4	570.3	525.0	489.7
5	2855.4	2613.6	2426.9
6	-1006.7	-932.5	-874.3
7	-392.5	-363.5	-340.8
8	-208.6	-193.7	-181.9
9	-107.2	-100.1	-94.5
10	-32.3	-31.2	-30.2

TABLE 15
RESISTANCE OF TLA WITH FOUR DIFFERENT SEGMENTATIONS

Frequency in MHz	5 segment	9 segment	15 segment	21 segment
2	0.01	0.01	0.01	0.01
3	0.09	0.09	0.09	0.09
4	0.73	0.75	0.75	0.75
5	32.15	34.08	33.76	33.55
6	8.13	8.08	8.17	8.22
7	2.34	2.34	2.36	2.36
8	1.45	1.45	1.45	1.46
9	1.17	1.17	1.17	1.17
10	1.09	1.09	1.09	1.09

TABLE 16
REACTANCE OF TLA WITH THREE DIFFERENT SEGMENTATIONS

Frequency in MHz	5 segment	9 segment	15 segment	21 segment
2	127.1	132.2	134.6	135.5
3	232.9	242.6	247.0	248.6
4	468.8	489.7	498.4	501.4
5	2280.1	2426.8	2454.7	2459.5
6	-846.1	-874.3	-895.1	-903.2
7	-327.6	-340.8	-348.6	-351.5
8	-174.0	-181.9	-186.3	-187.9
9	-89.7	-94.5	-97.1	-97.9
10	-27.7	-30.2	-31.4	-31.9

TABLE 17
RESISTANCE OF TLA WITH THREE DIFFERENT FEED POINTS

Frequency in MHz	EF-TLA	CEF-TLA	TF-TLA
2	0.01	0.01	0.01
3	0.09	0.09	0.05
4	0.75	0.82	0.17
5	34.08	55.54	0.49
6	8.08	7.08	1.33
7	2.34	2.27	3.57
8	1.45	1.46	10.68
9	1.17	1.21	45.01
10	1.09	1.16	924.12

TABLE 18
REACTANCE OF TLA WITH THREE DIFFERENT FEED POINTS

Frequency in MHz	EF-TLA	CEF-TLA	TF-TLA
2	132.2	136.9	117.4
3	242.6	253.3	183.6
4	489.7	522.3	260.8
5	2426.9	3147.5	356.7
6	-874.3	-827.5	485.6
7	-340.8	-337.4	678.6
8	-181.9	-182.7	1019.4
9	-94.5	-95.7	1841.2
10	-30.2	-30.6	5357.4

TABLE 19
RESISTANCE OF TLA WITH THREE DIFFERENT CAPACITORS

Frequency in MHz	$C = 10^{-6}$ in Farads	$C = 10^{-9}$ in Farads	$C = 10^{-12}$ in Farads
2	0.01	0.01	0.02
3	0.09	0.09	0.06
4	0.75	0.68	0.11
5	34.08	23.45	0.22
6	8.08	9.16	0.39
7	2.34	2.44	0.79
8	1.45	1.48	1.85
9	1.17	1.18	7.04
10	1.09	1.09	161.81

TABLE 20
REACTANCE OF TLA WITH THREE DIFFERENT CAPACITORS

Frequency in MHz	$C = 10^{-6}$ in Farads	$C = 10^{-9}$ in Farads	$C = 10^{-12}$ in Farads
2	132.2	120.9	-272.6
3	242.6	229.5	-144.9
4	489.7	461.9	-66.5
5	2426.8	2012.6	-3.7
6	-874.3	-934.5	58.2
7	-340.8	-350.4	132.7
8	-181.9	-185.8	248.3
9	-94.5	-96.8	521.9
10	-30.2	-31.8	2458.2

TABLE 21
RESISTANCE OF TLA WITH THREE DIFFERENT INDUCTORS

Frequency in MHz	$L = 10^{-2}$ in Henry	$L = 10^{-4}$ in Henry	$L = 10^{-6}$ in Henry
2	0.03	0.05	0.01
3	0.06	0.07	0.12
4	0.12	0.13	1.69
5	0.22	0.22	34.22
6	0.39	0.38	2.43
7	0.71	0.67	1.28
8	1.49	1.32	1.01
9	4.26	3.41	0.97
10	35.09	19.19	0.89

TABLE 22
REACTANCE OF TLA WITH THREE DIFFERENT INDUCTORS

Frequency in MHz	$L = 10^{-2}$ in Henry	$L = 10^{-4}$ in Henry	$L = 10^{-6}$ in Henry
2	-288.2	-411.4	151.4
3	-156.7	-192.4	297.3
4	-77.5	-98.4	762.9
5	-15.7	-30.9	-2410.6
6	42.9	28.9	-445.9
7	109.7	93.6	-211.9
8	203.9	179.9	-105.7
9	386.7	333.7	-33.2
10	1138.2	826.9	-30.9

TABLE 23
 INPUT IMPEDANCE FOR EF-TLA FROM 4.0 - 6.9 MHZ
 WITH 9 SEGMENTS AND A 0.05 METER RADIUS

Frequency in MHz	Resistance in Ohms (R)	Reactance in Ohms (jX)
4.0	0.75	489.7
4.1	0.96	535.7
4.2	1.23	589.9
4.3	1.62	654.9
4.4	2.17	734.4
4.5	2.97	834.1
4.6	4.21	963.1
4.7	6.24	1136.2
4.8	9.82	1383.7
4.9	16.95	1764.2
5.0	34.08	2426.8
5.1	92.34	3876.5
5.2	598.72	9563.4
5.3	2783.20	-19856.0
5.4	178.48	-4917.1
5.5	61.16	-2798.8
5.6	31.62	-1952.6
5.7	19.75	-1497.7

TABLE 23
INPUT IMPEDANCE FOR EF-TLA FROM 4.0 - 6.9 MHZ
WITH 9 SEGMENTS AND A 0.05 METER RADIUS

Frequency in MHz	Resistance in Ohms (R)	Reactance in Ohms (jX)
5.8	13.73	-1212.4
5.9	10.39	-1016.1
6.0	8.08	-874.3
6.1	6.58	-765.4
6.2	5.52	-679.5
6.3	4.73	-609.8
6.4	4.13	-552.2
6.5	3.66	-503.5
6.6	3.29	-461.8
6.7	2.98	-425.6
6.8	2.73	-393.9
6.9	2.52	-365.9

APPENDIX D

RADIATION PATTERNS FOR A CENTER-END FEED TRANSMISSION LINE ANTENNA

Contained in this appendix are radiation patterns produced by the NEC computer analysis for center-end feed transmission line antenna, the transmission line with dimensions 13.5 x 0.6 meters and above a perfect ground at 2, 5, 7, and 10 MHz.

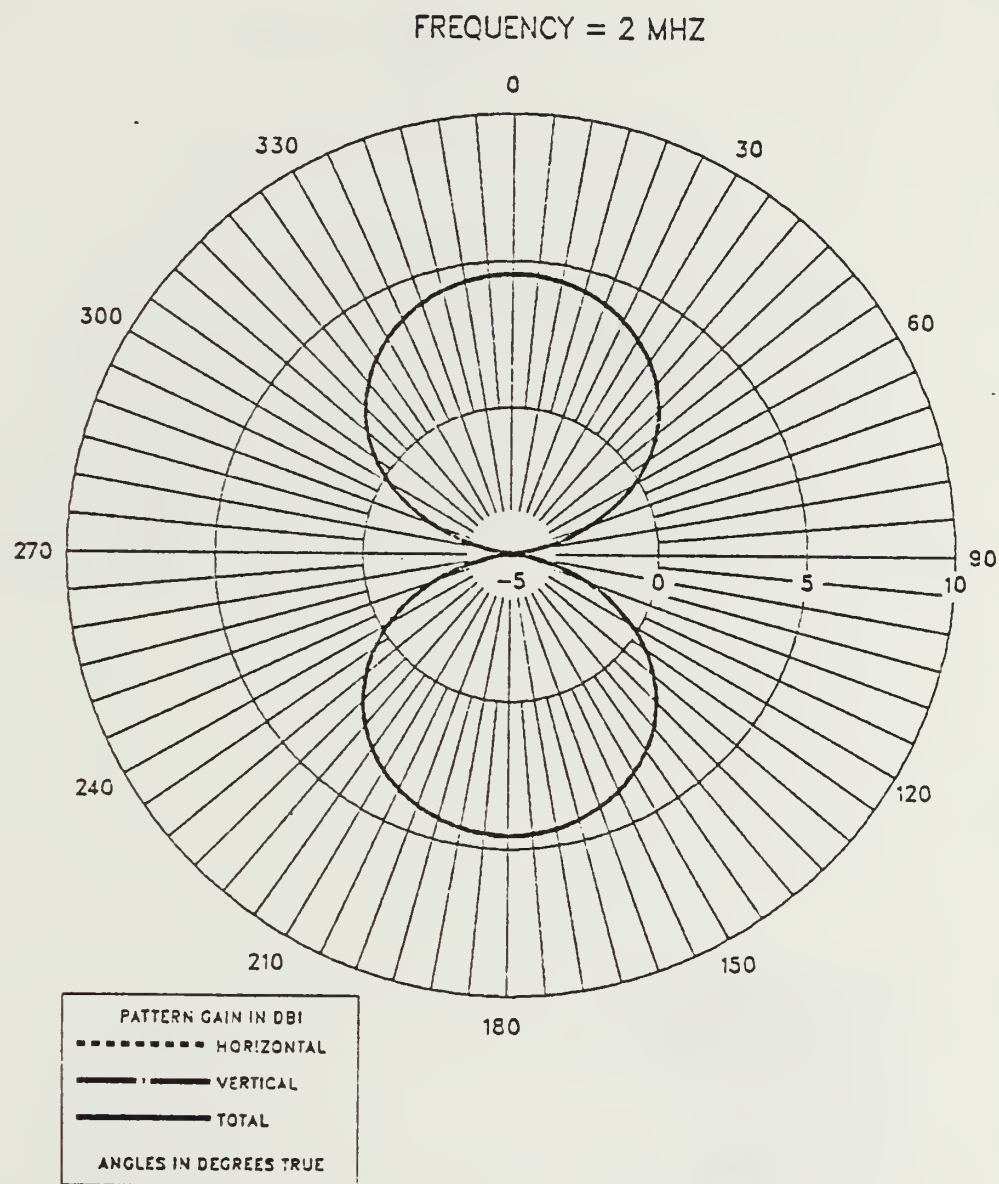


Figure D.1 E-Field Azimuth Pattern at 2 MHz
for CEF-TLA.

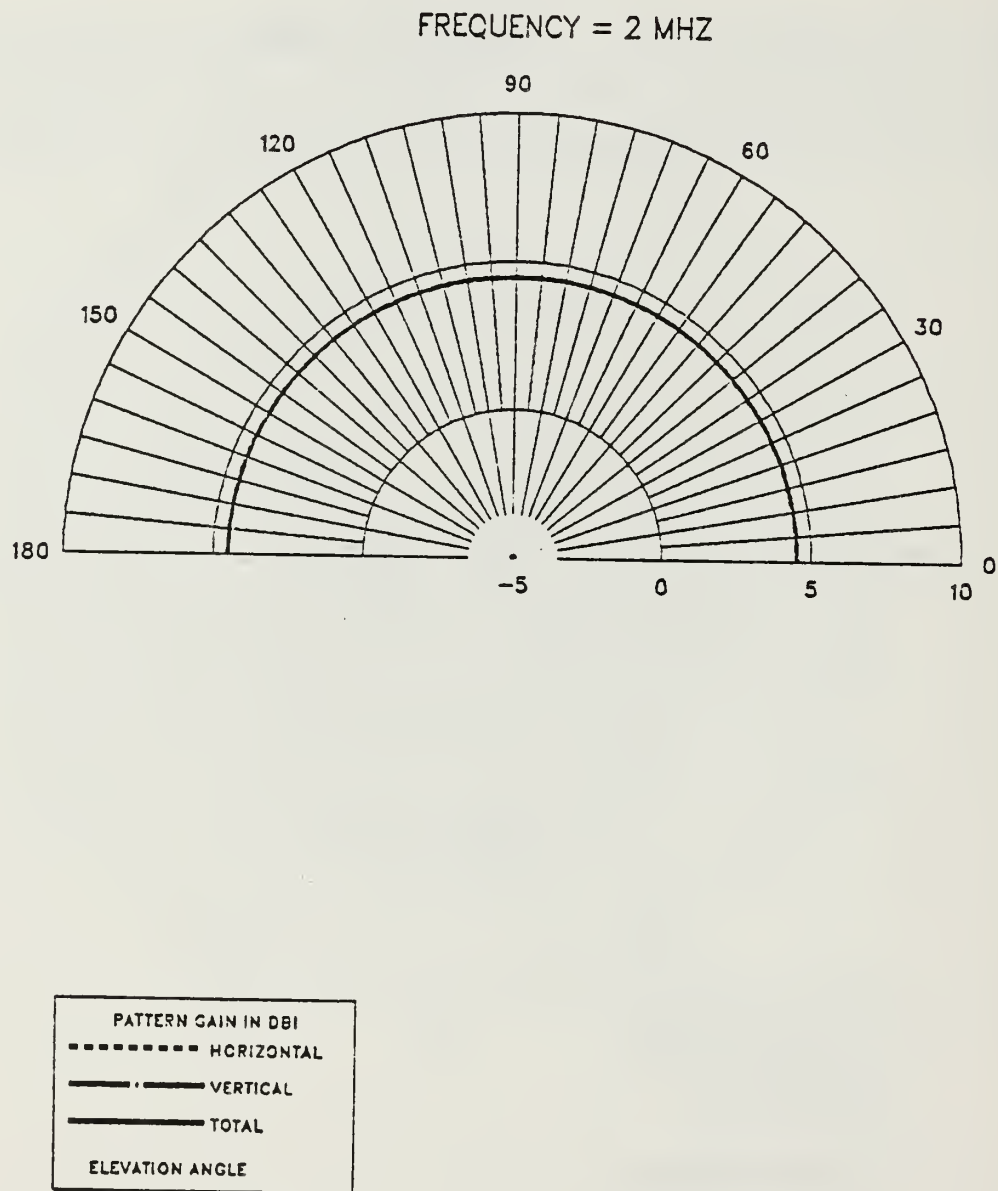


Figure D.2 E-Field Elevation Pattern at 2 MHz for CEF-TLA.

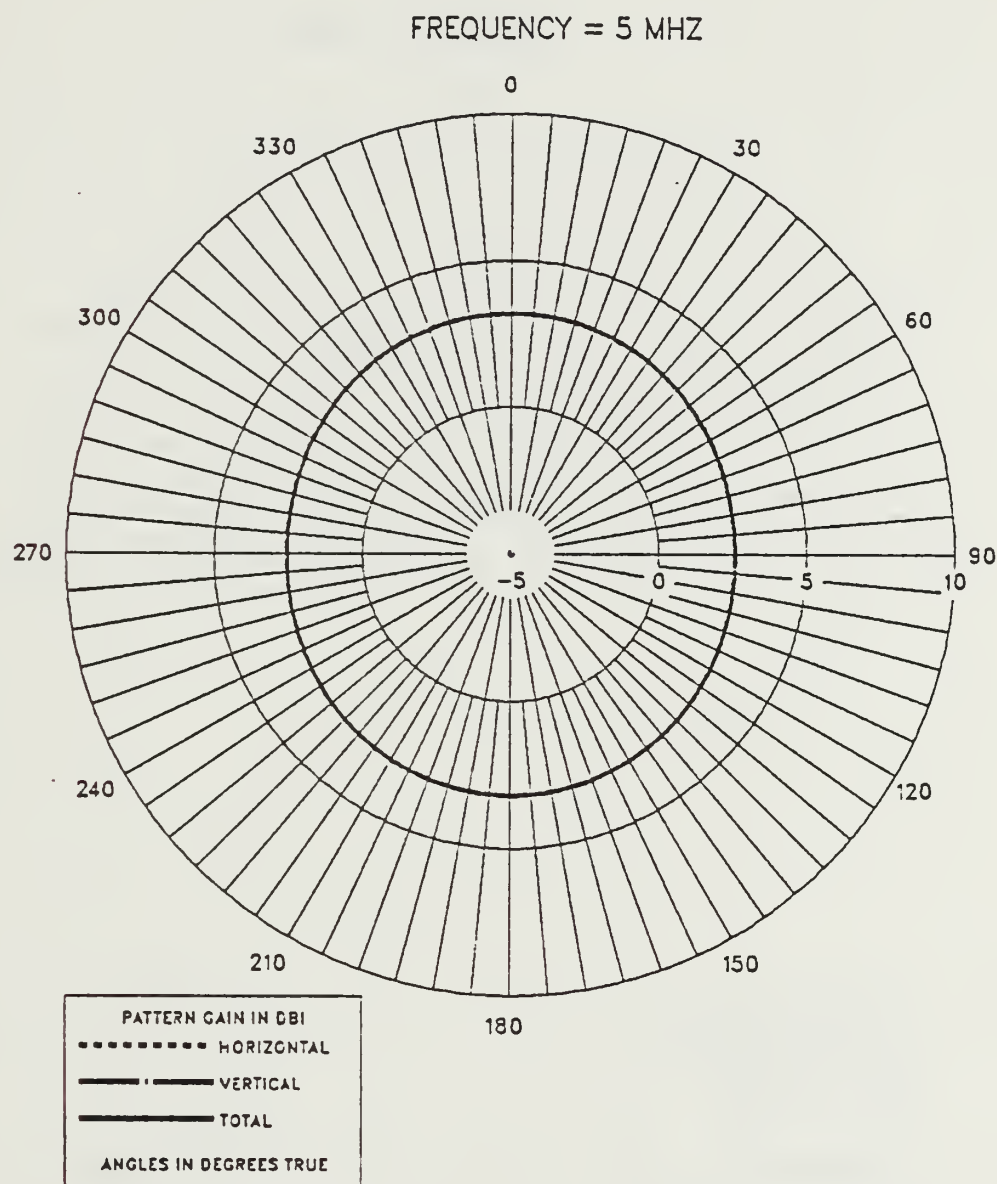


Figure D.3 E-Field Azimuth Pattern at 5 MHz
for CEF-TLA.

FREQUENCY = 5 MHZ

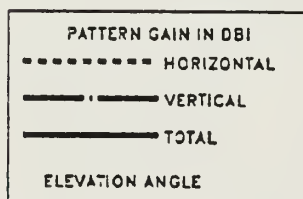
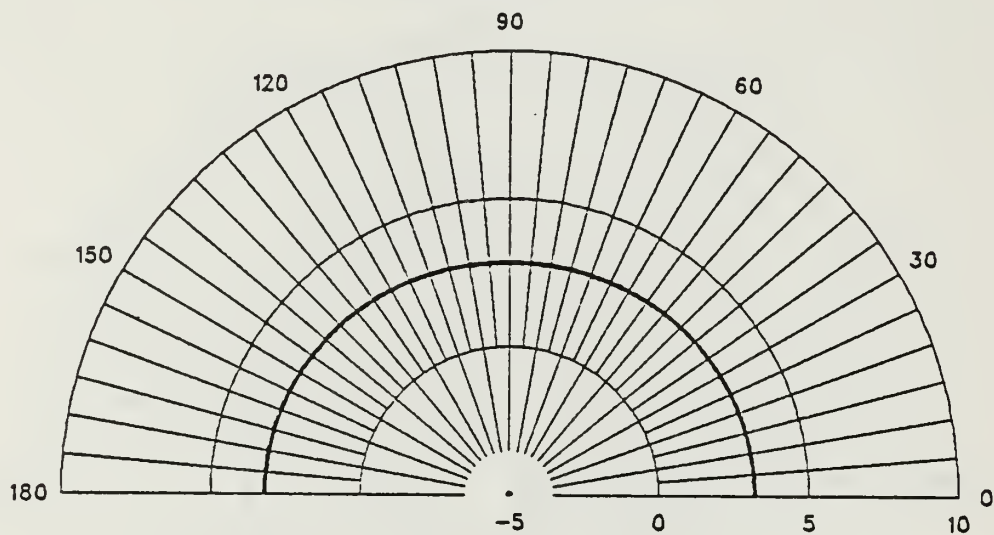


Figure D.4 E-Field Elevation Pattern at 5 MHz
for CEF-TLA.

FREQUENCY = 7 MHZ

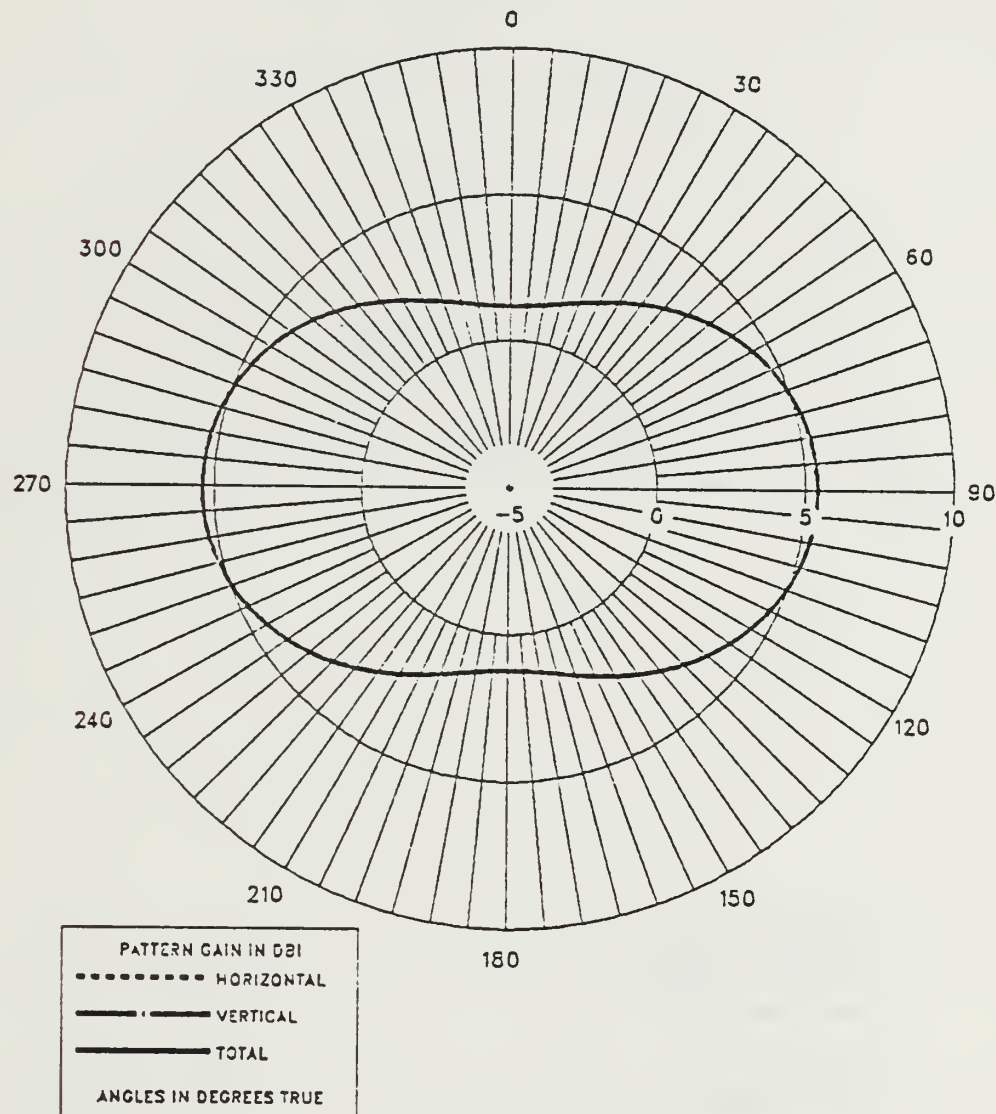


Figure D.5 E-Field Azimuth Pattern at 7 MHz
for CEF-TLA.

FREQUENCY = 7 MHZ

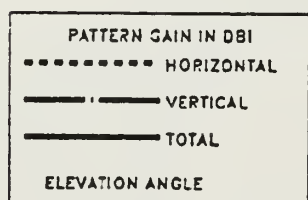
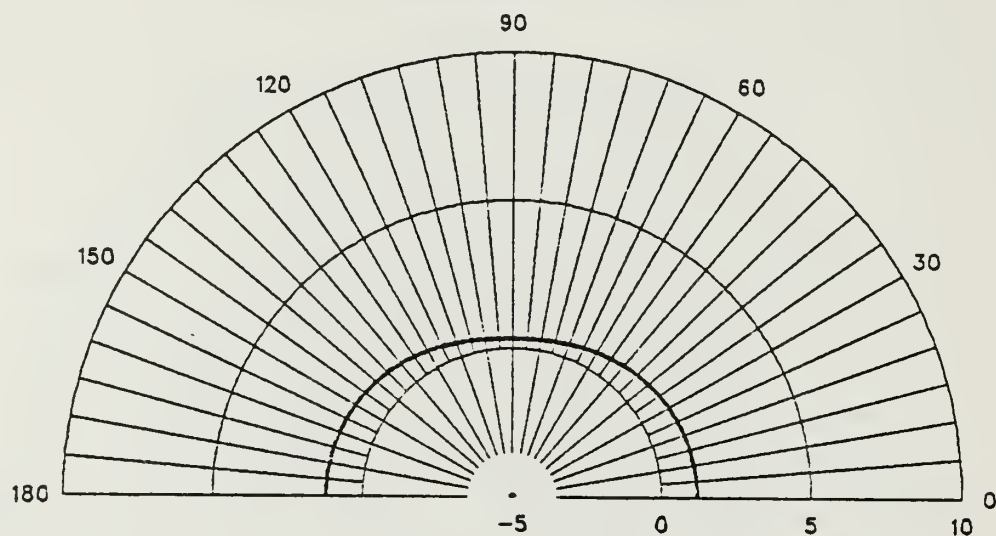


Figure D.6 E-Field Elevation Pattern at 7 MHz
for CEF-TLA.

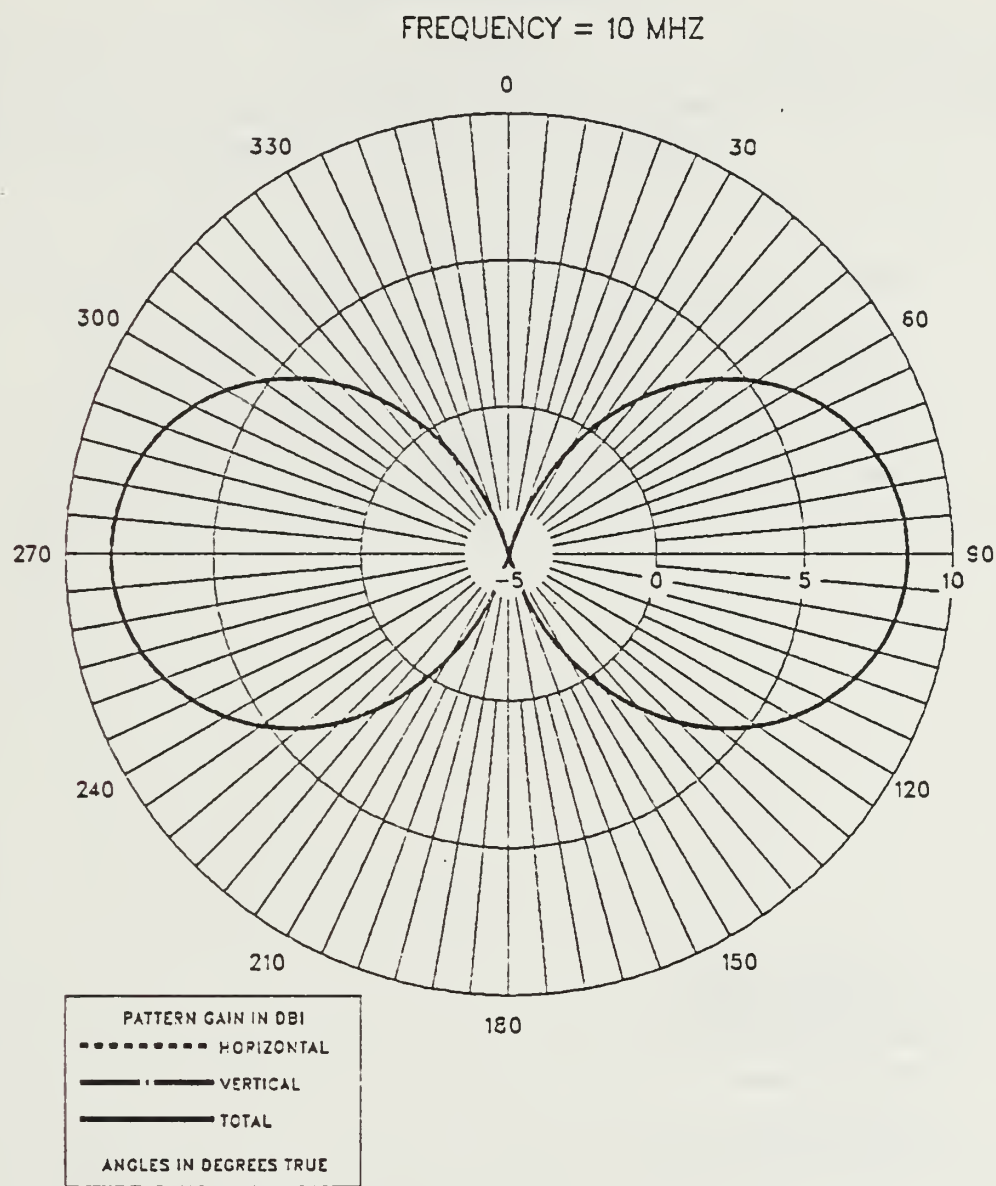


Figure D.7 E-Field Azimuth Pattern at 10 MHz
for CEF-TLA.

FREQUENCY = 10 MHZ

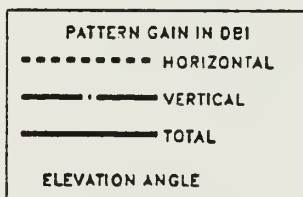
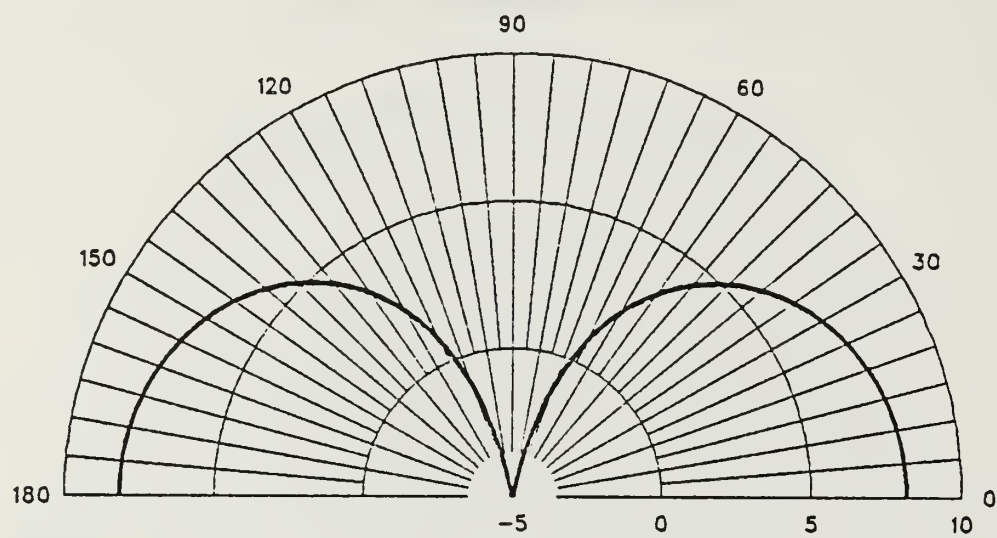


Figure D.8 E-Field Elevation Pattern at 10 MHz
for CEF-TLA.

APPENDIX E

**RADIATION PATTERNS FOR TRANSMISSION LINE ANTENNAS ON
THE BOW AND ON THE STERN**

Contained in this appendix are radiation patterns generated by the NEC computer analysis for the transmission line antenna computer models on the bow and on the stern of an FFG-45 frigate at 2, 4.5, 7.5, and 10 MHz.

EF-TLA ON THE BOW

FREQUENCY = 2 MHZ

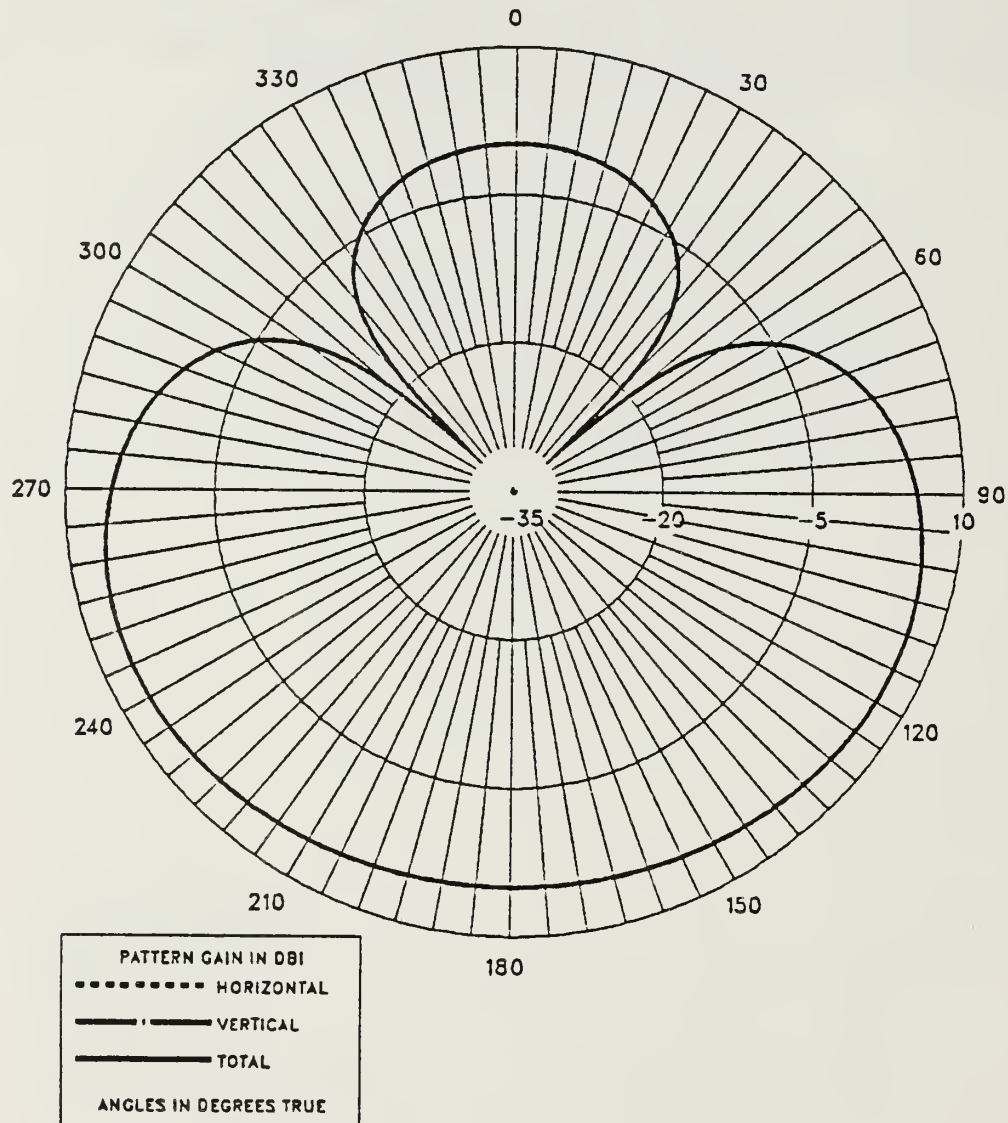


Figure E.1 E-Field Azimuth Pattern at 2.0 MHz
for EF-TLA on the Bow.

EF-TLA ON THE BOW

FREQUENCY = 2 MHZ

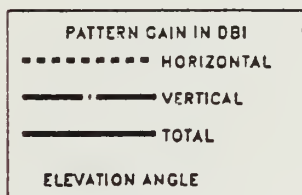
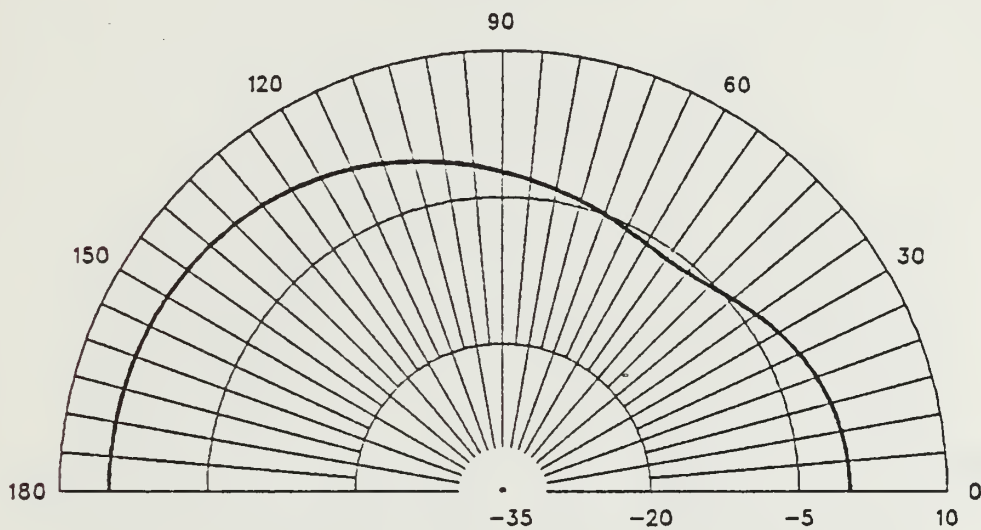


Figure E.2 E-Field Elevation Pattern at 2.0 MHz
for EF-TLA on the Bow.

EF-TLA ON THE STERN

FREQUENCY = 2 MHZ

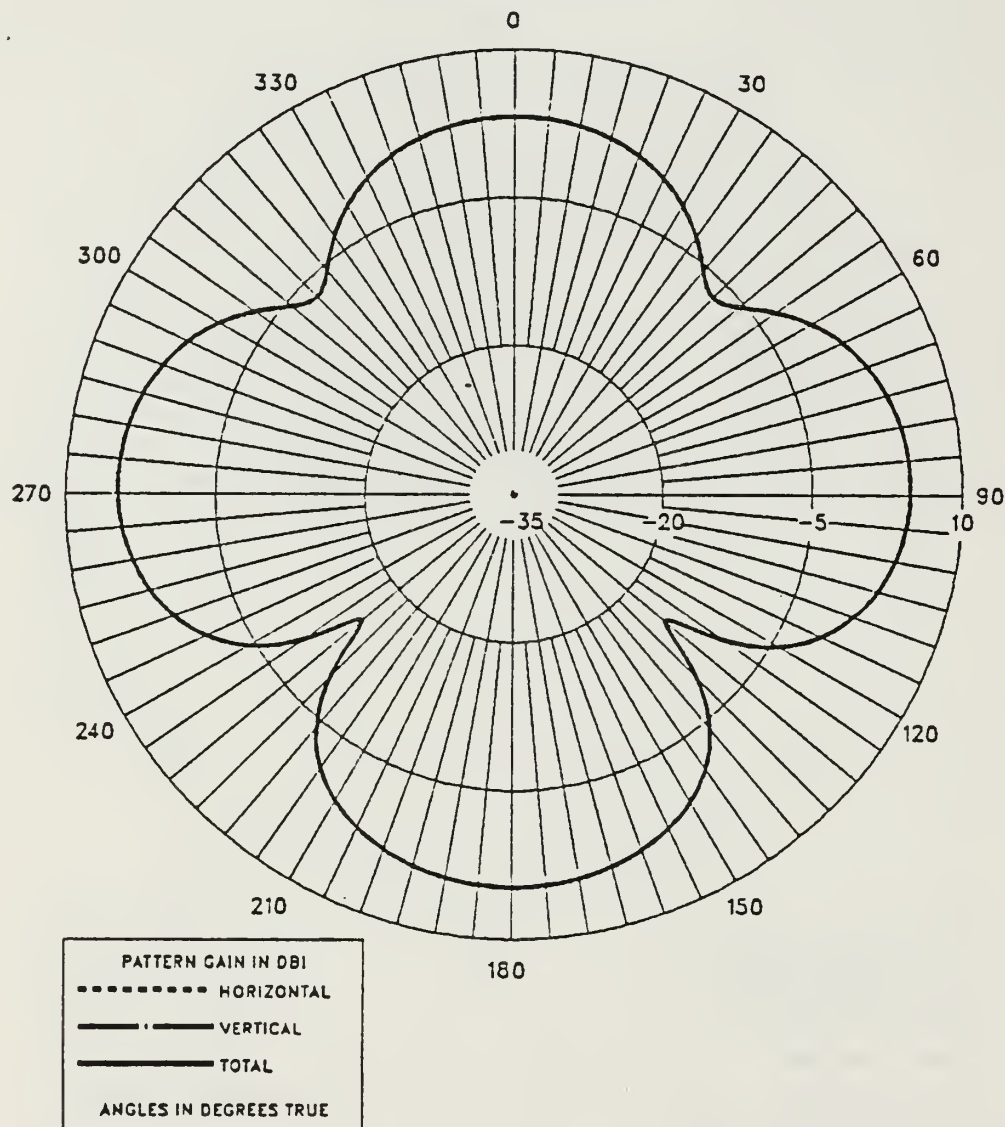


Figure E.3 E-Field Azimuth Pattern at 2.0 MHz
for EF-TLA on the Stern.

EF-TLA ON THE STERN

FREQUENCY = 2 MHZ

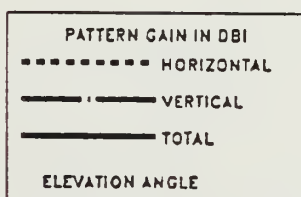
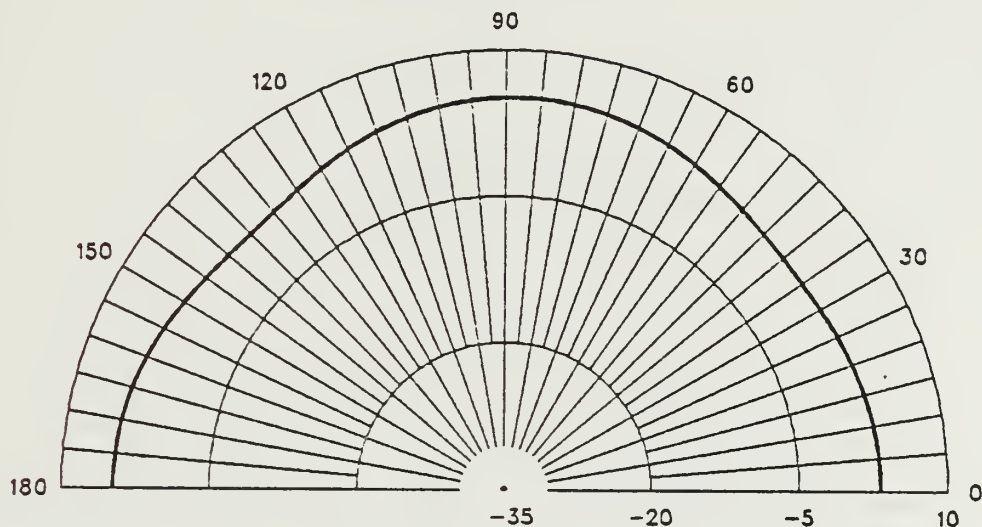


Figure E.4 E-Field Elevation Pattern at 2.0 MHz
for EF-TLA on the Stern.

EF-TLA ON THE BOW

FREQUENCY = 4.5 MHZ

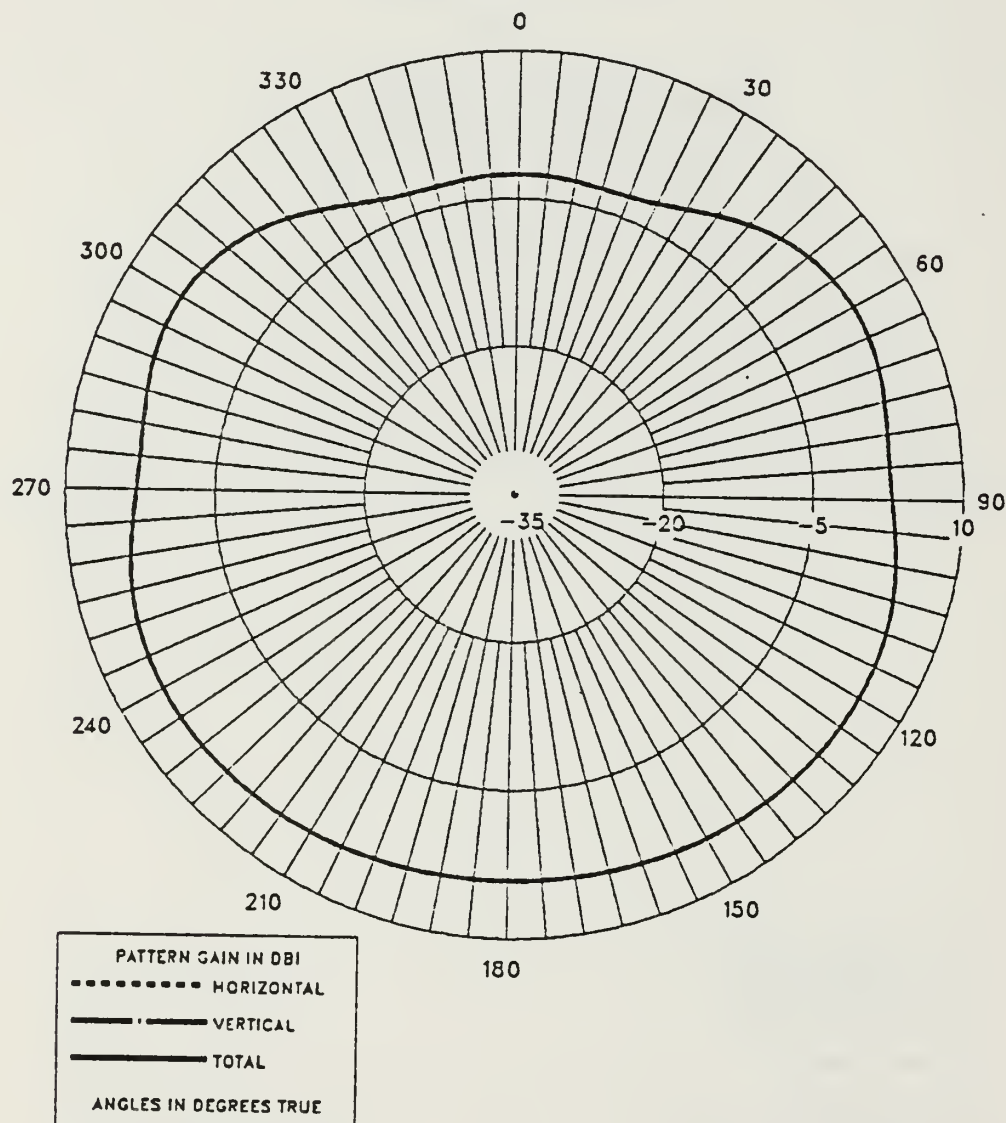


Figure E.5 E-Field Azimuth Pattern at 4.5 MHz
for EF-TLA on the Bow.

EF-TLA ON THE BOW

FREQUENCY = 4.5 MHZ

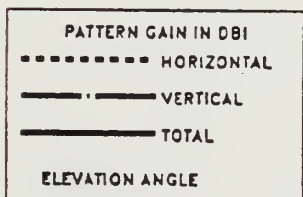
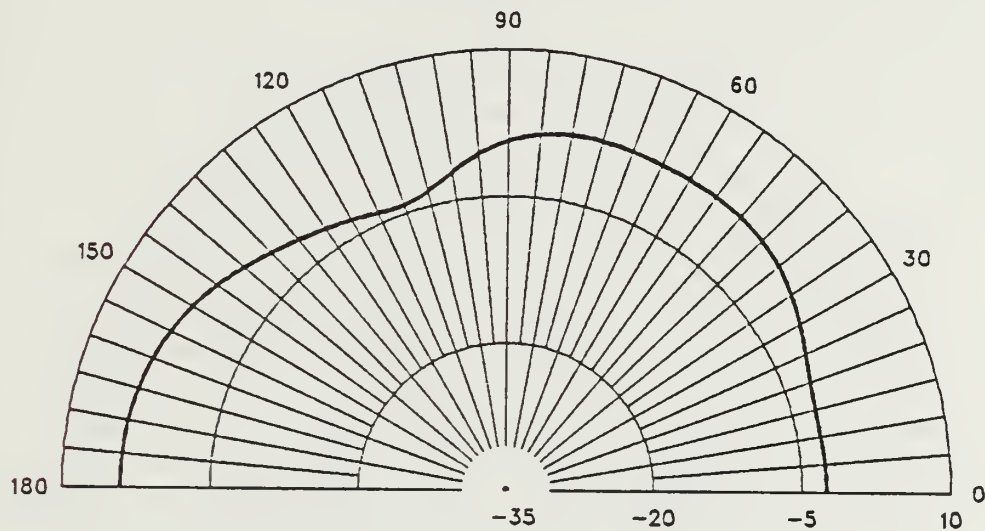


Figure E.6 E-Field Elevation Pattern at 4.5 MHz
for EF-TLA on the Bow.

EF-TLA ON THE STERN

FREQUENCY = 4.5 MHZ

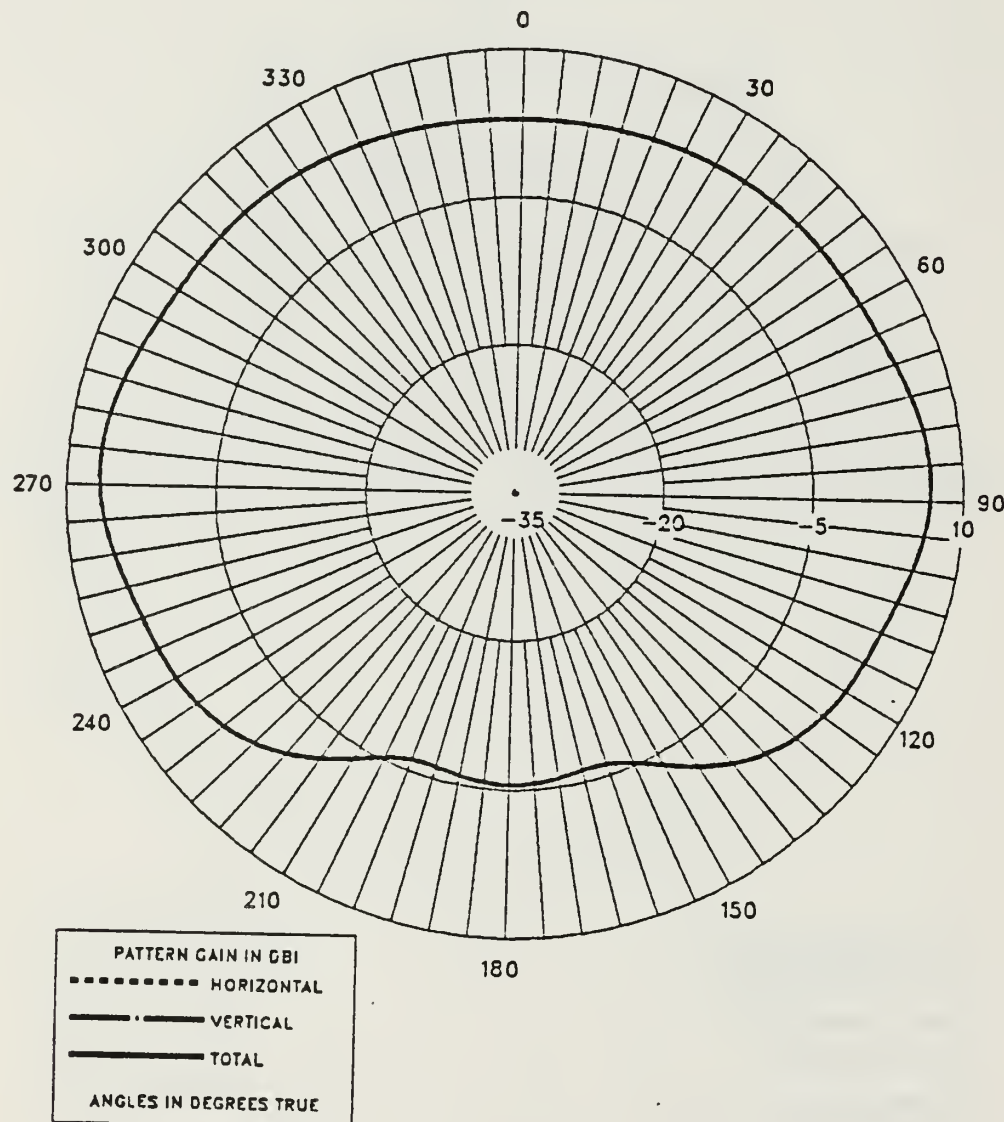
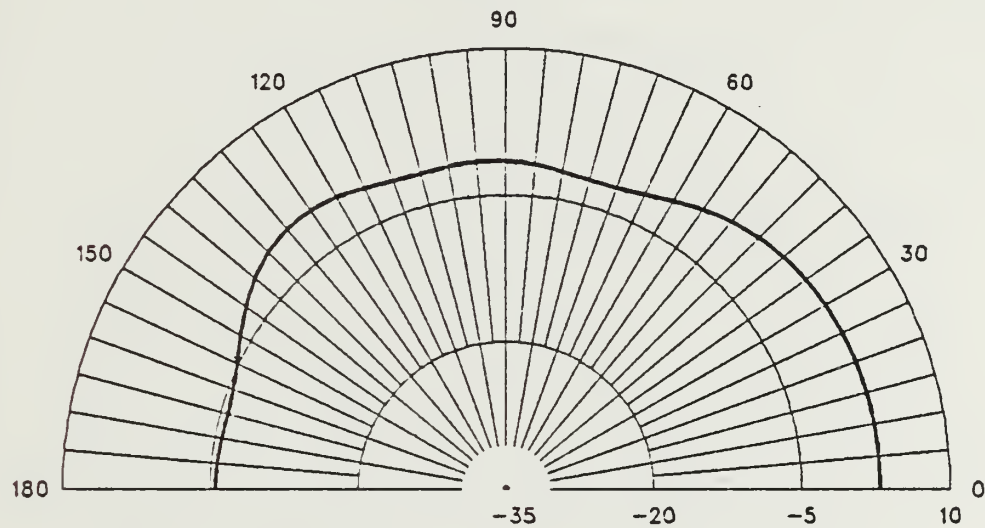


Figure E.7 E-Field Azimuth Pattern at 4.5 MHz
for EF-TLA on the Stern.

EF-TLA ON THE STERN

FREQUENCY = 4.5 MHZ



PATTERN GAIN IN DBI	
-----	HORIZONTAL
—	VERTICAL
—	TOTAL
ELEVATION ANGLE	

Figure E.8 E-Field Elevation Pattern at 4.5 MHz
for EF-TLA on the Stern.

EF-TLA ON THE BOW

FREQUENCY = 7.5 MHZ

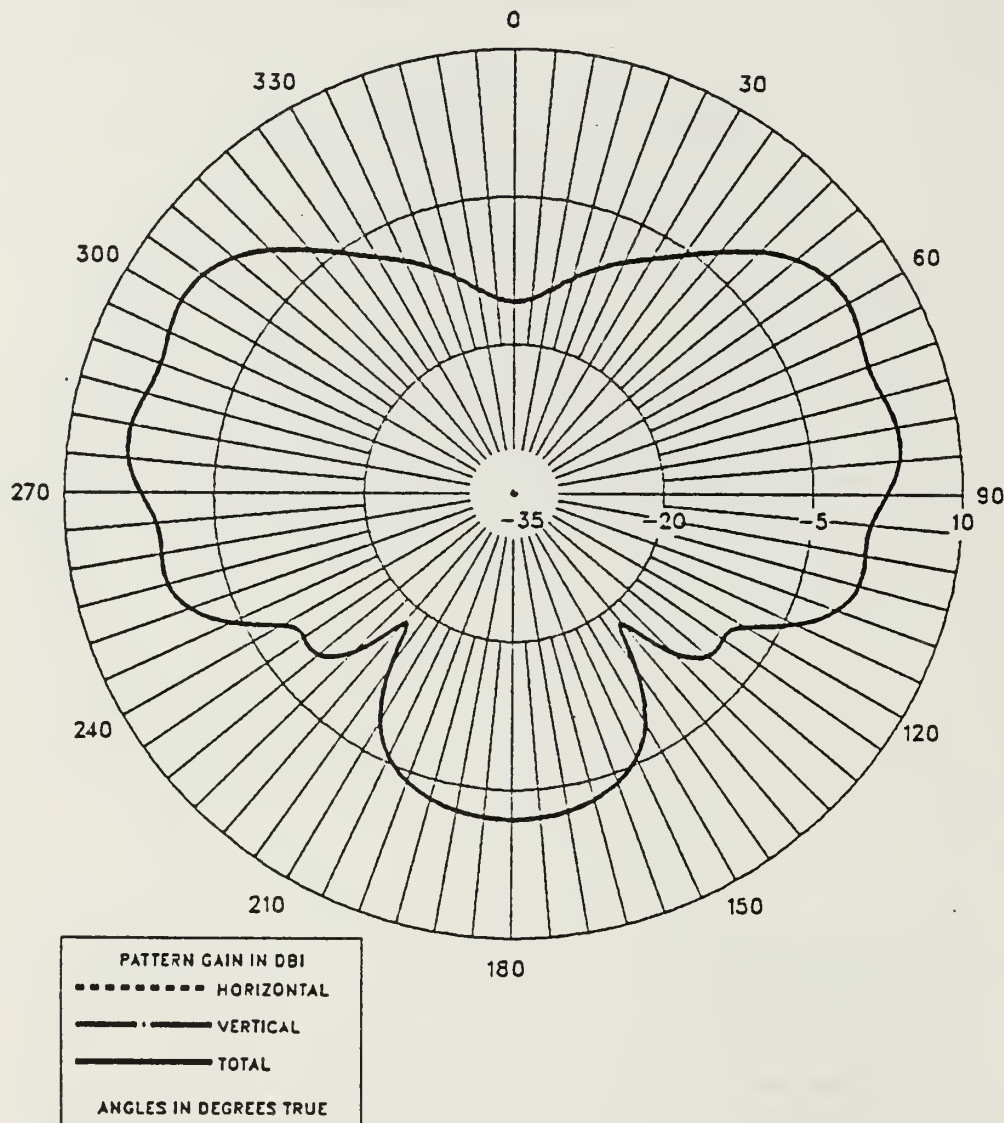


Figure E.9 E-Field Azimuth Pattern at 7.5 MHz for EF-TLA on the Bow.

EF-TLA ON THE BOW

FREQUENCY = 7.5 MHZ

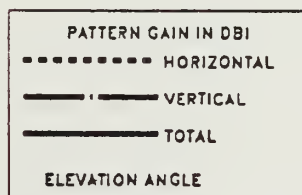
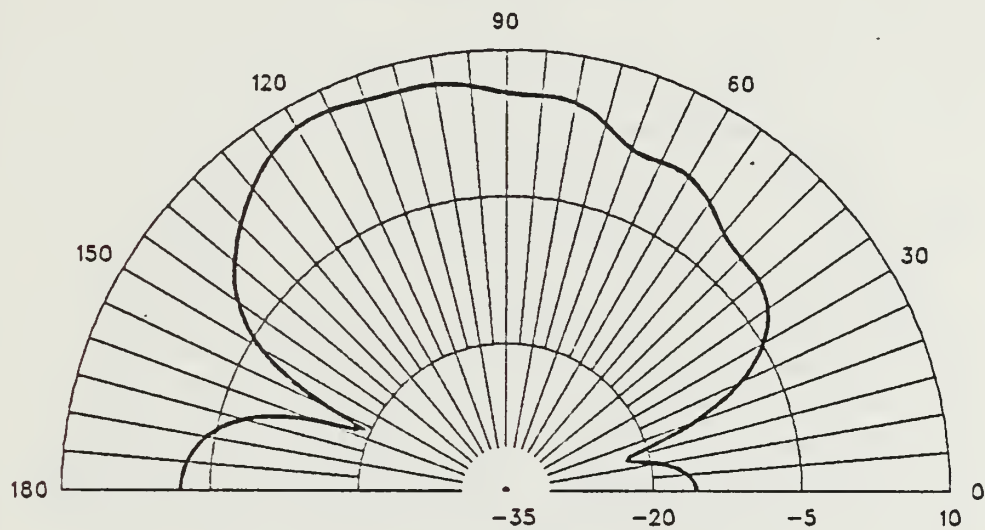


Figure E.10 E-Field Elevation Pattern at 7.5 MHz
for EF-TLA on the Bow.

EF-TLA ON THE STERN

FREQUENCY = 7.5 MHZ

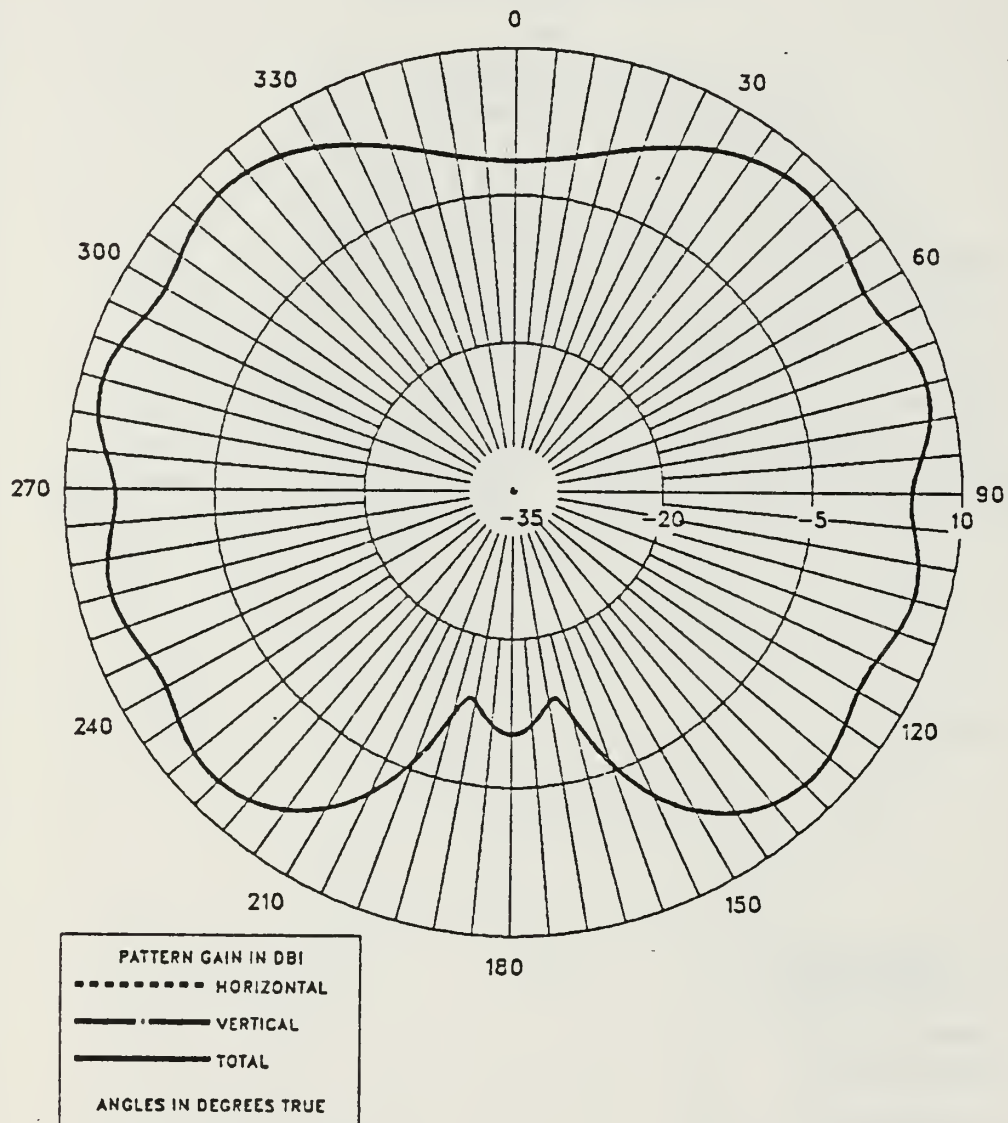


Figure E.11 E-Field Azimuth Pattern at 7.5 MHz
for EF-TLA on the Stern.

EF-TLA ON THE STERN

FREQUENCY = 7.5 MHZ

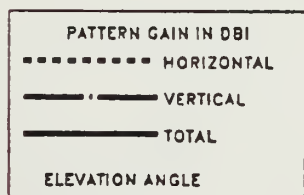
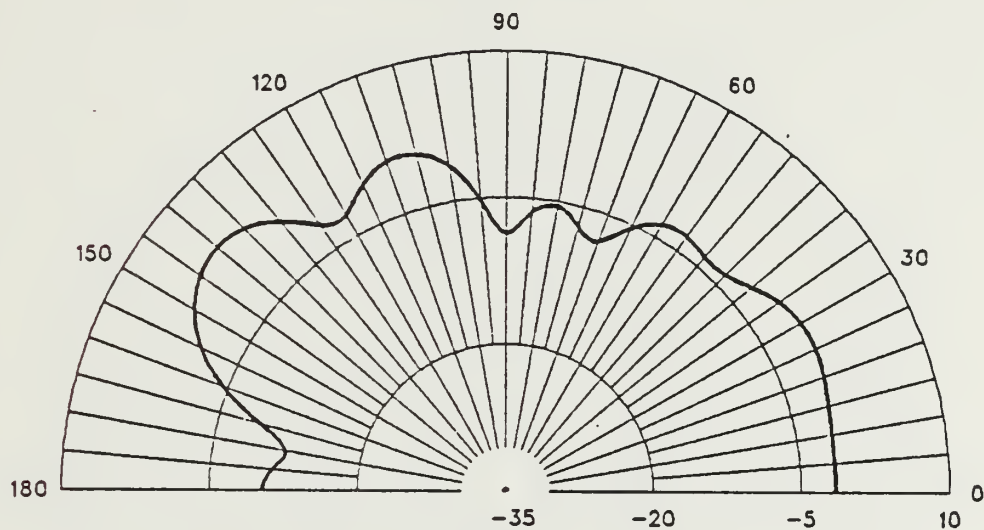


Figure E.12 E-Field Elevation Pattern at 7.5 MHz
for EF-TLA on the Stern.

EF-TLA ON THE BOW

FREQUENCY = 10 MHZ

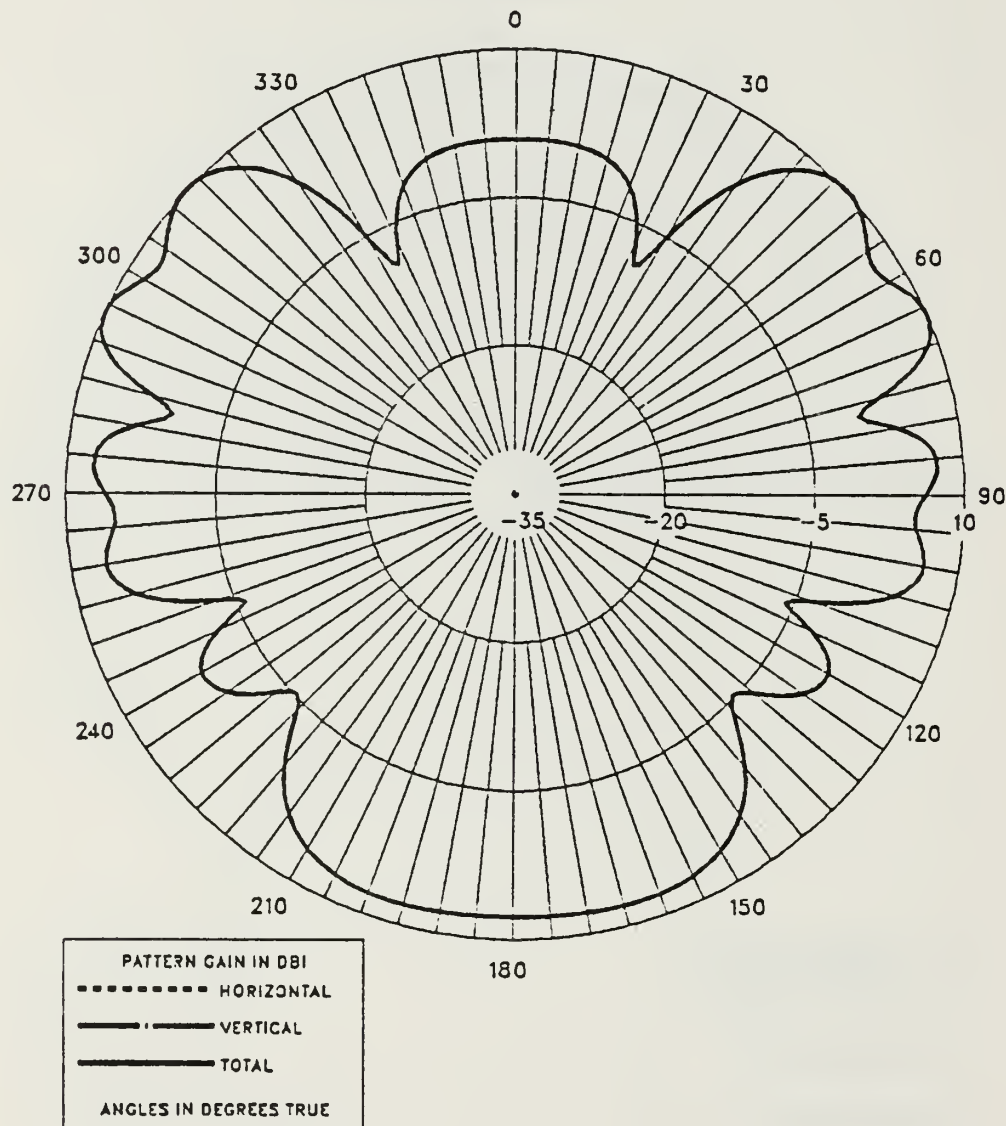


Figure E.13 E-Field Azimuth Pattern at 10.0 MHz for EF-TLA on the Bow.

EF-TLA ON THE BOW

FREQUENCY = 10 MHZ

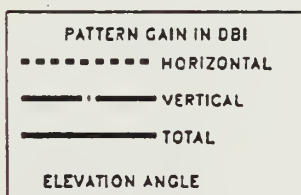
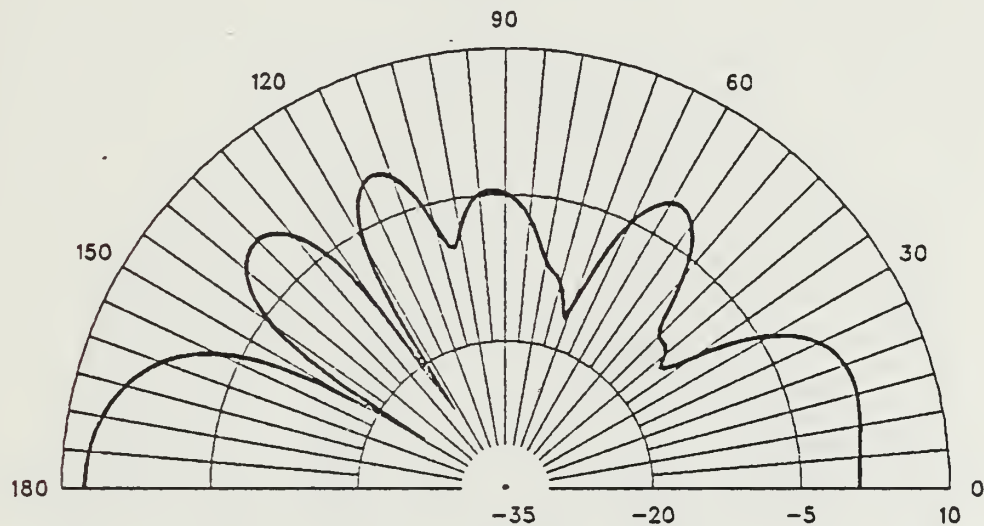


Figure E.14 E-Field Elevation Pattern at 10.0 MHz
for EF-TLA on the Bow.

EF-TLA ON THE STERN

FREQUENCY = 10 MHZ

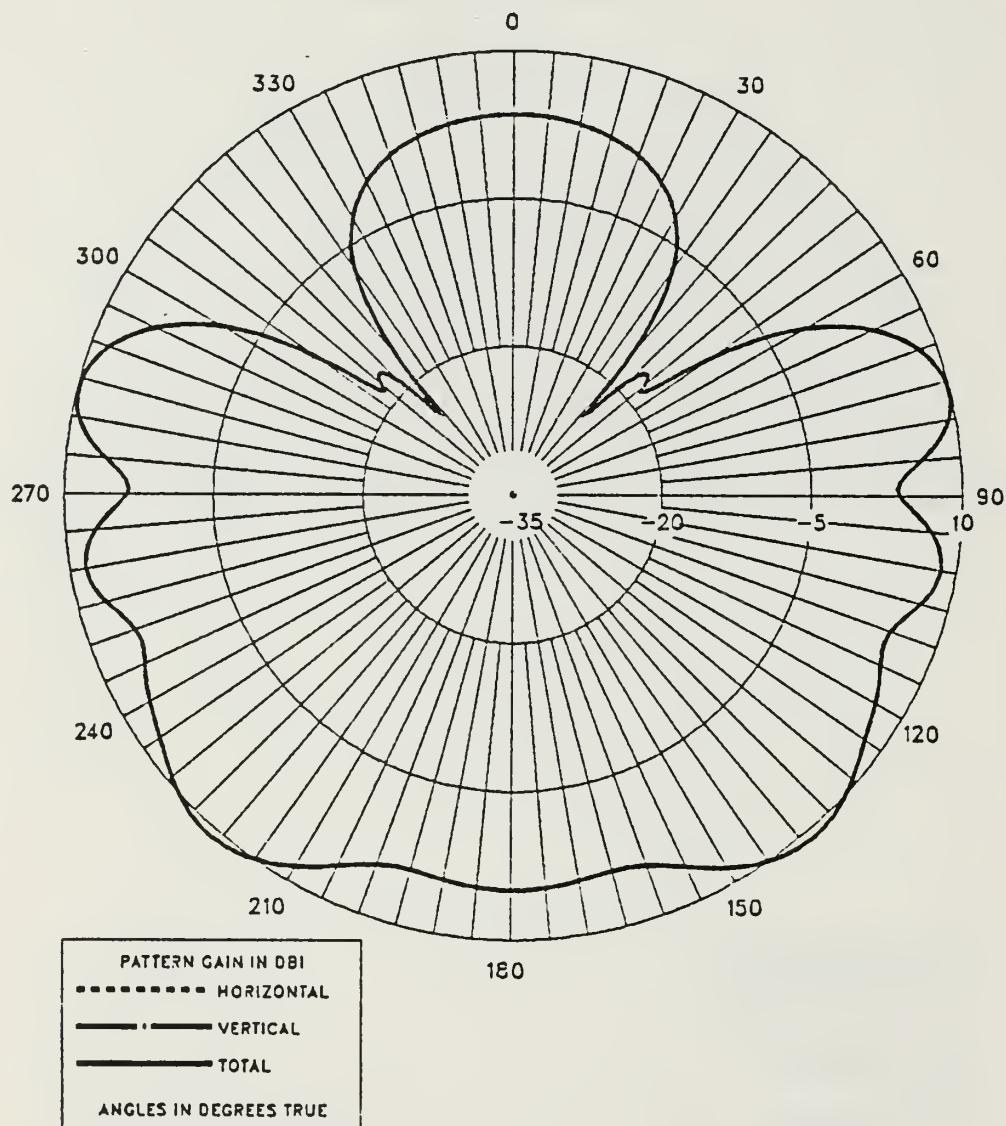


Figure E.15 E-Field Azimuth Pattern at 10.0 MHz for EF-TLA on the Stern.

EF-TLA ON THE STERN

FREQUENCY = 10 MHZ

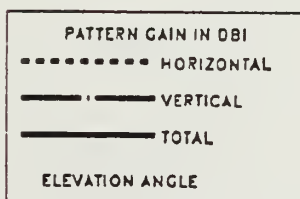
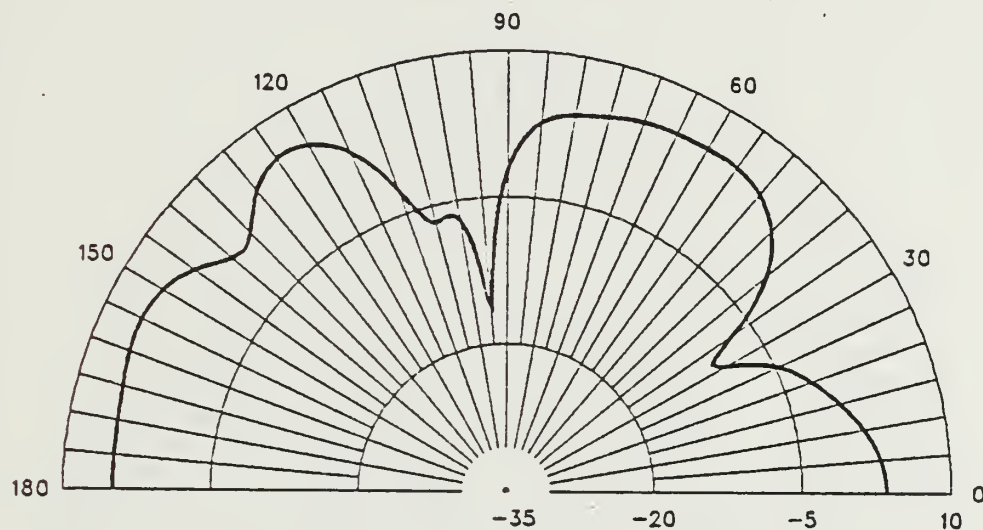


Figure E.16 E-Field Elevation Pattern at 10.0 MHz
for EF-TLA on the Stern.

TF-TLA ON THE BOW

FREQUENCY = 2 MHZ

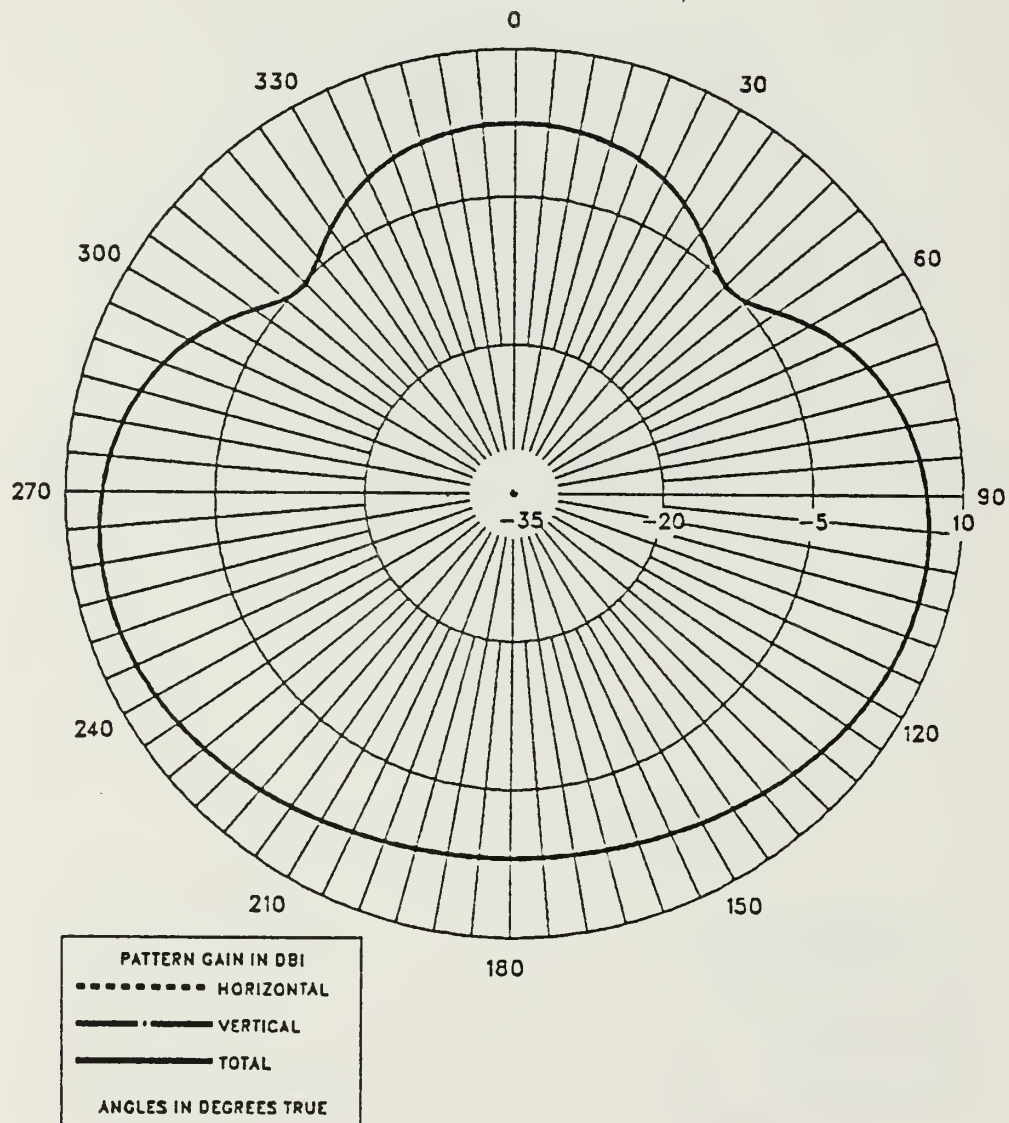


Figure E.17 E-Field Azimuth Pattern at 2.0 MHz
for TF-TLA on the Bow.

TF-TLA ON THE BOW

FREQUENCY = 2 MHZ

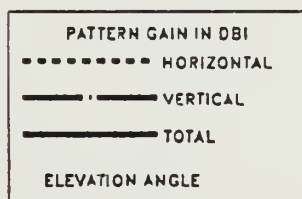
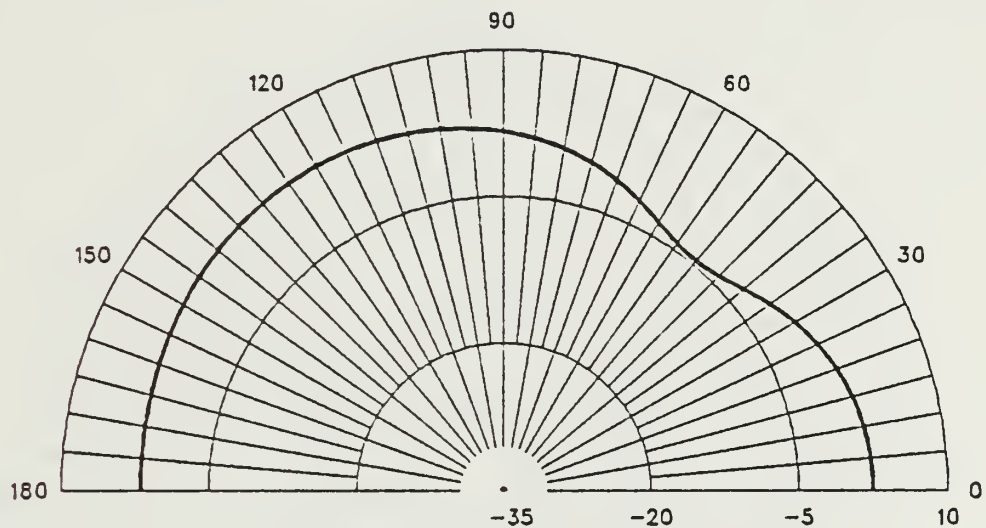


Figure E.18 E-Field Elevation Pattern at 2.0 MHz
for TF-TLA on the Bow.

TF-TLA ON THE STERN

FREQUENCY = 2 MHZ

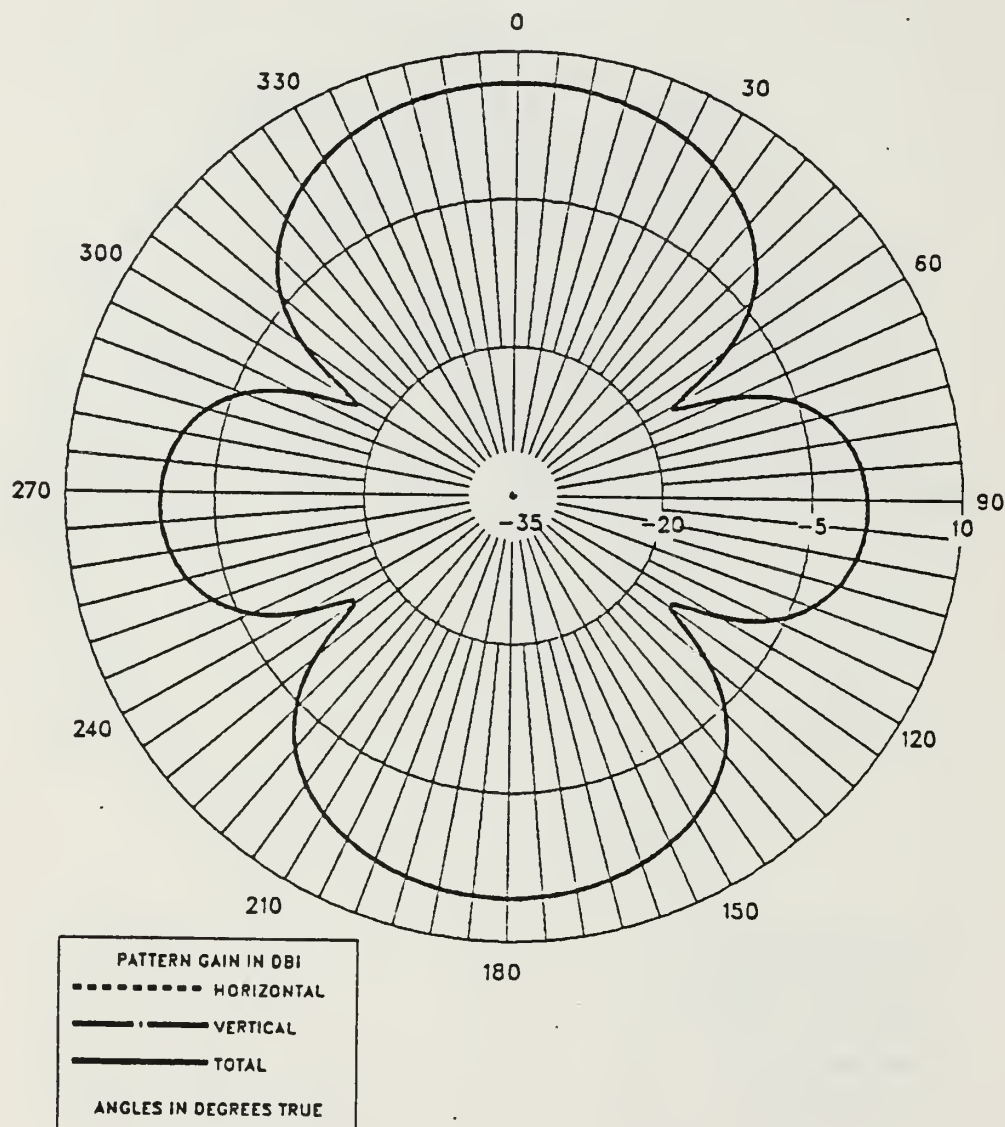


Figure E.19 E-Field Azimuth Pattern at 2.0 MHz
for TF-TLA on the Stern.

TF-TLA ON THE STERN

FREQUENCY = 2 MHZ

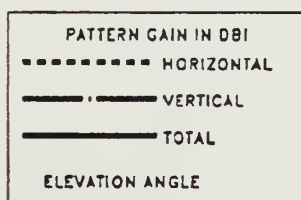
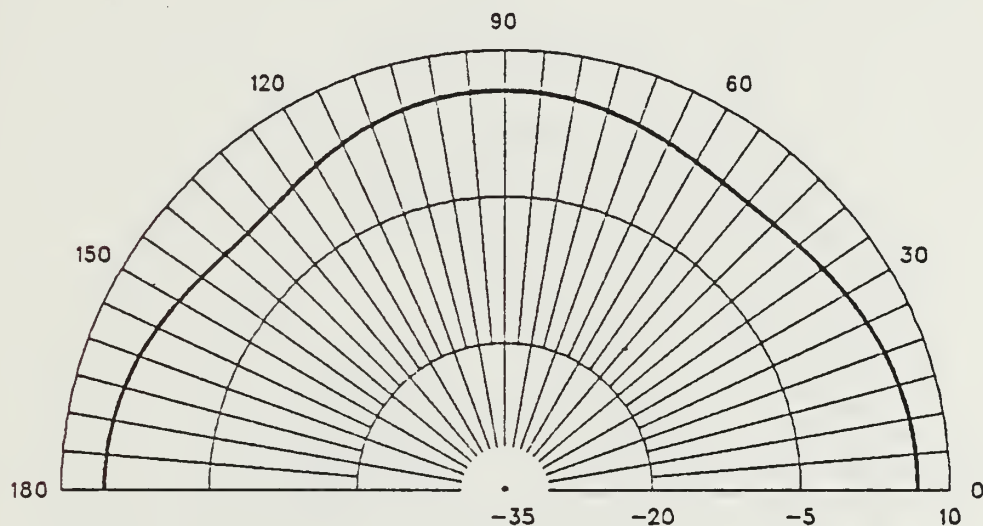


Figure E.20 E-Field Elevation Pattern at 2.0 MHz
for TF-TLA on the Stern.

TF-TLA ON THE BOW

FREQUENCY = 4.5 MHZ

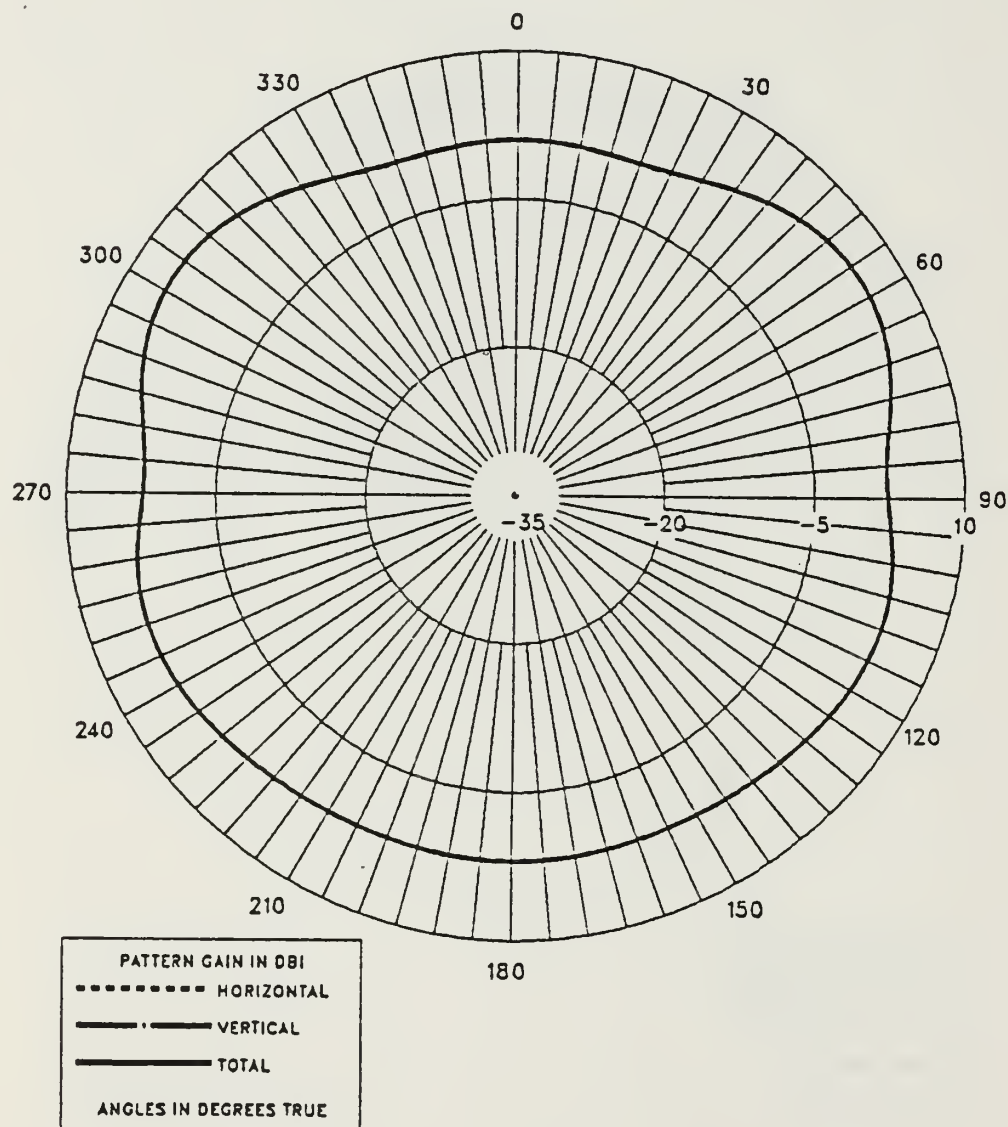


Figure E.21 E-Field Azimuth Pattern at 4.5 MHz
for TF-TLA on the Bow.

TF-TLA ON THE BOW

FREQUENCY = 4.5 MHZ

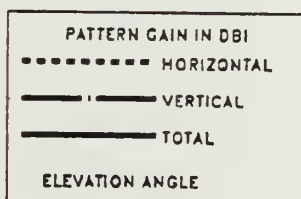
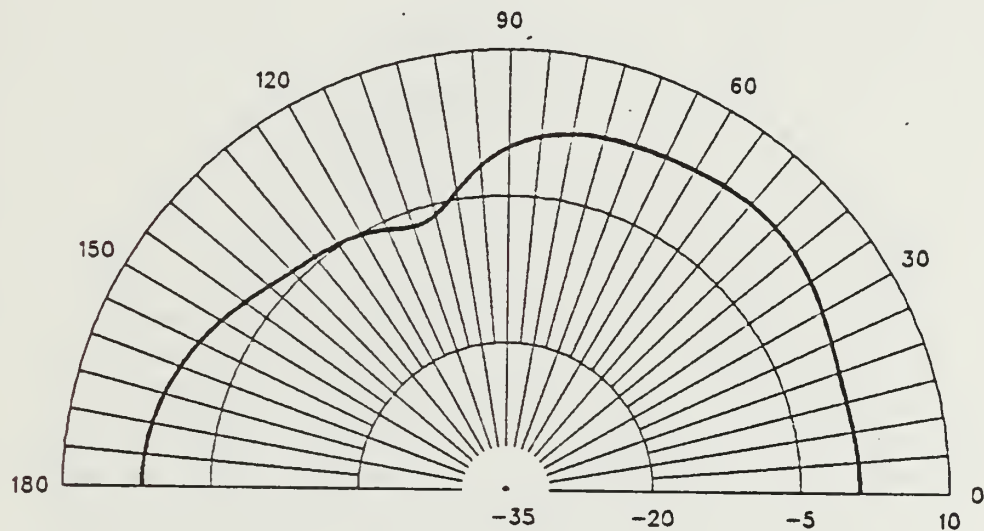


Figure E.22 E-Field Elevation Pattern at 4.5 MHz
for TF-TLA on the Bow.

TF-TLA ON THE STERN

FREQUENCY = 4.5 MHZ

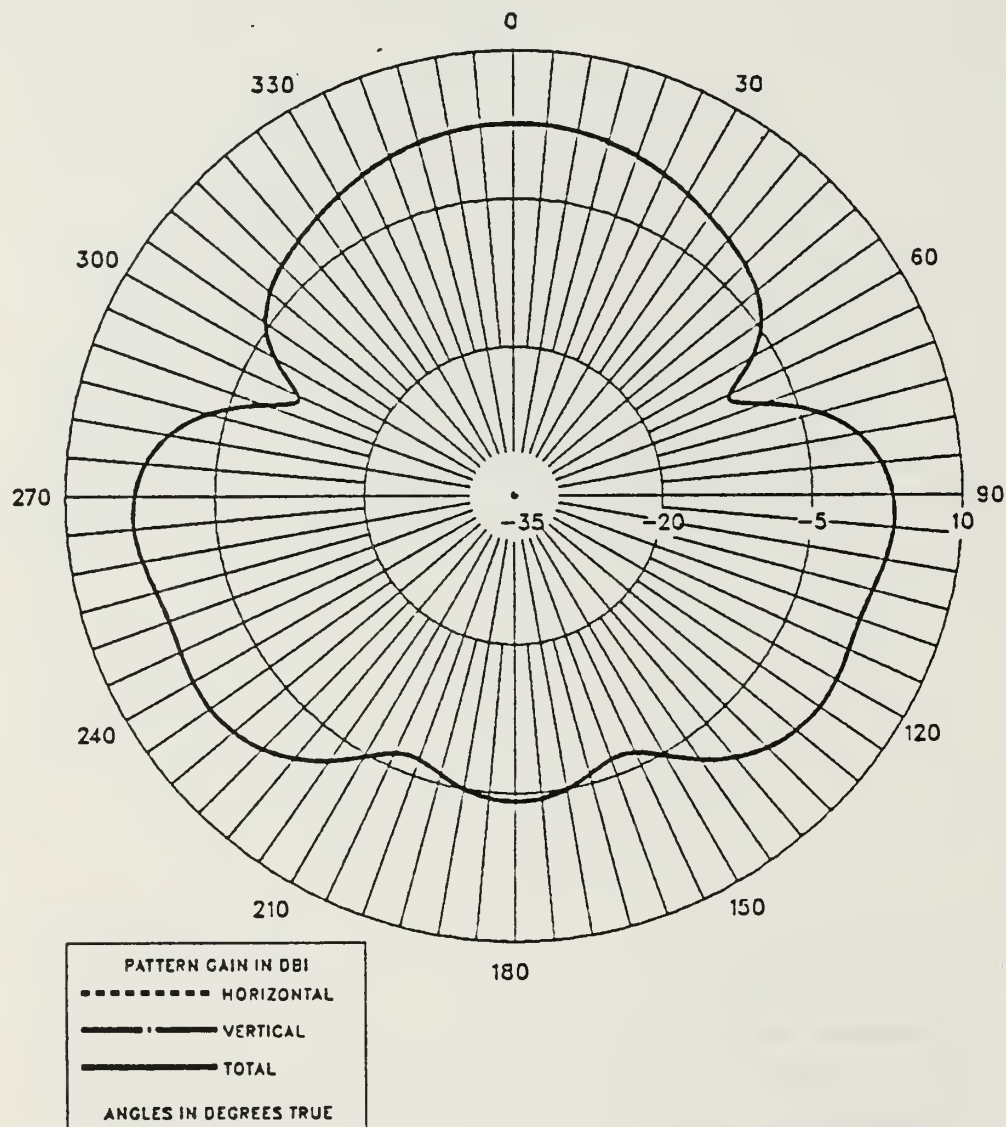


Figure E.23 E-Field Azimuth Pattern at 4.5 MHz
for TF-TLA on the Stern.

TF-TLA ON THE STERN

FREQUENCY = 4.5 MHZ

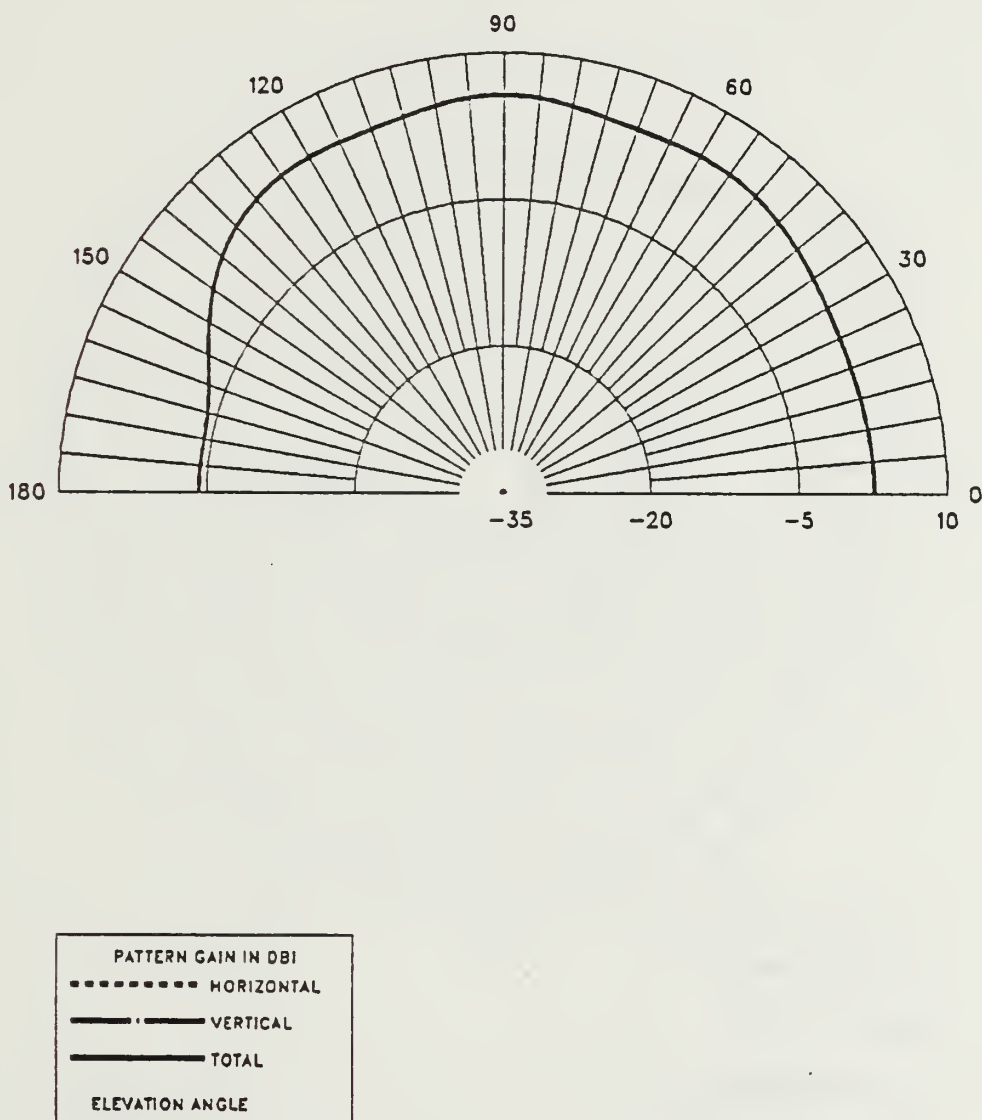


Figure E.24 E-Field Elevation Pattern at 4.5 MHz
for TF-TLA on the Stern.

TF-TLA ON THE BOW

FREQUENCY = 7.5 MHZ

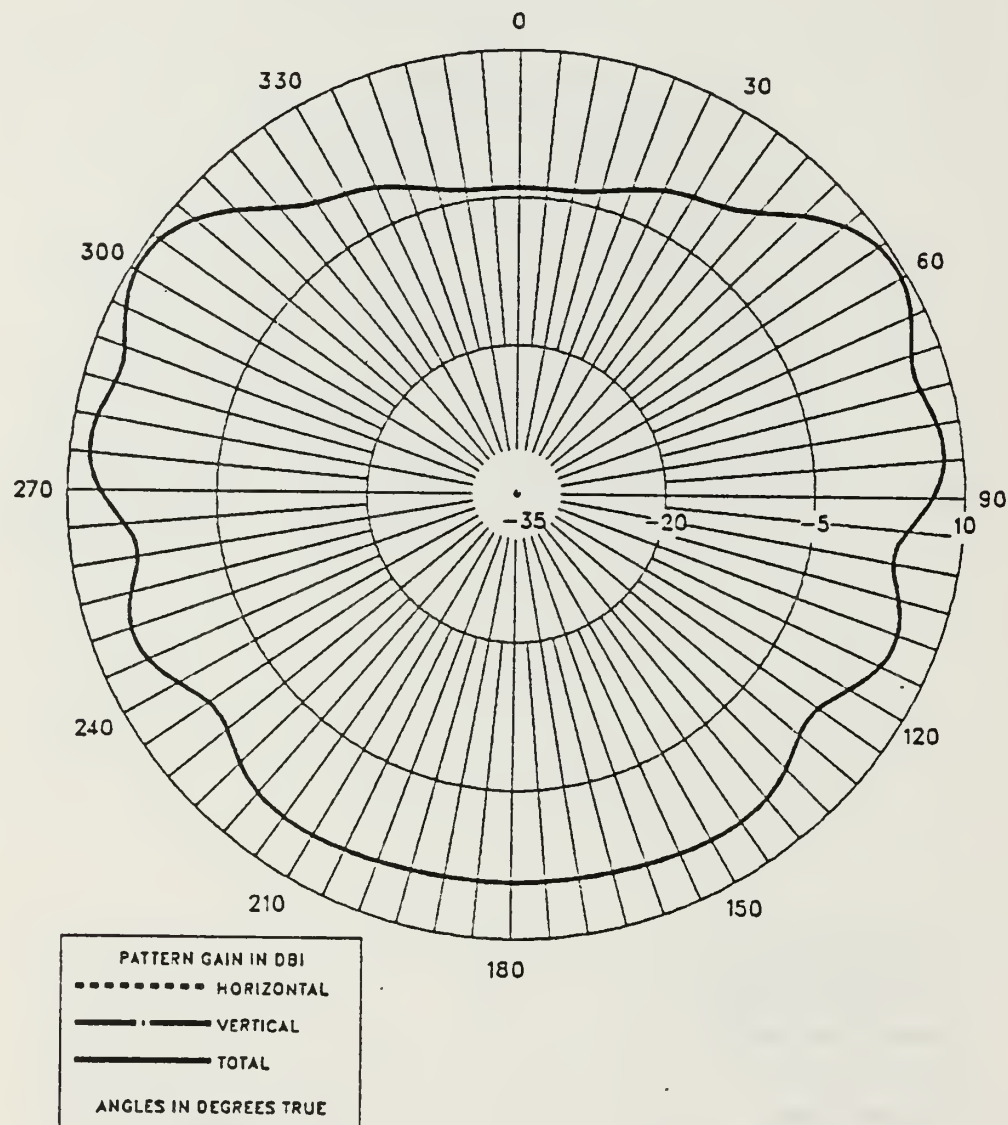


Figure E.25 E-Field Azimuth Pattern at 7.5 MHz
for TF-TLA on the Bow.

TF-TLA ON THE BOW

FREQUENCY = 7.5 MHZ

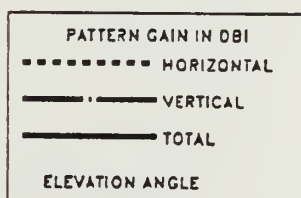
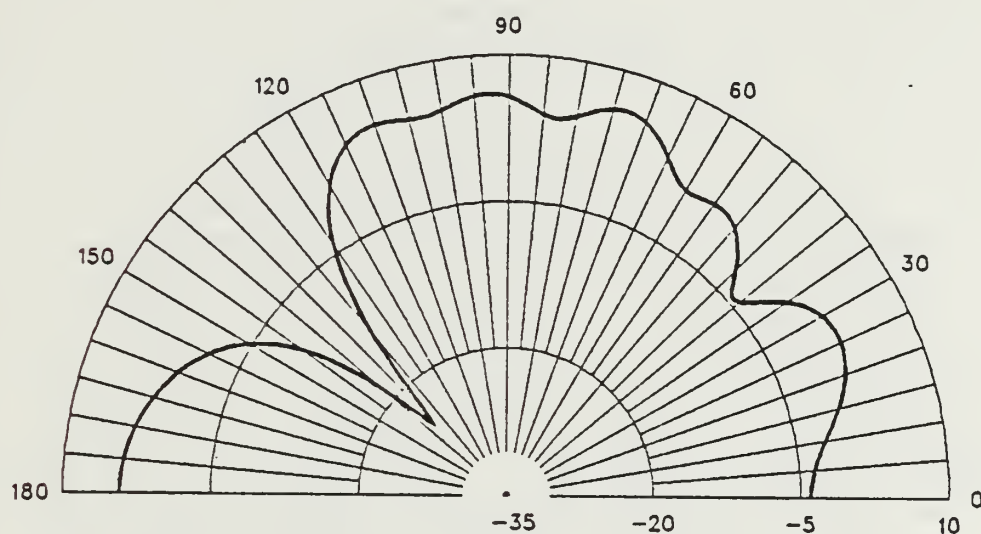


Figure E.26 E-Field Elevation Pattern at 7.5 MHz
for TF-TLA on the Bow.

TF-TLA ON THE STERN

FREQUENCY = 7.5 MHZ

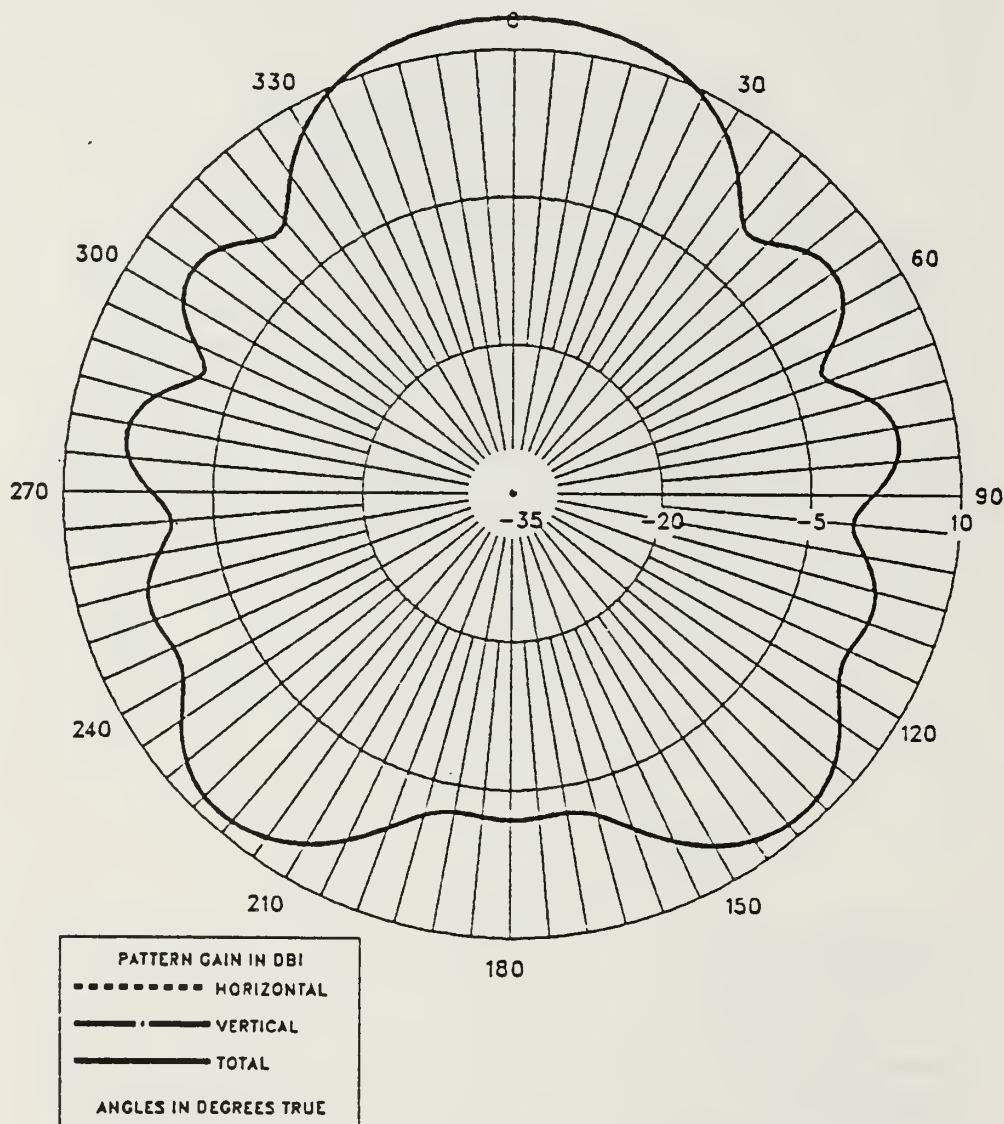


Figure E.27 E-Field Azimuth Pattern at 7.5 MHz
for TF-TLA on the Stern.

TF-TLA ON THE STERN

FREQUENCY = 7.5 MHZ

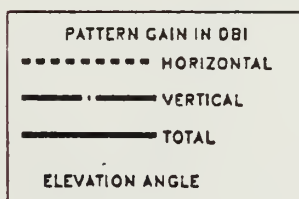
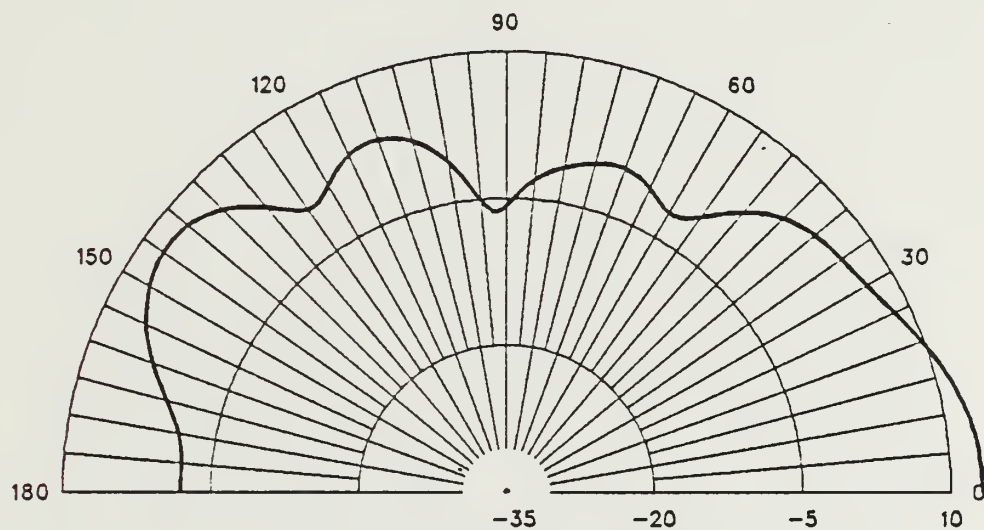


Figure E.28 E-Field Elevation Pattern at 7.5 MHz
for TF-TLA on the Stern.

TF-TLA ON THE BOW

FREQUENCY = 10 MHZ

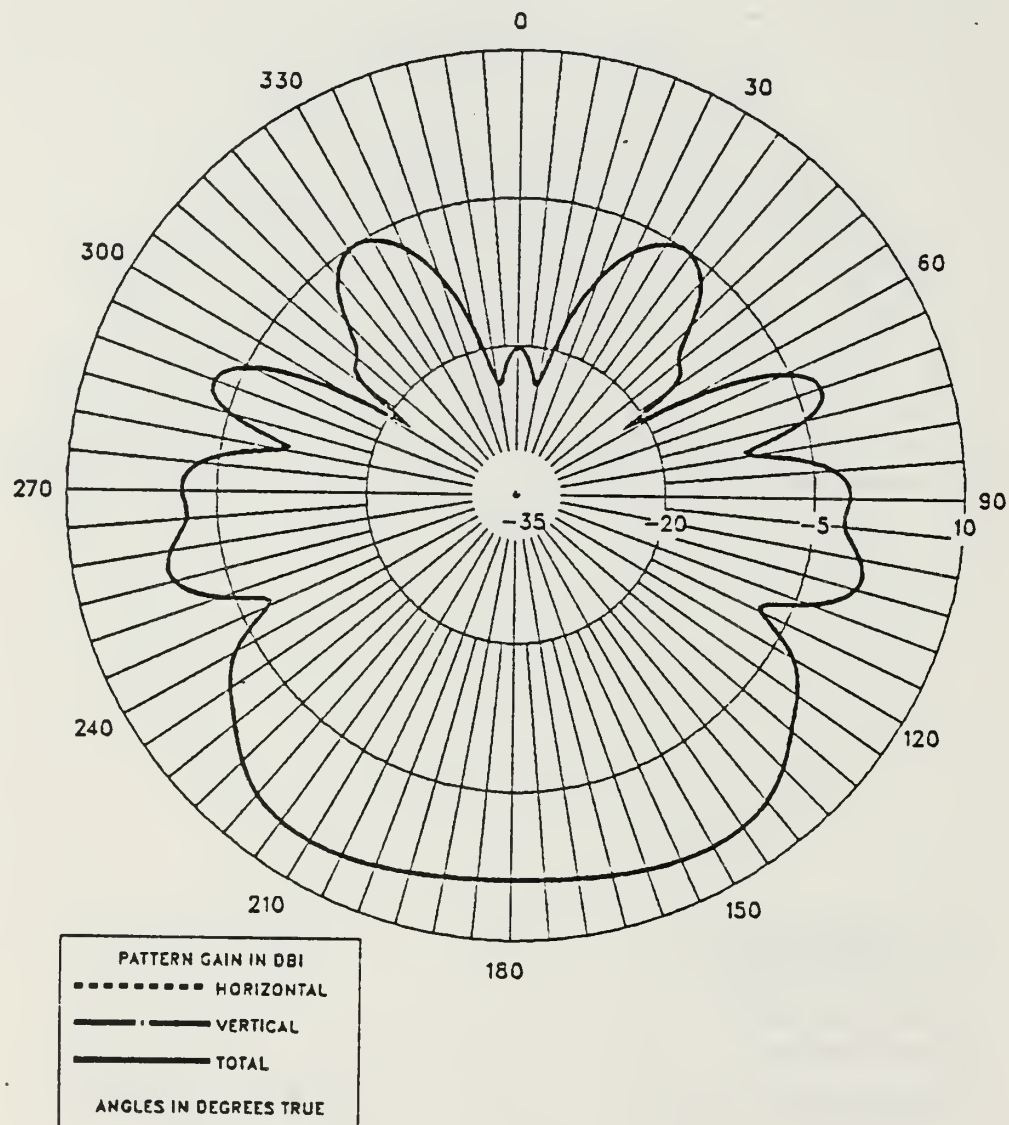


Figure E.29 E-Field Azimuth Pattern at 10.0 MHz for TF-TLA on the Bow.

TF-TLA ON THE BOW

FREQUENCY = 10 MHZ

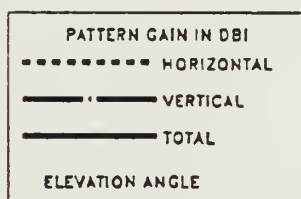
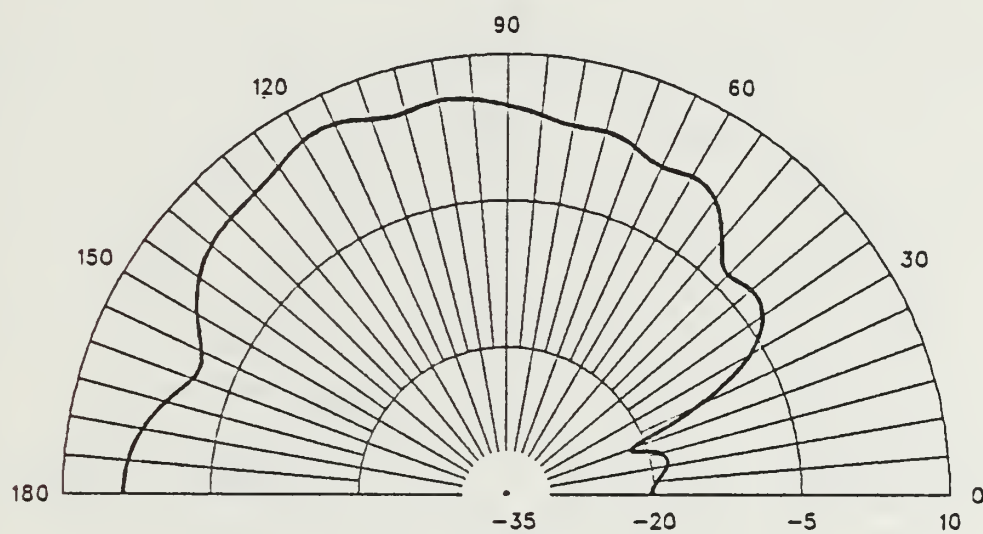


Figure E.30 E-Field Elevation Pattern at 10.0 MHz
for TF-TLA on the Bow.

TF-TLA ON THE STERN

FREQUENCY = 10 MHZ

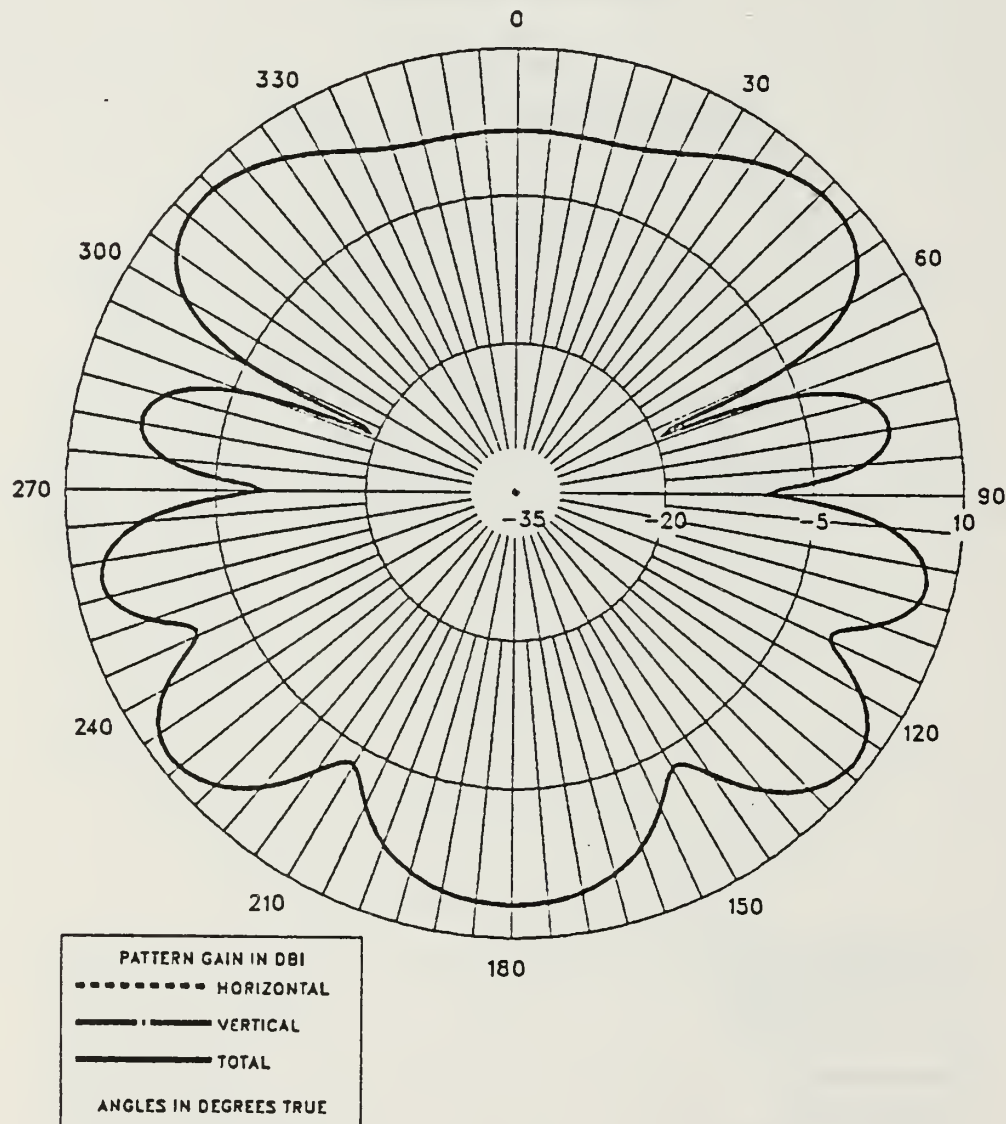


Figure E.31 E-Field Azimuth Pattern at 10.0 MHz
for TF-TLA on the Stern.

TF-TLA ON THE STERN

FREQUENCY = 10 MHZ

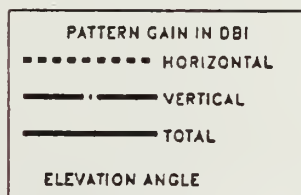
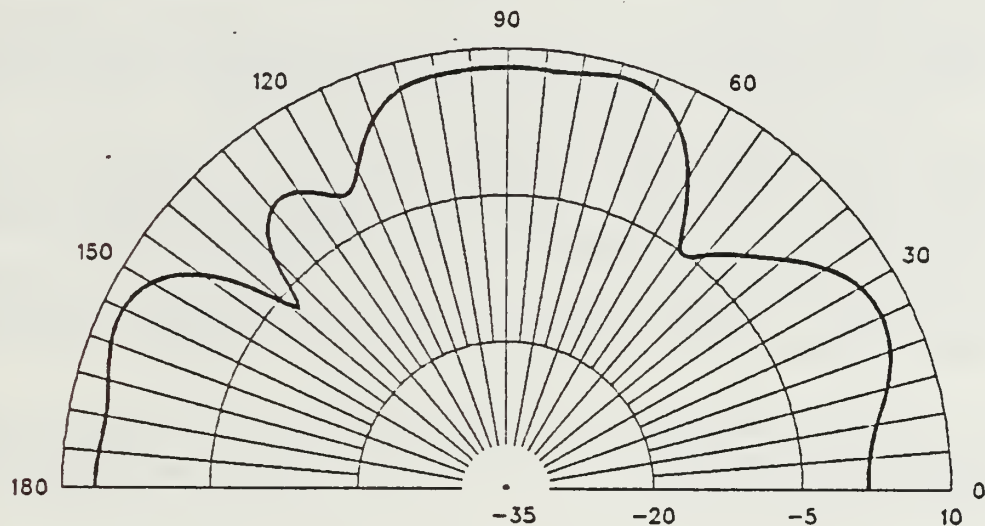


Figure E.32 E-Field Elevation Pattern at 10.0 MHz
for TF-TLA on the Stern.

LIST OF REFERENCES

1. Stutzman, W. L. and Thiele, G. A., *Antenna Theory and Design*, John Wiley & Sons., Chapter 5, 1981.
2. Burke, M. S., and Pogio, A. J., *Numerical Electromagnetics Code (NEC) - Method of Moments*, Lawrence Livermore Laboratory, January 1981.
3. Naval Ocean Systems Center Technical Document 116, Volume 2, *Numerical Electromagnetics Code (NEC) - Methods of Moments*, by G. J. Burke and A. J. Pogio of Lawrence Livermore Laboratory, pp. 3-6, January 1981.
4. Naval Electronic Systems Command, FFG-45 thru. FFG-55, *Communication Antenna Configuration Data*, Washington, DC. 20360, July 1984.
5. G. J. Burke, *Enhancements and Limitations of the Code NEC for Modeling Electrically Small Antennas*, Lawrence Livermore National Laboratory, Report UCID-20970, January 1987.
6. Naval Ocean Systems Center Technical Document 116, Volume 2, *Numerical Electromagnetics Code (NEC) - Methods of Moments*, by G. J. Burke and A. J. Pogio of Lawrence Livermore Laboratory, pp. 89-92, January 1981.
7. Tertocha, C. J., *A Feasibility Study of a Shipboard Combat Survivable HF Antenna Design*, M.S.E.E. Thesis, Naval Postgraduate School, Monterey, California, pp. 68-72, March 1986.

BIBLIOGRAPHY

Liberopoulos George L., *Numerical Models of New HF Shipboard Communication Antenna Systems for Improved Survivability*, M.S.E.E. Thesis, Naval Postgraduate School, Monterey, California, June 1986.

Neiva Mario Cabral, *Broadband Techniques Applied to Shipboard HF Slot Antennas*, M.S.E.E. Thesis, Naval Postgraduate School, Monterey, California, June 1986.

Vorrias Ioannis G., *Shipboard Combat Survivable HF Antenna Designs*, M.S.E.E. Thesis, Naval Postgraduate School, Monterey, California, December 1986.

Naval Postgraduate School Report MVS-01, *User's Guide to MVS at NPS*, by J. Favorite, pp. 29, November 1983.

Harrington, R. F., *Matrix Methods for Field Problems*, Proceedings of IEEE, Vol. 55, pp. 136-149, February 1967.

INITIAL DISTRIBUTION LIST

	No. Copies
1. Defense Technical Information Center Cameron Station Alexandria, VA 22304-6145	2
2. Library, Code 0142 Naval Postgraduate School Monterey, CA 93943-5002	2
3. Department Chairman, Code 62 Department of Electrical and Computer Engineering Naval Postgraduate School Monterey, CA 93943-5000	1
4. Prof. Richard W. Adler, Code 62 AB Department of Electrical and Computer Engineering Naval Postgraduate School Monterey, CA 93943-5000	5
5. Prof. Harry Atwater, Code 62 AN Department of Electrical and Computer Engineering Naval Postgraduate School Monterey, CA 93943-5000	1
6. Donald Wehner NOSC Code 744 San Diego, CA 92152	1
7. Bailey Aalfs SABRE Communications P. O. Box 536 Sioux city, IA 51102	1
8. CHU Associates Inc. 800 Fesler St El Cajon, CA 92020	1
9. Mr. R. D. Albus IIT Research Institute 207 Woodloch Ln Severna Park, MD 21146	1
10. Mr. R. Anders APPL. Electromagnetic Engineering Vorder Halden 11 D-7777 Salem 1 West Germany	1

11.	Dr. Harold W Askins, JR The Citadel Department of Electrical Engineering Charleston, SC 29409	1
12.	Capt. W.P. Averill U.S. Naval Academy Department of Electrical Engineering Annapolis, MD 21402	1
13.	Mr. L.R. Bachman Naval Electronics System Engineering Activity ST. Inigoes, MD 20684	1
14.	Dr. Duncan C. Baker Department of Electrical and Computer Engineering University of Pretoria 0002 Pretoria South Africa	1
15.	Mr. R.J. Balestri Booz, Allen and Hamilton 2201 Buena Vista, SE, #400 Albuquerque, NM 87106	1
16.	Mr. D. Baran IITRI 185 Admiral Cochrane DR Annapolis, MD 21401	1
17.	Mr. M. Barth Lawrence Livermore National Laboratories P. O. Box 5504, L-153 Livermore, CA 94550	1
18.	Mr. J. Belrose CRC/DRC Building 2A, Room 330 3701 Carling Ave Box 11490. Sta. H Ottawa, ONT K2H8S2 Canada	1
19.	Mr. T. Birnbaum OAR Corporation Engineering Department 10447 Roselle St San Diego, CA 92121	1

20.	Mr. L. Botha NIAST/CSIR P. O. Box 395 Pretoria South Africa	1
21.	Mr. J.K. Breakall Lawrence Livermore National Laboratories P. O. Box 5504, L-156 Livermore, CA 94550	1
22.	Mr. G.W. Browne Sperry Support SVCS Building 92 Benicia Ind PK Benicia, CA 94510	1
23.	Mr. G. Burke Lawrence Livermore National Laboratories P. O. Box 5504, L-156 Livermore, CA 94550	1
24.	Mr. Scott Burkhart Lawrence Livermore National Laboratories P. O. Box 5504, L-156 Livermore, CA 94550	1
25.	Mr. D. Cambell TRW Military Electronics Division RC2/266 7x San Diego, CA 92128	1
26.	Mr. B. Cambell ECAC, MS 21 N. Seven Naval Base Annapolis, MD 21401	1
27.	Mr. J. Cauffman Naval Electronics System Comm. Electronics 3041 Washington, DC 20360	1
28.	Mr. A. Christman Ohio University Stocker Center Athens, OH 45701	1
29.	Mr. D. Coblin Lockeed M & S Co. O/6242; B/130/Box 3504 Sunnyvale, CA 94088-3504	1

30.	Mr. P. Cunningham U. S. Army CECOM ATTN: AMSEL-RD-COM-TA-1 Ft. Monmouth, NJ 07703	1
31.	Mr. J. M. Devan NOSC Code 8122 San Diego, CA 92152	1
32.	Mr. W. Essig Naval Electronics System Comm. Code 51012 Washington, DC 20360	1
33.	Mr. D. Faust Eyring Research Institute 1455 W 820 N Provo, UT 84601	1
34.	Dr. A. J. Ferraro Penn. State University Ionosphere Research Laboratory University Park, PA 16802	1
35.	Mr. D. Fessenden Naval Underwater System Center New London Laboratory New London, CT 06320	1
36.	Mr. P. Gailey The EC Corporation 575 Oak Ridge Turnpike Oak Ridge, TN 37830	1
37.	Mr. G. H. Hagn SRI International 1611 N. Kent Street Arlington, VA 22209	1
38.	Mr. L. Harnish SRI International 1611 N. Kent Street Arlington, VA 22209	1
39.	Mr. J. B. Hatfield Hatfield & Dawson 4226 Sixth Ave., N. W. Seattle, WA 98107	1

40.	Mr. J. E. Hipp S W Research INST/EMA PO Drawer 28510 San Antonio, TX 78284	1
41.	Mr. H. Hochman GTE Sylvania MS 4G12, Box 7188 Mountain View, CA 94039	1
42.	Mr. D. E. Hudson Lockeed Aircraft Service Company Department 1-330 P. O. Box 33 Ontario, CA 91761	1
43.	Mr. K. Coburn/ DELHD-N-EMA Harry Diamond Laboratory 2800 Powder Mill Road Adelphi, MD 20783	1
44.	Dr. S. J. Kubina Concordia University 7141 Sherbrooke Street W. Montreal, QUE H4B1R6 Canada	1
45.	Mr. R. Latorre LLNL L156/ Box 5504 Livermore, CA 94550	1
46.	Mr. J. Logan NOSC Code 822 (T) 271 Catalina Boulevard San Diego, CA 92152	1
47.	Mr. F. Mace 11635 Havener Road Fairfax State, VA 22039	1
48.	Commander USAISEIC/ASBI-STS (J. McDonald) Ft. Huachuca, AZ 85613-7300	1
49.	Mr. B. J. Meloy 333 Ravenswood/Building G Menlo Park, CA 94025	1

50.	Mr. E. K. Miller Rockwell Science Center Box 1085 Thousand Oaks, CA 91365	1
51.	Mr. L. C. Minor IIT Research Institute/ECAC 185 Admiral Cochrane Drive Annapolis, MD 21401	1
52.	Mr. J. Molnar Naval Electrical System Command National Center #1 Washington, DC 20363	1
53.	Mr. C. A. Nelson NOSC Code 822 (T) 271 Catalina Boulevard San Diego, CA 92152	1
54.	Mr. I. C. Olson NOSC Code 822 (T) 271 Catalina Boulevard San Diego, CA 92152	1
55.	Mr. D. J. Pinion 12151/2 S. Alfred Street Los Angeles, CA 90035	1
56.	Mr. J. Cahill Kershner, Wright & Hagaman 5730 General Wash. Drive Alexandria, VA 22312	1
57.	Mr. J. J. Reaves, Jr. Naval Electrical System Engineering Center 4600 Marriott Drive N. Charleston, SC 29413	1
58.	Mr. T. Roach Microcube Corporation Box 488 Leesburg, VA 22075	1
59.	Mr. R. Royce Naval Research Laboratory Washington, DC 20375	1
60.	Mr. D. Rucker ESL 495 Java Drive, MS205 Sunnyvale, CA 94086	1

61.	Mr. T. Simpson University of South Carolina College of Engineering Columbia, SC 29208	1
62.	Mr. W. D. Stuart IIT Research Institute/ECAC 185 Admiral Cochrane Drive Annapolis, MD 21401	1
63.	Mr. R. Tell USEPA ORP P. O. Box 18416 Las Vegas, NV 89114	1
64.	Mr. J. Tertocha C-15 Tenbytown Apartments Delran, NJ 08075	1
65.	Mr. R. Thowless NOSC Code 822 (T) 271 Catalina Boulevard San Diego, CA 92152	1
66.	Mr. C. H. Vandment Rockwell International 802 Brentwood Richardson, TX 75080	1
67.	Dr. E. Villaseca Hughes Aircraft Co./GD System P. O. Box 3310 Fullerton, CA 92634	1
68.	Mr. W. P. Wheless, Jr. P. O. Box 3 CL Las Cruces, NM 88003	1
69.	Naval Academy Library Jinhae City, Gyungnam 602-00 Republic of Korea	2
70.	Maj. Choi, Seung Kyu Jangmi Yeollip A dong 102 Ho 462-9 Mangwon-dong Mapogu Seoul 121 Republic of Korea	8
71.	Director of Research Administration Code 012 Naval Postgraduate School Monterey, CA 93943	1

Thesis

C448861 Choi

c.1

A numerical modeling
study of the transmis-
sion line antenna for
use as an HF combat
survivable shipboard
antenna.

Thesis

C448861 Choi

c.1

A numerical modeling
study of the transmis-
sion line antenna for
use as an HF combat
survivable shipboard
antenna.



